UNIVERSITY OF MILANO-BICOCCA

DEPARTMENT OF STATISTICS AND QUANTITATIVE METHODS

DOCTORAL THESIS IN STATISTICS AND MATHEMATICAL FINANCE

Stochastic Systemic LCOE with Time-Varying Pricing Schedule and Agent-Based Interaction Modelling

Author: **SONUBI**, Adeyemi Adewale
Registration No.: 798856

Tutor: Prof. ssa. Silvana Stefani
Advisor: Prof. Carlo Mari

ACADEMIC YEAR   2016/2017

Abstract

A methodological scheme to diversify the portfolio of generating technologies, through a Levelized Cost of Electricity (LCOE) analysis is explored in this research, in order to minimize the cost and risk involved in the production of electricity. We investigate the cost effect of the time-varying pricing schedule when the intermittent renewable energy source is integrated into a dispatchable resource-based power system, under a stochastic systemic framework. The unpredictability of fossil fuel prices and the uncertainty in the environmental policies constitute the financial risk in the purely thermal technology portfolio. The fossil fuel is modeled using mean-reverting Levy models, which captures the complicated behavior in the observed dynamics of market prices; this ensured a more accurate computation of LCOE. The Conditional Value at Risk Deviation (CVaRD) measure is used to capture the tail risk in the systemic LCOE portfolio for the assessment of the worst-case scenario. We observe that the inclusion of solar and wind components, which represent the riskless asset of the portfolio, shows a combined effect of extra cost and risk reduction in the systemic frontier produced through the mean-CVaRD optimization approach. This research is useful for a policymaker in measuring the overall competitiveness of an energy system.

The second part of this research, which is based on agent interaction, shows the effect of competition and cooperation among interacting agents along a generalized Verhulst-Lotka-Volterra model. We investigate analytically and numerically how interaction among agents affect satisfying demand, that is, reaching the market capacity, and the effect on the systemic stability. Agents in this analysis are the energy investors/firms. Systemic stability is observed when agents grew in size to the market capacity. Agents which collaborated better also tend to perform better in the market.

Acknowledgements

Contents

List of Figures

List of Tables

Introduction

Investment decisions and investment assessment in electricity production are usually supported by a Levelized Cost Of Electricity (LCOE) analysis, where the LCOE is obtained as the deterministic solution of an algebraic equation, in which fuel prices and CO_2 costs are included as dynamic deterministic variables (expected values of future prices and costs) [23, 32]. LCOE is calculated as the break-even price that investors would receive on average per kilowatt-hour (kWh) generated in order to cover all costs and receive an adequate return on their initial investment. In corporate finance, an investment is profitable if the present value of revenues is greater than the present value of the costs of the project, which is the LCOE.

LCOE is an economic measure that estimates the cost of lifetime-generated energy; it is used as a benchmarking tool to assess the cost-effectiveness of different energy generation technologies per unit of electricity (MWh) [37]. It allows investors to compare generating costs of alternative technologies. Generation costs of conventional plants with intermittent renewable sources such as wind and solar PV (photovoltaics) can be compared, despite their different cost of investment and maintenance. LCOE plays a crucial role in a free market context because through it, market risks can be incorporated into the value of the cost of capital used to discount cash flows [28]. For a multi-technology project, LCOE determines the minimum selling price of electricity produced by its generation technology mix which is necessary to cover all the operation cost, principal and interest repayment obligation on debt incurred on the investment cost and to provide equity investors the adequate return for the assumed risk [24].

This research is based on the methodological scheme to diversify the portfolio of generating technologies. This includes, the purely thermal technology mix portfolio (i.e. coal and gas technology mix), which satisfy the baseload demand of electricity, and the integrated intermittent non-dispatchable energy sources (solar and wind energy). The choice of solar and wind energy is based on the fact that "wind resource tends to complement solar resource" [18], since "wind blows during stormy conditions when the sun does not shine and the sun often shines on calm days with little wind, combining wind and solar can go a long way toward meeting demand, especially when a steady base can be called on to fill in the gaps" [19]. The unpredictability of fossil fuel prices as well as

the uncertainty in the environmental policies constitute the financial risk in a purely thermal technology portfolio. The integration of renewable energy sources into the power system has the same diversification effect as a riskless asset in a portfolio, where the purely thermal plant represents the risky asset in the portfolio. This helps to minimize the electricity price risk induced by the high volatility of fuel and CO_2 market prices.

Motivated by the works of Mari & Lucheroni [27] and Reichelstein & Sahoo [41], we investigate, from a single investor perspective, the effect of a time-varying pricing schedule in the LCOE computation of intermittent energy sources integrated in a purely thermal resource based power system in a stochastic systemic framework. This is done by considering the extra costs and gains imposed on the power system which is not reflected in the classical LCOE definition. The extra costs considered in our LCOE analysis are stated below:

Firstly, the systemic constraints, which are due to the intermittency of the renewable energy that are integrated into the power system. Systemic constraints affect the computation of the LCOE through energy and capacity reduction. When an intermittent energy source is generated and injected into the grid, energy generated from the purely thermal technology must be reduced of the same quantity in order to have a demand-supply balance, since energy storage is quite expensive. This energy reduction must be considered in the LCOE computation. In addition to this, the inclusion of the solar and wind power capacity component in a generation portfolio may not be completely equivalent to the power capacity of the dispatchable energy, since wind might not blow during peak hours which is often late afternoons in summer, when the demand for air-conditioning places utility systems under greatest stress. Also, the Sun might not shine on cloudy days which mostly occur during winter. Therefore, in order to have a balance on the expected power capacity demanded, some backup dispatchable power capacity needs to be maintained. Inputing cost variation due to systemic constraints into the computation of the LCOE is called the 'systemic LCOE theory' [27].

Secondly, the time-varying pricing schedule, which is due to time of day fluctuations and seasonal cycles of the renewable energy sources integrated into the power system. Classical LCOE calculations are prone to neglect substantial aspect of the economics of renewable energy sources [20]. This can be appended through a multiplicative correction factor called the co-variation coefficient introduced by Reichelstein and Sahoo [41]. The co-variation coefficient captures any interaction and/or relationship between the time-varying patterns of electricity generation and pricing due to time of day fluctuations and seasonal cycles. It can be noted that by construction, co-variation coefficient is equal to one for a base-load energy system such as fossil fuel power plants because electricity generation is assumed to be constant throughout the lifecycle of the power plant. Also, the co-variation coefficient is equal to one for an intermittent energy source under a time-invariant pricing schedule.

Financial risk analysis is introduced into LCOE computation by the stochastic LCOE approach, which accounts for the variability of LCOE due to risky factors. The main sources of financial risk in this analysis are the dynamics of coal market prices, the dynamics of gas market prices and the dynamics of CO_2 prices. Although, the Geometric Brownian Motion (GBM) is sometimes used to model fossil fuel prices dynamics, it should be noted that such a stochastic process may not capture completely the observed dynamics of market prices. Some evidence exist for more complicated behaviors showing mean reversion around some long run value, jumps and stochastic volatility [13]. Therefore the dynamics used for the analysis of fossil fuel price is a mean-reverting Levy model as suggested in [24]; this accurately describes the time evolution of the coal and gas prices. The dynamics of coal prices is chosen to follow a mean-reverting stochastic differential equation, while the dynamics of gas prices is chosen to follow a mean-reverting jump-diffusion equation due to the high volatility of gas prices, which includes spikes. The continuous model dynamics chosen for CO_2 prices is a GBM.

In general, LCOE distributions are not gaussian, having asymmetric long thick tails [14], therefore the Markowitz mean-variance analysis used in the systemic LCOE risk analysis is considered only as the starting point. The analysis can be extended with a more suitable dispersion measure called CVaR deviation (CVaRD), which plays the same role as the standard deviation in a Markowitz approach. The results of these analyses will be compared.

The second part of this research work is based on a complex system perspective. A complex system is composed of many interacting parts called agents, which display collective behavior that does not follow trivially from the behavior of the individual parts [2, 5, 33]. Over the years, it has been discovered that non-linear mathematical models replicate the dynamics of real systems better than the linear ones [15, 49]. An example of such non-linear models is the Lotka-Volterra model [22, 53]. The Lotka-Volterra model has been used in various ways to model complex systems [6, 7, 8, 30].

A more specific analysis based on our previous research [48] on the effect of competition and cooperation among interacting agents along a generalized Verhulst-Lotka Volterra model in the presence of a market capacity, will be done. In this case, the interacting agents are the energy firms/investors, that minimize cost and the risk involved in the production of electricity in order to maximize their profits while keeping the environment clean. The agent's interaction is analyzed based on the size of agent with common resources to share, that is, the consumers of electricity. Agents tend to increase in size when they acquire more of the market share and reduce when any market portion is lost. A network effect was introduced through an undirected but weighted graph in order to enable a mixed-type of interactions, that is, having a system in which competitive and cooperative scenarios are considered to occur simultaneously among various interacting agents in the presence of a realistic constraint called

the market capacity. Such competition, cooperation, and mixed type of interactions are analyzed below for a triad of interacting agents through the evaluation of the eigenvalues of the relevant Jacobian matrix computed at corresponding fixed points in order to investigate the system stability. This triad system has been chosen as the most simple, yet complex enough as representative of basic networks.

The main contributions in this thesis are outlined as follows:

1. An extension of the Stochastic Systemic LCOE Theory is proposed by introducing time-varying pricing schedules into LCOE analysis of intermittent renewable energy sources integrated into a dispatchable resource based power system.

2. A modeling of fossil-fuel prices with stochastic processes that capture more complicated behaviors characterizing the dynamics of market prices of energy commodities is advanced. This enables a more accurate LCOE analysis.

3. LCOE risk analysis using the deviation measure called CVaRD to capture tail risk is presented. This is an extension to the Markowitz mean-variance analysis done in [27] as a starting point of systemic LCOE risk analysis.

4. Agent interaction is investigated along the generalized Verhulst-Lotka Volterra model. We considered how interactions among agents affect satisfying demands (i.e. market capacity) and the effect on the systemic stability. Agents in this analysis are the energy investors/firms.

The thesis is organized as follows. In the first chapter, the stochastic LCOE theory is reviewed. In computing the LCOE of coal and gas technologies, the dynamics of fossil fuel prices is modeled using mean-reverting stochastic differential equations. LCOE analysis based on these dynamic models is compared to previous analyses in the literature. The extra cost of integrating intermittent renewable energy sources into a dispatchable resource-based power system is analyzed in the second chapter. The analysis is done by considering the systemic constraints involved in the integration of renewables and the synergies that exist in the time-varying patterns of electricity generation and pricing of renewables when computing the LCOE of the portfolio of generation technologies. LCOE risk analysis is performed in the third chapter starting from the Markowitz mean-variance analysis approach, and then extended to the CVaR deviation in order to capture the tail risk. The second part of the thesis which includes the fourth and the fifth chapter, is based on the published paper [48] on the effect of competition and cooperation among interacting agents in the presence of a market capacity.

Chapter 1

LCOE Theory

1.1 Introduction

In this chapter, the economic and financial analysis of fundamental terms in LCOE analysis is presented. Background studies on the computation of the classical LCOE is reviewed. An extension to the stochastic form which accounts for the variability of LCOE due to risky factors is also reviewed from past literatures. LCOE analysis of coal and gas through geometric Brownian motion and mean-reverting stochastic differential equation is shown. The fossil fuel models were compared with historical data of fuel prices in the US in order to validate the model appropriate for our analysis.

1.2 Fundamental terms in LCOE Analysis

The overview of the basic concepts and elements of the economic and financial analysis of the LCOE from [46] is presented below:

1.2.1 Cash Flows

Cash flow is the net amount of cash and cash-equivalents moving into and out of a project or business, as the case may be. Cash flow can be defined in terms of three different activities performed by a company, which are operation, investment and financing. Cash flows from operating activities of a company includes all revenue obtained minus operation and maintenance cost, interest paid and the income tax. Cash flow from Investment includes the capital expenditures while financing activities cash flow includes the repayment of principal debt and dividends.

1.2.2 Inflation Rates

The revenue and cost of a company can be measured in terms of current or constant dollar rates. Current money unit cash flow is the actual cash flow observed in the market place, that is, the actual cash required in the year the cost is incurred. This changes over time due to inflation or deflation of the economy. Constant money unit cash flow represent the amount of money that would have been required if the cost is paid in the base year. Therefore, the relationship between the two cash rate is:

$$C_n = \frac{C_m}{(1+i)^{m-n}} \tag{1.2.1}$$

Where C_n represents the constant rate cash flow in the base year n, C_m is the current rate cash flow in year m and i is the inflation rate which is assumed to be constant during the $m - n$ years.

1.2.3 Time Points and Periods

Time points considered critical in an LCOE analysis includes the base year, dollar year and the investment year. The *base year (zero year)* is the year in which all cash flows are converted, the *dollar year* is the year to which base year results are converted and reported while the *investment year* is the year the actual investment occurs. The important time periods for LCOE analysis includes the *investment lifetime*, which is the estimation of a particular investment useful life; *Analysis period*, this is the period for which the evaluation is conducted; *Depreciation Period*, this is the period of time over which an investment is amortized (usually for tax purposes); *Finance period*, this is the period for which an investment financing is structured and *Levelization Period*, which is the period of time used when calculating a levelized cash flow stream.

1.2.4 Discounted Rates

Discounted rates are often used to account for the risk inherent in an investment. It acts as a measure of time value of return (i.e. the price put on the time that an investor waits for a return on an investment) and it is central to the calculation of present value. Nominal discount rate are discount rates with inflationary effects while real discount rates excludes inflation. Discount rate can be converted from real to nominal and vice versa with the following formula:

$$(1 + d_n) = (1 + d_r)(1 + i) \tag{1.2.2}$$

Where d_n is the nominal discount rate, d_r is the real discount rate and i is the inflation rate. From Equation 1.2.2, we can deduce that the nominal discount rate d_n is explicitly given by :

$$d_n = [(1 + d_r)(1 + i)] - 1 \tag{1.2.3}$$

while the real discount rate d_r is given by:

$$d_r = \frac{(1 + d_n)}{(1 + i)} - 1 \qquad (1.2.4)$$

1.2.5 Cost of Capital

This involves determining the cost of the various capital components which majorly include debt, preferred stock and equity, then applying these costs to the capitalization ratio of the firm to arrive at a *Weighted Average Cost of Capital (WACC)*. It is the rate of return needed to induce investors to invest in a project of similar risk and duration. The price of a good or service to a consumer in a competitive market or regulated market will include a return approximately equal to the cost of capital of the industry. Higher returns attract increased investment, whereas lower returns discourage investment and leads to inadequate supplies and sources of investment capital. The general formulation of WACC is calculated by:

$$\text{WACC} = R_e \frac{C_e}{C_e + P_s + D} + R_p \frac{P_s}{C_e + P_s + D} + (1 - T)R_d \frac{D}{C_e + P_s + D}, \quad (1.2.5)$$

where R_e is the rate of return on common equity, C_e is the common stock and corporate retained earnings, P_s is the preferred stock, D is debt issues, R_p is the rate of return on the preferred stock, T is the corporate tax and R_d is the interest paid on the debt. Accessing the LCOE through the WACC method allows one to include the level of risk perceived by investors (both equity and bondholders) through the debt fraction of the investment in the discounting rate [27].

1.2.6 Present Value

It is the measure of today's value of revenue or cost to be incurred in the future. Present value analysis is used to calculate the worth of transaction today with respect to the future changing money valuation.

$$PV = PVIF_n \times C_n, \qquad (1.2.6)$$

where PV is the present value, $PVIF_n = \frac{1}{(1+d)^n}$ is the present value interest factor, C_n is the cash flow n years in the future and d is the annual discount rate. When future cash flow are fixed in size and regularly over a specific number of periods, the situation is known as an annuity. The present value formula for an annuity is given by:

$$PV = C \times \frac{(1 + d)^N - 1}{(d(1 + d)^N)}, \qquad (1.2.7)$$

where C is the cash flow in each of N future years.

1.2.7   Taxes

The most complete analysis of an investment in a technology or a project requires the analysis of each year of the life of the investment, taking into account relevant costs, including taxes. Cash flow is the basis for analyzing alternative investment in energy production, therefore, after-tax cash flow is the most appropriate to be used for analysis since it accounts for federal and state income taxes.

1.2.8   Depreciation

This is a means of recovering, through an income tax deduction, the cost of property used in a trade or business or of property held for the production of income. The capital sum to be recovered by depreciation is the depreciation base, which when adjusted annually by the amount depreciable, becomes the adjusted base. The Modified Accelerated Cost Recovery System (MACRS) is the name given to the federal tax rules for recovering cost through depreciation in the US.

1.3   Background Study

The method of LCOE has been widely used for the estimation of power generation costs (among others see [3, 4, 24, 28, 37, 38, 45, 47]). A methodological approach based on the LCOE was proposed in a risk analysis of portfolios of power generating technologies in [28]. This was done in a stochastic framework, in which, fossil fuel prices and carbon credit prices were assumed to evolve in time according to well defined Brownian processes. Nuclear power was considered as a hedging asset to reduce CO_2 emission in the atmosphere, thereby minimizing the volatility of electricity prices. Starting from market data, and using Monte Carlo techniques to stimulate generating cost values, portfolio optimization of the power generating technologies was performed by using the mean-variance approach. However, the stochastic processes used in this paper may not completely capture the observed dynamics of market prices of energy commodities. Also, the mean-variance analysis is not useful when considering the worst case assessment of a portfolio.

The research on stochastic LCOE for optimizing multi-asset risky energy portfolios was reviewed and extended in [24] by using two different stochastic models, a Lognormal model and an extended Levy model, which properly replicates the dynamics of the real market prices of coal and gas in the US for 20 years respectively. In addition, risk analysis was carried out using the mean-variance approach and the mean-CVaR analysis, which is useful for cases with asymmetric distributions. The two risk analysis had different results in terms of optimal portfolios. It can be noted that the WACC, which includes the risk

perception of investors in nuclear business, was kept constant during the analyses. The research can be extended through the inclusion of different WACC scenarios, in order to study the tradeoff between different but concurrent environmental risks (i.e., in this case, CO_2 price volatility and nuclear business risk). Renewable energy sources may also be chosen as a preferable option of a riskless asset to hedge the risky energy portfolio.

Due to the intermittency of renewable energy sources, electricity demand can only be met at all times of the day and season if energy production through renewable energy sources is backed up with a dispatchable energy source, which provides a steady source of energy for the production of electricity. Earlier literatures has argued that LCOE analysis may be inappropriate when applied to intermittent power sources [20]. This argument was addressed in [41], where the authors demonstrated that LCOE analysis remains appropriate for accessing the cost competitiveness of an renewable energy sources, provided that the figure obtained from the traditional average LCOE computation is adjusted by a multiplicative correction factor called the co-variation coefficient. The co-variation coefficient captures any interaction and/or relationship between the time-varying patterns of electricity generation and pricing, due to time of day fluctuations and seasonal cycles. It can be noted that, by construction, the co-variation coefficient is equal to one for a base-load energy system, such as fossil fuel power plants. However, *the authors did not consider systemic constraints related to intermittency,* even though the authors admitted that the effects of such constraints will become increasingly prominent as renewable energy sources provide a more substantial share of the overall supplied electricity.

A systemic deterministic LCOE was introduced in [27] by taking into consideration the cost generated from constraints imposed on system through the integration of an intermittent energy sources in a given power system operated on dispatchable energy sources. The stochastic version takes into consideration the volatility of fossil fuel and CO_2 emission prices. The inclusion of intermittent energy source act as a riskless asset in a given power system. It was used to investigate the diversification effect and the CO_2 emission reduction due to the electricity generation portfolio selection. Markowitz mean-variance analysis was used to analyze the financial risk of the electricity prices. Nevertheless, the LCOE analysis of the intermittent renewable energy integrated into the power system can be extended, by considering not only the systemic constraints, but also the synergies that exist between the time-varying patterns of electricity generation and pricing, due to time of day fluctuations and seasonal cycles.

1.4 Deterministic LCOE Model

Classically, the LCOE is defined as the non-negative price P_{LC}^α (which is assumed constant in time, and expressed in real monetary units) of the electricity produced by a specific generation technology α, which makes the present value

of the expected revenues from electricity sales equal to the present value of all expected costs met during the plant life-cycle (which includes investment costs, operating costs, fuel costs and carbon charges when due). The LCOE represents generating cost at the plants level (i.e. busbar costs) and does not include transmission costs, distribution cost and all possible network infrastructure adjustments costs [32].

A project of an electricity generating plant with a project timeline $p(t)$ given by:

$$p(t) = \{t \in \mathbf{Z} : -n \leq t \leq N\}$$

has a construction period $t = [-n, 0]$, with $t = 0$, as the end of construction time, evaluation time and operation starting time. N is the end of operation time. After equating the present values of expected revenues and costs, the LCOE for a specific technology α evaluated at time $t = 0$ is implicitly defined as:

$$\sum_{t=0}^{N} \frac{P_{\mathrm{LC}}^{\alpha} Q_t^{\alpha} (1+i)^{t-t_0}}{(1+r_w)^t} = \sum_{t=0}^{N} \frac{C_t^{\alpha} + T_t^{\alpha}}{(1+r_w)^t} + I_0^{\alpha}. \qquad (1.4.1)$$

From the l.h.s of Equation (1.4.1), Q^{α} denotes the amount of electricity produced during period t, it is assumed to be constant in time. Also for a period of one year,

$$Q^{\alpha} = W^{\alpha} \times 8760 \times CF^{\alpha}, \qquad (1.4.2)$$

where W^{α} denotes the nameplate capacity of the plant, and CF^{α} denotes the capacity factor of the plant for 8760 hours. In Equation (1.4.1), i is the expected yearly inflation rate, t_0 refers to the base year used to compute nominal prices from real prices and r_w is the WACC discount rate, which is kept constant for the whole life of the project. From the r.h.s of Equation (1.4.1), C_t^{α} denotes the nominal operating expenses incurred throughout the operational life of the generating plant, which includes the expected real escalation rate of the fixed and variable operational & maintenance (O & M) costs, the time-varying fossil fuel and CO_2 emission prices. The yearly nominal tax liabilities denoted by T_t^{α} and given by

$$T_t^{\alpha} = T_c(R_t^{\alpha} - C_t^{\alpha} - D_t^{\alpha}), \qquad (1.4.3)$$

is calculated by subtracting costs C_t^{α} and asset depreciation D_t^{α} from the revenues R_t^{α} which stems from the sales of the generated electricity, with T_c being the tax rate. The revenue R_t^{α} are computed by the equation given below:

$$R_t^{\alpha} = P_{\mathrm{LC}}^{\alpha} \times Q^{\alpha} (1+i)^{t-t_0}. \qquad (1.4.4)$$

The second term on the r.h.s of Equation (1.4.1), I_0^{α}, denotes the pre-operations nominal investment expenses. It is computed as a lump sum, starting at $t = -n$

and ending at $t = 0$. Within the WACC approach, I_0^α given by

$$
\begin{aligned}
I_0^\alpha &= \sum_{t=-n}^{0} A_t^\alpha (1 + r_w)^{-t}, & (1.4.5) \\
&= A_{-n}^\alpha (1 + r_w)^n + \cdots + A_{-1}^\alpha (1 + r_w) + A_0^\alpha,
\end{aligned}
$$

where the nominal amount A_t^α at year t, computed in terms of the overnight cost O_t^α, allocated to year t, can be expressed as

$$
A_t^\alpha = (1 + i)^{t-t_0} O_t^\alpha, \qquad t = -n, \ldots, -1, 0. \tag{1.4.6}
$$

The solution of the LCOE for a specific technology α (i.e. P_{LC}^α) can be obtained simply by following the steps outlined below:

(a.) Substituting T_t^α, which is in Equation (1.4.3) into Equation (1.4.1), we obtain

$$
\begin{aligned}
\sum_{t=0}^{N} \frac{P_{\mathrm{LC}}^\alpha Q_t^\alpha (1 + i)^{t-t_0}}{(1 + r_w)^t} &= \sum_{t=0}^{N} \frac{C_t^\alpha + T_c(R_t^\alpha - C_t^\alpha - D_t^\alpha)}{(1 + r_w)^t} + I_0^\alpha, \\
&= \sum_{t=0}^{N} \frac{C_t^\alpha (1 - T_c) + T_c(R_t^\alpha) - T_c(D_t^\alpha))}{(1 + r_w)^t} + I_0^\alpha, \\
\sum_{t=0}^{N} \frac{P_{\mathrm{LC}}^\alpha Q_t^\alpha (1 + i)^{t-t_0} - T_c(R_t^\alpha)}{(1 + r_w)^t} &= \sum_{t=0}^{N} \frac{C_t^\alpha (1 - T_c) - T_c(D_t^\alpha)}{(1 + r_w)^t} + I_0^\alpha. \quad (1.4.7)
\end{aligned}
$$

(b.) Substituting Equation (1.4.4) into Equation (1.4.7) gives,

$$
\begin{aligned}
\sum_{t=0}^{N} \frac{P_{\mathrm{LC}}^\alpha Q_t^\alpha (1 + i)^{t-t_0} - T_c(P_{\mathrm{LC}}^\alpha \times Q_t^\alpha (1 + i)^{t-t_0})}{(1 + r_w)^t} &= \sum_{t=0}^{N} \frac{C_t^\alpha (1 - T_c) - T_c(D_t^\alpha)}{(1 + r_w)^t} + I_0^\alpha, \\
\sum_{t=0}^{N} \frac{P_{\mathrm{LC}}^\alpha Q_t^\alpha (1 + i)^{t-t_0}(1 - T_c)}{(1 + r_w)^t} &= \sum_{t=0}^{N} \frac{C_t^\alpha (1 - T_c) - T_c(D_t^\alpha)}{(1 + r_w)^t} + I_0^\alpha,
\end{aligned}
$$

(c.) Simplify by substituting $F_{0,t} = \frac{1}{(1+r_w)^t}$ into the equations above,

$$
\begin{aligned}
P_{\mathrm{LC}}^\alpha (1 - T_c) \sum_{t=0}^{N} Q_t^\alpha (1 + i)^{t-t_0} F_{0,t} &= \sum_{t=0}^{N} (C_t^\alpha (1 - T_c) - T_c(D_t^\alpha)) F_{0,t} + I_0^\alpha, \\
P_{LC}^\alpha (1 - T_c) &= (1 - T_c) \frac{\sum_{t=0}^{N} C_t^\alpha F_{0,t}}{\sum_{t=0}^{N} Q_t^\alpha (1 + i)^{t-t_0} F_{0,t}} + \frac{I_0^\alpha - T_c \sum_{t=0}^{N} D_t^\alpha F_{0,t}}{\sum_{t=0}^{N} Q_t^\alpha (1 + i)^{t-t_0} F_{0,t}}.
\end{aligned}
$$

Therefore, P_{LC}^α is explicitly written as:

$$
P_{\mathrm{LC}}^\alpha = \frac{\sum_{t=0}^{N} C_t^\alpha F_{0,t}}{\sum_{t=0}^{N} Q_t^\alpha (1 + i)^{t-t_0} F_{0,t}} + \frac{I_0^\alpha - T_c \sum_{t=0}^{N} D_t^\alpha F_{0,t}}{(1 - T_c) \sum_{t=0}^{N} Q_t^\alpha (1 + i)^{t-t_0} F_{0,t}}. \tag{1.4.8}
$$

(d.) Equation (1.4.8) can be further simplified by defining

$$\hat{Q}^\alpha = \sum_{t=0}^{N} Q_t^\alpha (1+i)^{t-t_0} F_{0,t}, \qquad (1.4.9)$$

and by defining unitary costs as follows

$$\hat{C}^\alpha = \frac{\sum_{t=0}^{N} C_t^\alpha F_{0,t}}{\hat{Q}^\alpha}, \quad \hat{I}_0^\alpha = \frac{I_0^\alpha}{\hat{Q}^\alpha}, \quad \hat{D}^\alpha = \frac{\sum_{t=0}^{N} D_t^\alpha F_{0,t}}{\hat{Q}^\alpha}. \qquad (1.4.10)$$

Therefore, the LCOE for a specific technology α can be simply rewritten as

$$P_{\text{LC}}^\alpha = \hat{C}^\alpha + \frac{\hat{I}_0^\alpha - T_c \hat{D}^\alpha}{1 - T_c}. \qquad (1.4.11)$$

For the derivation of the LCOE of a multi-technology project or a portfolio of technologies, the total quantity of electricity production must be equal to the sum of production from each technology. That is,

$$\hat{Q}^\Sigma = \sum_\alpha \hat{Q}^\alpha, \qquad (1.4.12)$$

if the expected amount of electricity produced during each period is constant then, $Q^\Sigma = \sum_\alpha Q^\alpha$. The total LCOE for a portfolio of technology is derived from the assumption that the total expected revenues generated by the generation portfolio must be equal to the total expected cost. This implies that

$$
\begin{aligned}
\hat{Q}^\Sigma P_{\text{LC}}^\Sigma &= \sum_\alpha \hat{Q}^\alpha \hat{C}^\alpha + \sum_\alpha \hat{Q}^\alpha \left(\frac{\hat{I}_0^\alpha - T_c \hat{D}^\alpha}{1 - T_c} \right), \\
&= \sum_\alpha \hat{Q}^\alpha \left(\hat{C}^\alpha + \frac{\hat{I}_0^\alpha - T_c \hat{D}^\alpha}{1 - T_c} \right), \\
&= \sum_\alpha \hat{Q}^\alpha P_{\text{LC}}^\alpha.
\end{aligned}
$$

Consequently,

$$P_{\text{LC}}^\Sigma = \sum_\alpha \frac{\hat{Q}^\alpha}{\hat{Q}^\Sigma} P_{\text{LC}}^\alpha = \sum_\alpha w^\alpha P_{\text{LC}}^\alpha, \qquad (1.4.13)$$

where

$$w^\alpha = \frac{\hat{Q}^\alpha}{\hat{Q}^\Sigma} \qquad (1.4.14)$$

is the weight of technology α in the portfolio, which satisfies the condition $\sum_\alpha w^\alpha = 1$. Equation (1.4.13) implies that the total LCOE over portfolio of technologies (i.e. P_{LC}^Σ) is a linear combination of individual technologies LCOE weighted by the fraction of electricity generated by each technology.

12

1.5 Stochastic LCOE Model

The LCOE analysis developed in the previous section does not account for the stochasticity of LCOE. The portfolios of generating technologies in this research work include purely thermal technology mix portfolios (i.e., coal and gas technology mix), which satisfies the baseload demand of electricity, and integrated intermittent non-dispatchable energy sources (solar and wind energy). The unpredictability of fossil fuel prices as well as the uncertainty in the environmental policies, constitutes financial risk in a purely thermal technology portfolio. Thereby, making the purely thermal plant represent the risky asset in the portfolio, while the integration of renewable energy sources into the power system has the same diversification effect as a riskless asset in a portfolio. This helps to minimize the electricity price risk induced by the high volatility of fossil fuel and CO_2 market prices. Therefore the main sources of financial risk in this analysis are the dynamics of coal market prices, the dynamics of gas market prices, and the dynamics of CO_2 prices. Although, the geometric Brownian motion is sometimes used to model fossil fuel price dynamics, it should be noted that such a stochastic process may not capture completely the observed dynamics of market prices. Some evidence exists for more complicated behaviors showing mean reversion around some long run value, jumps and stochastic volatility [13]. The dynamics used for fossil fuel prices is a mean-reverting Levy model, as suggested in [24], which accurately describes the time evolution of the coal and gas prices. The dynamics of coal prices P_c is chosen to follow a mean-reverting stochastic differential equation, while the dynamics of gas price P_g is chosen to follow a mean-reverting jump-diffusion stochastic differential equation, due to the high volatility of gas prices which includes spikes, see for instance [16, 55]. The two equations are written as follows:

$$
\begin{aligned}
d\hat{P}_{\mathrm{co}} &= (\mu^{\mathrm{co}} - \theta^{\mathrm{co}}\hat{P}_{\mathrm{co}})dt + \sigma^{\mathrm{co}}dB_{\mathrm{co}}, & (1.5.1) \\
d\hat{P}_{\mathrm{ga}} &= (\mu^{\mathrm{ga}} - \theta^{\mathrm{ga}}\hat{P}_{\mathrm{ga}})dt + \sigma^{\mathrm{ga}}dB_{\mathrm{ga}} + J(\sigma_J)dN(\lambda), & (1.5.2)
\end{aligned}
$$

where $\hat{P}_{\mathrm{co}}$ and $\hat{P}_{\mathrm{ga}}$ are, respectively, the natural logarithm of coal and gas market prices; $\mu^{\mathrm{co}}, \theta^{\mathrm{co}}$ and $\mu^{\mathrm{ga}}, \theta^{\mathrm{ga}}$ are, respectively, the mean-reversion parameters of the logarithm of the coal and gas prices; σ^{co} and σ^{ga} are, respectively, the volatilities of coal and gas prices; B_{co} and B_{ga} are independent standard Brownian motions; J is the jump amplitude distributed as a normal random variable with zero mean and standard deviation σ_J; N is a Poisson process with constant jump intensity λ. The dynamical parameters are chosen according to the estimates reported in [25], obtained by discretizing the stochastic differential equations on a monthly time grid to give discrete time series that stimulate the fuel dynamics of coal and gas real price monthly time series from Jan. 1990 to Aug. 2013 in the US market.

The continuous model dynamics chosen for the CO_2 emission prices P_{em} is

	coal	gas
	$\mu^{\mathrm{co}} = 0.0000$	$\mu^{\mathrm{ga}} = 0.0373$
	$\theta^{\mathrm{co}} = 0.0000$	$\theta^{\mathrm{ga}} = 0.0292$
	$\sigma^{\mathrm{co}} = 0.0139$	$\sigma^{\mathrm{ga}} = 0.0737$
		$\sigma_J = 0.1258$
		$\lambda = 0.2542$

Table 1.1: Parameters of coal and gas stochastic price processes.

a simple geometric Brownian motion given by:

$$\frac{dP_{\mathrm{em}}}{P_{\mathrm{em}}} = \pi dt + \sigma^{\mathrm{em}} dB_{\mathrm{em}}, \tag{1.5.3}$$

where π is the natural logarithm of one plus the expected inflation rate, $\pi = \ln(1+i)$; σ^{em} is the CO_2 emission price volatility, and B_{em} is a standard Brownian motion that is assumed to be independent of B_{co} and B_{ga}.

Therefore, the classical LCOE P_{LC}^{α} becomes a stochastic variable $P_{\mathrm{LC}}^{\alpha}(\omega)$ due to a set of risky sources stochastic paths ω present in the cost term C_t^{α}. This implies that from Equation (1.4.11), the stochastic LCOE for a specific technology α can be defined by the following equation:

$$
\begin{aligned}
P_{\mathrm{LC}}^{\alpha}(\omega) &= \hat{C}^{\alpha}(\omega) + \frac{\hat{I}_0^{\alpha} - T_c \hat{D}^{\alpha}}{(1 - T_c)}, \\
P_{\mathrm{LC}}^{\alpha}(\omega) &= \hat{C}^{\alpha,\mathrm{var}}(\omega) + \hat{C}^{\alpha,\mathrm{fix}} + \frac{\hat{I}_0^{\alpha} - T_c \hat{D}^{\alpha}}{(1 - T_c)},
\end{aligned}
\tag{1.5.4}
$$

where $\hat{C}^{\alpha,\mathrm{var}}$ is denoted as the unitary variable cost which depends on the stochastic factors and $\hat{C}^{\alpha,\mathrm{fix}}$ is the unitary fixed cost of technology α, such that

$$\hat{C}^{\alpha} = \hat{C}^{\alpha,\mathrm{var}} + \hat{C}^{\alpha,\mathrm{fix}}.$$

1.6 Empirical Analysis

Technical data used in the empirical analysis are extracted from the "Annual Energy Outlook 2016" [10] as reported in the "Updated Capital Cost Estimates For Utility Scale Electricity Generating Plants" [11] provided by the United States Energy Information Administration. All technical data and costs included in the analysis are denominated in US dollars with 2016 as the base

year. Table (1.3) shows some important rates used in the empirical analysis. A nominal WACC of 7.9% is adopted, in agreement with the recent literature [27].

	Units	Coal	Gas
Techology symbol		co	ga
Nominal capacity	MW	650	702
Capacity factor		85%	87%
Heat rate	Btu/kWh	8800	6600
Overnight cost	$/kW	3636	978
Fixed O&M rate	$/kW/year	42.1	11.00
Variable O&M rate	mills/kWh	4.6	3.50
Fuel costs	$/mmBtu	2.42	3.91
CO_2 intensity	Kg-C/mmBtu	25.8	14.5
Fuel real escalation rate		0.3%	2.0%
Construction period	years	4	4
Operation start		2022	2022
Plant life	years	30	30
Depreciation scheme		MACRS,20	MACRS,15

Table 1.2: Technical data for LCOE Analysis.

All dollar amounts are in year 2016 dollars. Overnight costs are assumed to be uniformly distributed on the construction period. Depreciation is developed according to MACRS (Modified Accelerated Cost Recovery System) scheme described in Appendix A. O&M denotes operation and maintenance. Mills stands for 1/1000 of a dollar, while mmBtu denotes one million BTUs.

Inflation rate $(i) = 2.2\%$	Tax rate $(T_c) = 40\%$
WACC $= 7.9\%$	CO_2 emission volatility $(\sigma^{\mathrm{em}}) = 0.20$

Table 1.3: Important rates for LCOE analysis.

LCOE values for purely thermal technology project were computed using data from Table 1.2. They were computed through a Monte Carlo simulation techniques in Matlab. Different LCOE values of coal and gas were generated using a geometric Brownian motion as the dynamic model that described the prices of fossil fuels as done in previous literature. These values were compared with the LCOE values of coal and gas generated if the dynamics of the coal

	LCOE coal	LCOE gas
Mean	102.62	64.16
Standard Deviation	5.90	20.28
Skewness	1.07	2.64
Kurtosis	5.21	16.72

Table 1.4: Descriptive statistics of coal and gas LCOE when fossil fuel is modeled using Geometric Brownian Motion.

	LCOE coal	LCOE gas
Mean	102.53	63.84
Standard Deviation	3.73	6.72
Skewness	0.59	0.73
Kurtosis	3.64	4.9

Table 1.5: Descriptive statistics of coal and gas LCOE when fossil fuel is modeled using Mean-Reverting SDE model.

prices P_{co} was chosen to follow a mean-reverting stochastic differential equation and the dynamics of gas price P_{ga} was chosen to follow a mean-reverting jump-diffusion stochastic differential equation due to the high volatility of gas prices, which include spikes. The LCOE values generated with the different dynamic models is shown in Figure (1.1) and Figure (1.2). It is observed that the LCOE of gas in Figure (1.1) contains too many spikes. This implies that the underlying fossil fuel is extremely volatile and this seems to be unrealistic when compared with the historical data in Fig (1.3), which contains the logarithmic monthly changes of fossil fuel market prices in the United States from January 1990 to August 2013 [25]. Even though there exist spikes in the underlying fossil fuel for the gas power plant, a mean-reverting property also exist in the figure that contains the historical data due to the possibility of storage. Therefore Figure (1.2) seem to be more appropriate LCOE values with dynamic models that replicate fossil fuel prices shown in the historical data. Furthermore, comparing the descriptive statistics of the LCOE values shown in Table (1.4) and Table (1.5), even though the means of the LCOE of coal and gas are similar, the standard deviations are markedly different (5.90 against 3.73 for coal and 20.28 against 6.72 for gas respectively). The high value of volatility in the rise
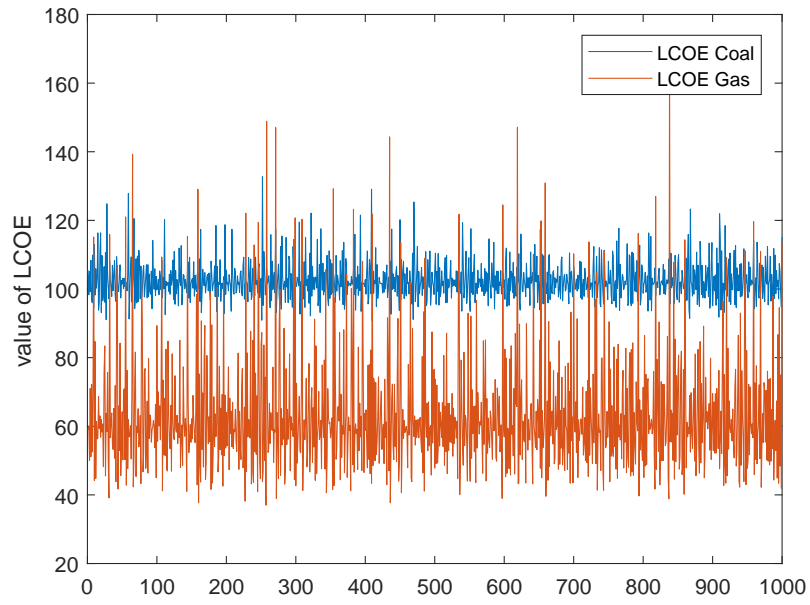
Figure 1.1: LCOE values of coal and gas when fossil fuel is modeled using Geometric Brownian Motion.
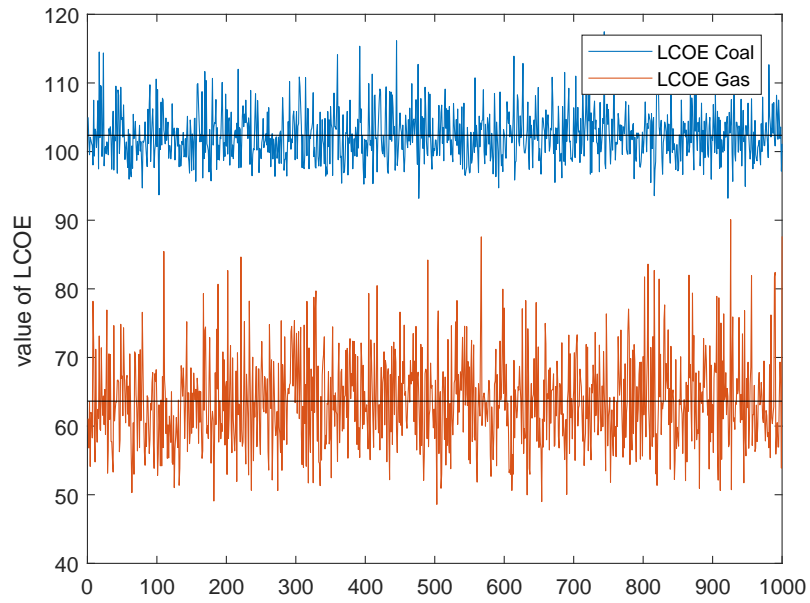
Figure 1.2: LCOE values of coal and gas when fossil fuel is modeled using Mean-Reverting Stochastic processes.
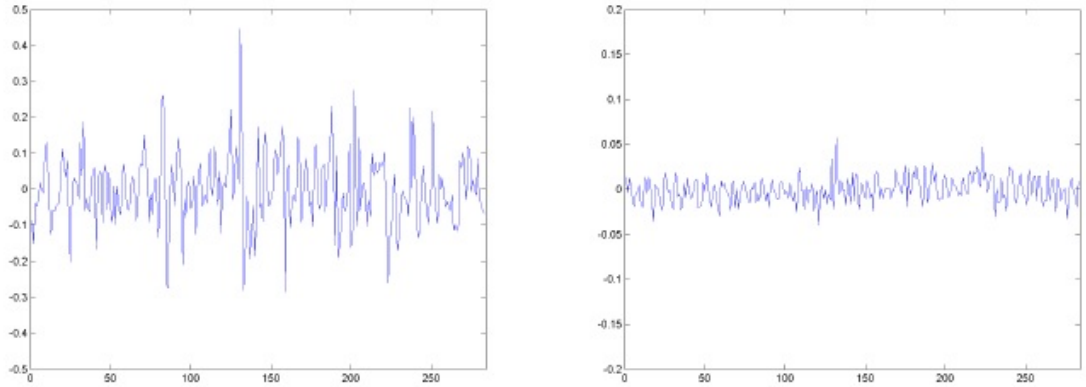
Figure 1.3: logarithmic monthly changes of fossil fuel market prices in the U.S. from January 1990 to August 2013 (gas left, coal right)

of geometric Brownian motion does not correspond to what is observed in the historical data of the underlying fossil fuel as shown in Fig (1.3). This may eventually affect the portfolio selection of the generation technology mix which minimizes the cost and the risk involved in electricity generation through individual generation technology. In addition to this, the skewness of 0.59 and 0.73 in Table (1.5) show that the LCOE distribution is positively skewed but closer to normal distribution than the values in Table (1.4) whose skewness is 1.07 and 2.64 for coal and gas LCOE respectively. Lastly, the kurtosis in Table (1.5) signal fat tails since its values are above 3.0, which is the kurtosis for a normal distribution. On the other hand, the values in Table (1.4) contains too many outliers especially for gas LCOE with kurtosis of 16.72. These observations justify the reasons for choosing mean-reverting Levy models for the modeling of the fossil fuel of coal and gas technology in our LCOE analysis.

1.7 Conclusion

LCOE theory was introduced. Background studies were reviewed and the deterministic LCOE model formulation was shown analytically. A stochastic form of the LCOE model due to the uncertainty in the fossil fuel prices and CO_2 emission prices was also reviewed. Modeling of coal and gas prices was done through mean-reverting stochastic differential equation and mean-reverting jump-diffusion stochastic differential equation, respectively, as an improvement on previous fossil fuel modeling with the geometric Brownian motion. The empirical analysis showed that, despite the similarity of LCOE mean, the LCOE volatilities of coal and gas when fossil fuel is modeled with geometric

Brownian motion tended to be too high when compared to historical data. Mean-reverting modeling of fossil fuel prices replicated better the historical data, which makes it more realistic to be used for our analysis.

Chapter 2

Systemic LCOE Theory

2.1   Introduction

In this chapter, two main issues are addressed: Firstly, Systemic LCOE with time-invariant pricing, that is, cost variation due to systemic constraints is introduced into the computation of LCOE in a system whose pricing does not depend explicitly on time; Secondly, a time-varying pricing schedule due to time of day fluctuations and seasonal cycles of the renewable energy sources integrated into the power system is introduced into the Systemic LCOE theory, that is, in addition to the cost variation due to systemic constraints, a multiplicative correction factor which captures any interaction and/or relationship between the time-varying patterns of electricity generation and pricing, is appended to the LCOE computation. These are analyzed under stochastic framework.

2.2   Systemic LCOE Theory with Time-Invariant Pricing

A portfolio of energy generation technologies is said to be technically feasible if the the power capacity and energy demanded at each hour of the year is balanced. That is, if the portfolio of energy generation technology matches the yearly load duration curve. The purely thermal technology portfolio, which satisfies the baseload demand of electricity, is assumed to be technically feasible in this research work. This technically feasible set consists of single fuel portfolio such as coal only generation portfolio or gas only generation portfolio and mixed portfolio including both dispatchable technologies, coal and gas. The power system of all these individual portfolio matches the yearly load duration curve but they differ in terms of their cost of energy generation and financial risks. This shall be discussed in details later.

Due to the intermittency of solar and wind energy, two major issues need

to be considered when evaluating their inclusion as renewable energy sources into a feasible portfolio: Firstly, when solar and wind energy is generated and injected into the grid, energy generated from purely thermal technologies must be reduced of the same quantity in order to have a balanced demand/supply due to the high cost of energy storage. Secondly, the inclusion of the solar and wind power capacity component in a generation portfolio may not be completely equivalent to the power capacity of the dispatchable energy, since wind might not blow during peak hours which is often late afternoons in summer, when the demand for air-conditioning places utility systems under greatest stress. Also, Sun might not shine on cloudy days which mostly occurs during winter. Therefore, in order to have a balance on the expected power capacity demanded, some backup dispatchable power capacity needs to be maintained. The capacity value quantifies how much of dispatchable power generation capacity the solar and wind power sources can replace in a given portfolio. Capacity value of zero is adopted by most conservative operators of intermittent sources such as wind plants [50]. The inclusion of solar and wind power into the feasible generation portfolio increases the portfolio cost due to high construction cost of wind turbine onshore or offshore and solar PV (even though the cost has considerably fallen due to advancement in technology). On the other hand, such an inclusion reduces the total cost of the feasible portfolios because of the energy and capacity reduction.

2.2.1   Cost Effect of Energy and Capacity Reduction

Suppose the index α denotes the dispatchable technologies which contains coal and gas, i.e., $\alpha = \mathrm{co}, \mathrm{ga}$. After the inclusion of the non-dispatchable technology, the energy generation reduction imposed on the technically feasible portfolio α in one year is given by

$$Q^{\alpha,\mathrm{red}} = \gamma^{\alpha} Q^{\beta}, \tag{2.2.1}$$

where $\gamma^{\mathrm{co}} + \gamma^{\mathrm{ga}} = 1$, such that $0 \leq \gamma^{\alpha} \leq 1$; the parameter Q^{β} denotes the yearly power production from non-dispatchable technology, where $\beta = \mathrm{wi}, \mathrm{so}$. This can be simplified as $Q^{\beta} = Q^{\mathrm{wi},\mathrm{so}} = Q^{\mathrm{wi}} + Q^{\mathrm{so}}$, where Q^{wi} represents the yearly wind power production and Q^{so} is the yearly solar power production. The maximum energy reducible is equivalent to the amount of energy generated by non-dispatchable technology integrated into the power system, since $0 \leq Q^{\alpha,\mathrm{red}} \leq Q^{\beta}$.

The yearly capacity reduction is deduced from the yearly avoided energy generation due to the substitution of dispatchable capacity with solar and wind capacity. This will be denoted by

$$Q^{\alpha,\mathrm{av}} = W^{\alpha,\mathrm{av}} \times 8760 \times CF^{\alpha}, \tag{2.2.2}$$

where $W^{\alpha,\mathrm{av}}$ is the nameplate capacity reduction of the dispatchable technology α, i.e., avoided (av); CF^{α} denotes the capacity factor of the technology α for

8760 hours (i.e., one calendar year).

2.2.2 Integration of One Renewable Power Source

The total present value of the augmented feasible portfolio with the inclusion of the solar and wind component is evaluated based on the systemic constraints. This is given by:

$$
\begin{aligned}
\hat{Q}^{\Sigma} P_{LC}^{\Sigma} = & \left(\sum_{\alpha} \hat{Q}^{f,\alpha} P_{\text{LC}}^{\alpha} + \hat{Q}^{\text{wi}} P_{\text{LC}}^{\text{wi}} + \hat{Q}^{\text{so}} P_{\text{LC}}^{\text{so}} \right) \\
& - \left(\hat{Q}^{\text{wi}} + \hat{Q}^{\text{so}} \right) \sum_{\alpha} \gamma^{\alpha} \hat{C}^{\alpha,\text{var}} - \sum_{\alpha} \hat{Q}^{\alpha,\text{av}} \left(\hat{C}^{\alpha,\text{fix}} + \frac{\hat{I}_0^{\alpha} - T_c \hat{D}^{\alpha}}{1 - T_c} \right).
\end{aligned}
$$
$$(2.2.3)$$

In Equation (2.2.3), $\hat{Q}^{\Sigma} = \hat{Q}^{f,\text{co}} + \hat{Q}^{f,\text{ga}}$ denotes the technically feasible portfolio which consist of the dispatchable technologies; $\sum_{\alpha} \hat{Q}^{f,\alpha} P_{LC}^{\alpha}$ is the total cost of the feasible portfolio; $P_{\text{LC}}^{\text{wi}}$ and $P_{\text{LC}}^{\text{so}}$ are the LCOE of 'bare' wind and solar technologies respectively such that,

$$
P_{\text{LC}}^{\text{wi}} = \hat{C}^{\text{wi}} + \frac{\hat{I}_0^{\text{wi}} - T_c \hat{D}^{\text{wi}}}{1 - T_c}, \qquad P_{\text{LC}}^{\text{so}} = \hat{C}^{\text{so}} + \frac{\hat{I}_0^{\text{so}} - T_c \hat{D}^{\text{so}}}{1 - T_c}, \qquad (2.2.4)
$$

that is, without consideration of the systemic interactions due to the inclusion of the solar and wind technology into a technically feasible portfolio.

In order to evaluate the consistent LCOE for solar ($P_{\text{LC}}^{\text{so}*}$) and wind ($P_{\text{LC}}^{\text{wi}*}$) power that properly accounts for the extra cost imposed on the power system, we shall evaluate further the total cost of the augmented portfolio which can be expressed as:

$$
\hat{Q}^{\Sigma} P_{\text{LC}}^{\Sigma} = \sum_{\alpha} \left(\hat{Q}^{f,\alpha} - \gamma^{\alpha} \hat{Q}^{\beta} \right) P_{\text{LC}}^{\alpha} + \hat{Q}^{\beta} P_{\text{LC}}^{\beta*}. \qquad (2.2.5)
$$

In the absence of solar power, that is $Q^{\text{so}} = 0$, we have $Q^{\beta} = Q^{\text{wi}}$. By equating Equations (2.2.3) and (2.2.5), the LCOE of wind power is evaluated as:

$$
P_{\text{LC}}^{\text{wi}*} = P_{\text{LC}}^{\text{wi}} + \sum_{\alpha} \gamma^{\alpha} P_{\text{LC}}^{\alpha} - \sum_{\alpha} \gamma^{\alpha} \hat{C}^{\alpha,\text{var}} - \sum_{\alpha} \frac{Q^{\alpha,\text{av}}}{Q^{\text{wi}}} \left(\hat{C}^{\alpha,\text{fix}} + \frac{\hat{I}_0^{\alpha} - T_c \hat{D}^{\alpha}}{1 - T_c} \right).
$$
$$(2.2.6)$$

This is expressed as a sum of the 'bare' wind LCOE and the cost of the interaction of the wind component with the technically feasible portfolio and it is equivalent to the results from previous literature [27]. The wind LCOE can be expressed in terms of fixed cost only, by substituting the value of P_{LC}^{α} into

the second term of Equation (2.2.6) with $\hat{C}^\alpha = \hat{C}^{\alpha,\text{var}} + \hat{C}^{\alpha,\text{fix}}$. The equation obtained is:

$$P_{\text{LC}}^{\text{wi}*} = P_{\text{LC}}^{\text{wi}} + \sum_\alpha \left(\gamma^\alpha - \frac{Q^{\alpha,\text{av}}}{Q^{\text{wi}}} \right) \left(\hat{C}^{\alpha,\text{fix}} + \frac{\hat{I}_0^\alpha - T_c \hat{D}^\alpha}{1 - T_c} \right). \tag{2.2.7}$$

Equation (2.2.7) implies that the extra cost on the wind LCOE depends on the mix technologies used to reduce both the electricity generation and the power capacity from the feasible portfolio. Similarly, in the absence of wind power, that is $Q^{\text{wi}} = 0$, we have $Q^\beta = Q^{\text{so}}$. Therefore evaluating from Equations (2.2.3) and (2.2.5), the LCOE of solar power is given as:

$$P_{\text{LC}}^{\text{so}*} = P_{\text{LC}}^{\text{so}} + \sum_\alpha \left(\gamma^\alpha - \frac{Q^{\alpha,\text{av}}}{Q^{\text{so}}} \right) \left(\hat{C}^{\alpha,\text{fix}} + \frac{\hat{I}_0^\alpha - T_c \hat{D}^\alpha}{1 - T_c} \right), \tag{2.2.8}$$

which is the addition of the 'bare' solar LCOE to the cost of interaction of the solar component with the technically feasible portfolio. It must be noted that the ratio

$$\frac{\hat{Q}^{\alpha,\text{av}}}{\hat{Q}^{\text{wi}}} = \frac{Q^{\alpha,\text{av}}}{Q^{\text{wi}}}$$

in Equation (2.2.6) because the yearly electricity production by each technology is assumed constant over time under this section.

Capacity values of solar and wind power can be included in their LCOE analysis in Equations (2.2.7) and (2.2.8) by solving the fraction

$$\frac{Q^{\alpha,\text{av}}}{Q^\beta} \tag{2.2.9}$$

in terms of the capacity value and substituting the solution into the equations. Firstly, suppose $w^{f,\text{ga}}$ and $w^{f,\text{co}}$ denotes the composition of a technically feasible generation portfolio, such that $w^{f,\text{ga}} + w^{f,\text{co}} = 1$. Let

$$w^\beta = \frac{Q^\beta}{Q^\Sigma}, \tag{2.2.10}$$

denote portfolio of wind or solar penetration ($\beta = \text{so, wi}$). It can be assumed that the electricity reduction from fossil fuel generation is proportional to the share of single fuel electricity generated by the technically feasible portfolio, so that

$$\gamma^\alpha = w^{f,\alpha}, \tag{2.2.11}$$

and the capacity reduction of technology α is proportional to the share of power capacity of technology α in the technically feasible portfolio such that,

$$W^{\alpha,\text{av}} = c_v W^\alpha, \tag{2.2.12}$$

23

where c_v is defined as the capacity value of the power system. Under the assumptions above,

$$
\begin{aligned}
\frac{Q^{\alpha,\mathrm{av}}}{Q^{\beta}} &= \frac{W^{\alpha,\mathrm{av}} \times 8760 \times CF^{\alpha}}{w^{\beta} \times Q^{\Sigma}}, \\
&= \frac{c_v W^{\alpha} \times 8760 \times CF^{\alpha}}{w^{\beta} \times Q^{\Sigma}}, \\
&= \frac{c_v Q^{\alpha}}{w^{\beta} \times Q^{\Sigma}}, \\
&= \frac{c_v w^{f,\alpha}}{w^{\beta}}.
\end{aligned}
\tag{2.2.13}
$$

Substituting Equations (2.2.13) into Equations (2.2.7) and (2.2.8) enables us to analyze the solar and wind LCOE using their capacity values. The wind LCOE in the absence of solar power becomes:

$$
P_{\mathrm{LC}}^{\mathrm{wi}*} = P_{\mathrm{LC}}^{\mathrm{wi}} + \sum_{\alpha} w^{f,\alpha} \left(1 - \frac{c_v}{w^{wi}}\right) \left(\hat{C}^{\alpha,\mathrm{fix}} + \frac{\hat{I}_0^{\alpha} - T_c \hat{D}^{\alpha}}{1 - T_c}\right).
\tag{2.2.14}
$$

Similarly, the solar LCOE in the absence of wind power becomes:

$$
P_{\mathrm{LC}}^{\mathrm{so}*} = P_{\mathrm{LC}}^{\mathrm{so}} + \sum_{\alpha} w^{f,\alpha} \left(1 - \frac{c_v}{w^{so}}\right) \left(\hat{C}^{\alpha,\mathrm{fix}} + \frac{\hat{I}_0^{\alpha} - T_c \hat{D}^{\alpha}}{1 - T_c}\right).
\tag{2.2.15}
$$

2.2.3 Integration of Two Renewable Power Sources

In this section, an evaluation of the solar LCOE in the presence of wind power will be shown. The vice-versa follows a similar argument. The evaluation of the solar LCOE when integrated into the systemic portfolio, which contains the technically feasible portfolio plus a wind component, is done by rewriting Equations (2.2.5) as:

$$
\hat{Q}^{\Sigma} P_{\mathrm{LC}}^{\Sigma} = \sum_{\alpha} \left(\hat{Q}^{f,\alpha} - \gamma^{\alpha}(\hat{Q}^{\mathrm{wi}} + \hat{Q}^{\mathrm{so}})\right) P_{\mathrm{LC}}^{\alpha} + \hat{Q}^{\mathrm{so}} P_{\mathrm{LC}}^{\mathrm{so}*} + \hat{Q}^{\mathrm{wi}} P_{\mathrm{LC}}^{\mathrm{wi}*}.
\tag{2.2.16}
$$

From Equation (2.2.3) and (2.2.16), we can deduce that the solar LCOE in the presence of wind power is given by:

$$
\begin{aligned}
P_{\mathrm{LC}}^{\mathrm{so}*} &= P_{\mathrm{LC}}^{\mathrm{so}} + \sum_{\alpha} \gamma^{\alpha} P_{\mathrm{LC}}^{\alpha} - \sum_{\alpha} \gamma^{\alpha} \hat{C}^{\alpha,\mathrm{var}} - \sum_{\alpha} \frac{Q^{\alpha,\mathrm{av}}}{Q^{\mathrm{so}}} \left(\hat{C}^{\alpha,\mathrm{fix}} + \frac{\hat{I}_0^{\alpha} - T_c \hat{D}^{\alpha}}{(1 - T_c)}\right) \\
&\quad - \frac{Q^{\mathrm{wi}}}{Q^{\mathrm{so}}} \left(P_{\mathrm{LC}}^{\mathrm{wi}*} - P_{\mathrm{LC}}^{\mathrm{wi}} - \sum_{\alpha} \gamma^{\alpha} P_{\mathrm{LC}}^{\alpha} + \sum_{\alpha} \gamma^{\alpha} \hat{C}^{\alpha,\mathrm{var}}\right)
\end{aligned}
\tag{2.2.17}
$$

The last term of Equation (2.2.17) can be simplified from Equation (2.2.6). This is substituted into Equation (2.2.17) to obtain:

$$
\begin{aligned}
P_{\text{LC}}^{\text{so*}} \;=\;& P_{\text{LC}}^{\text{so}} + \sum_{\alpha} \gamma^{\alpha} P_{\text{LC}}^{\alpha} - \sum_{\alpha} \gamma^{\alpha} \hat{C}^{\alpha,\text{var}} - \sum_{\alpha} \frac{Q^{\alpha,\text{av}}}{Q^{\text{so}}} \left(\hat{C}^{\alpha,\text{fix}} + \frac{\hat{I}_0^{\alpha} - T_c \hat{D}^{\alpha}}{1 - T_c} \right) \\
& - \frac{Q^{\text{wi}}}{Q^{\text{so}}} \left[-\sum_{\alpha} \frac{Q^{\alpha,\text{av}}}{Q^{\text{wi}}} \left(\hat{C}^{\alpha,\text{fix}} + \frac{\hat{I}_0^{\alpha} - T_c \hat{D}^{\alpha}}{1 - T_c} \right) \right].
\end{aligned}
\tag{2.2.18}
$$

Therefore, the solar LCOE, which is expressed as a sum of 'bare' solar LCOE plus the cost of the interaction of the solar component with the technically feasible portfolio in the presence of wind power is given by:

$$
P_{\text{LC}}^{\text{so*}} = P_{\text{LC}}^{\text{so}} + \sum_{\alpha} \gamma^{\alpha} P_{\text{LC}}^{\alpha} - \sum_{\alpha} \gamma^{\alpha} \hat{C}^{\alpha,\text{var}}.
\tag{2.2.19}
$$

The solar LCOE can be expressed in terms of fixed cost only, by substituting the value of P_{LC}^{α} into the second term of Equation (2.2.19) with $\hat{C}^{\alpha} = \hat{C}^{\alpha,\text{var}} + \hat{C}^{\alpha,\text{fix}}$ and $\gamma^{\alpha} = w^{f,\alpha}$. The equation obtained is:

$$
P_{\text{LC}}^{\text{so*}} = P_{\text{LC}}^{\text{so}} + \sum_{\alpha} w^{f,\alpha} \left(\hat{C}^{\alpha,\text{fix}} + \frac{\hat{I}_0^{\alpha} - T_c \hat{D}^{\alpha}}{1 - T_c} \right).
\tag{2.2.20}
$$

Equation (2.2.20) implies that the extra cost addition to the 'bare' solar LCOE depends on the mix technologies used to reduce the electricity generation only but in this case does not include power capacity reduction. The LCOE of wind can be similarly evaluated after solar inclusion into a dispatchable resource based power system.

Furthermore, the systemic LCOE of a generation portfolio that includes intermittent sources can be defined from Equation (2.2.16). This is given by:

$$
P_{\text{LC}}^{\text{sys}} = \sum_{\alpha} \left(\frac{Q^{f,\alpha} - \gamma^{\alpha}(Q^{\text{wi}} + Q^{\text{so}})}{Q^{\Sigma}} \right) P_{\text{LC}}^{\alpha} + \frac{Q^{\text{so}}}{Q^{\Sigma}} P_{\text{LC}}^{\text{so*}} + \frac{Q^{\text{wi}}}{Q^{\Sigma}} P_{\text{LC}}^{\text{wi*}}.
\tag{2.2.21}
$$

This implies that the systemic portfolio LCOE can be expressed as a linear combination of single technology LCOEs

$$
P_{\text{LC}}^{\text{sys}} = w^{\text{co}} P_{\text{LC}}^{\text{co}} + w^{\text{ga}} P_{\text{LC}}^{\text{ga}} + w^{\text{wi}} P_{\text{LC}}^{\text{wi*}} + w^{\text{so}} P_{\text{LC}}^{\text{so*}},
\tag{2.2.22}
$$

with portfolio weights defined as follows:

$$w^{\text{co}} = \frac{Q^{f,\text{co}} - \gamma^{\text{co}}\left(Q^{\text{wi}} + Q^{\text{so}}\right)}{Q^{\Sigma}},$$

$$w^{\text{ga}} = \frac{Q^{f,\text{ga}} - \gamma^{\text{ga}}\left(Q^{\text{wi}} + Q^{\text{so}}\right)}{\hat{Q}^{\Sigma}},$$

$$w^{\text{wi}} = \frac{Q^{\text{wi}}}{Q^{\Sigma}},$$

$$w^{\text{so}} = \frac{Q^{\text{so}}}{Q^{\Sigma}}.$$

The portfolio weight sums to one, since it was stated earlier that the portfolio weights of the dispatchable technology given by $\gamma^{\text{co}} + \gamma^{\text{ga}} = 1$. Therefore,

$$w^{\text{co}} + w^{\text{ga}} + w^{\text{wi}} + w^{\text{so}} = 1. \tag{2.2.23}$$

It must be noted that the systemic LCOE equation expressed in Equation (2.2.21) reduces to the corresponding technically feasible portfolio if there is no integration of the intermittent energy into the power grid. That is, when $Q^{\text{wi}} = Q^{\text{so}} = 0$ in Equation (2.2.21), systemic LCOE equation will be equal to the technically feasible portfolio which contains the purely thermal mix technology.

In the stochastic framework, as stated earlier, the unpredictability of fossil fuel prices and the uncertainty in the environmental policies constitute financial risk in a purely thermal technology portfolio, thereby making the purely thermal plant represent the risky asset in the portfolio, while integration of renewable energy into the power system has the same diversification effect as a riskless asset in a portfolio. Therefore, the LCOE P^{α}_{LC} becomes a time-independent stochastic variable $P^{\alpha}_{\text{LC}}(\omega)$ due to a set of risky sources stochastic paths ω present in the cost term. Following the same line of argument, the stochastic form of the systemic LCOE of a generation portfolio with the integration of solar and wind power can be expressed as follows,

$$P^{\text{sys}}_{\text{LC}}(\omega) = \sum_{\alpha} \left(\frac{Q^{f,\alpha} - \gamma^{\alpha}\left(Q^{\text{wi}} + Q^{\text{so}}\right)}{Q^{\Sigma}} \right) P^{\alpha}_{\text{LC}}(\omega) + \frac{Q^{\text{so}}}{Q^{\Sigma}} P^{\text{so}*}_{\text{LC}} + \frac{Q^{\text{wi}}}{Q^{\Sigma}} P^{\text{wi}*}_{\text{LC}}. \tag{2.2.24}$$

This also implies that the stochastic systemic portfolio can be expressed as a linear combination of single technology LCOEs

$$P^{\text{sys}}_{\text{LC}}(\omega) = w^{\text{co}} P^{\text{co}}_{\text{LC}}(\omega) + w^{\text{ga}} P^{\text{ga}}_{\text{LC}}(\omega) + w^{\text{wi}} P^{\text{wi}*}_{\text{LC}} + w^{\text{so}} P^{\text{so}*}_{\text{LC}}. \tag{2.2.25}$$

The portfolio weights is the same as the deterministic case since it is a constant, with all the weights summing up to one as in Equation (2.2.23).

	Units	Coal	Gas	Wind	Solar PV
Techology symbol		co	ga	wi	so
Nominal capacity	MW	650	702	100	20
Capacity factor		85%	87%	42%	33%
Heat rate	Btu/kWh	8800	6600	0	0
Overnight cost	$/kW	3636	978	1877	2671
Fixed O&M rate	$/kW/year	42.1	11.00	39.7	23.4
Variable O&M rate	mills/kWh	4.6	3.50	0	0
Fuel Costs	$/mmBtu	2.42	3.91	0	0
CO_2 intensity	Kg-C/mmBtu	25.8	14.5	0	0
Fuel real escalation rate		0.3%	2.0%	0%	0%
Construction period	years	4	4	3	3
Operation start		2022	2022	2022	2022
Plant life	years	30	30	30	30
Depreciation scheme		MACRS,20	MACRS,15	MACRS,20	MACRS,20

Table 2.1: Extended Technical data for LCOE Analysis.

All dollar amounts are in year 2016 dollars. Overnight costs are assumed to be uniformly distributed on the construction period. Depreciation is developed according to MACRS (Modified Accelerated Cost Recovery System) scheme described in Appendix A. O&M denotes operation and maintenance. Mills stands for 1/1000 of a dollar, while mmBtu denotes one million BTUs.

2.2.4 Empirical Analysis

Table (2.1) is the extension of Table (1.2). The Table (1.2) is updated with technical data of solar and wind power extracted from the "Annual Energy Outlook 2016" [10] as reported in "Updated Capital Cost Estimates For Utility Scale Electricity Generating Plants" [11] provided by the United State Energy Information Administration. All technical data and cost included in the analysis are denominated in US dollars with 2016 as the base year. The following assumptions were made in accordance to the Annual Energy Outlook 2016 [10]; expected inflation rate = 2.2% per annum and tax rate $T_c = 40\%$. A nominal WACC rate of 7.9% is adopted, this is in agreement with most studies proposed in recent literatures [27]. LCOE values for single-technology project is first computed using data from Table (2.1). The result is shown in Table (2.2). It must be noted that the LCOE values of solar and wind shown in Table (2.2) is the 'bare' wind and solar technology without considering the cost of integration.

The values of LCOE of solar (P_{LC}^{so*}) and wind (P_{LC}^{wi*}) can be analyzed using their capacity values in a single asset integration. This can be done under three scenarios. Firstly, when there is full energy and capacity reduction from the

	LCOE coal	LCOE gas	LCOE solar	LCOE wind
	102.53	63.84	99.70	56.79

Table 2.2: LCOE values.

Capacity value	Coal reduction	Gas reduction	Mixed reduction		
c_v	$\text{co}^{1.0}$	$\text{ga}^{1.0}$	$\text{co}^{0.25}\,\text{ga}^{0.75}$	$\text{co}^{0.5}\,\text{ga}^{0.5}$	$\text{co}^{0.75}\,\text{ga}^{0.25}$
0%	154.38	113.55	123.76	133.97	144.17
5%	145.27	111.24	119.75	128.25	136.76
10%	136.16	108.93	115.74	122.55	129.35
15%	127.04	106.63	111.73	116.83	121.93
20%	117.93	104.32	107.72	111.12	114.52

Table 2.3: Value of solar LCOE ($P_{\text{LC}}^{\text{so}*}$) at different scenarios of energy and capacity reduction with a 30% solar penetration.

gas component of the feasible portfolio, this scenario is termed 'gas reduction' ($\text{ga}^{1.0}$). That is, $\gamma^{\text{ga}} = 1$. This implies that $\gamma^{\text{co}} = 0$, since $\gamma^{\text{co}} + \gamma^{\text{ga}} = 1$. Also, the power capacity avoided of the coal energy $W^{\text{av,co}} = 0$, therefore, $W^{\text{av,ga}} = c_v W^{\text{ga}}$. The term c_v denotes the capacity value of the renewable source integrated into the power grid. Secondly, when there is full energy and capacity reduction from the coal component of the feasible portfolio, this scenario is termed 'coal reduction' ($\text{co}^{1.0}$). That is, $\gamma^{\text{co}} = 1$. This implies that $\gamma^{\text{ga}} = 0$. Also, the power capacity avoided from the gas energy $W^{\text{av,ga}} = 0$, therefore, $W^{av,\text{co}} = c_v W^{\text{co}}$. The third scenario is when there is a mixed reduction of energy and capacity from the coal and gas component, this scenario is termed 'mixed reduction'. In the literature [27], under the mixed reduction scenario, the case $\gamma^{\text{ga}} = 0.5$ and $\gamma^{\text{co}} = 0.5$ was considered. In this case, the power capacity avoided from the coal component is $W^{\text{av,co}} = c_v W^{\text{co}}$ and for the gas component, it is $W^{\text{av,ga}} = c_v W^{\text{ga}}$. The scenario is extended in this thesis to other proportions of the mixture of energy and capacity reduction (see Table (2.3) and Table (2.4)). For each integration scenario, five capacity values are chosen as done in the literature. These cases are $0\%, 5\%, 10\%, 15\%, 20\%$. Solar and wind penetration shares of 30% and 40% are assumed in agreement with the US planned targets as reported in 'Renewable Electricity Futures Study' published by the National Renewable Energy Laboratory [34]. It can be observed from Table (2.3) and Table (2.4) that the higher the capacity value, that is, the higher the percentage of reliability of solar or wind power to meet demand, the lower the value of solar and wind LCOE. Consequently, the LCOE for all the scenarios considered were at their lowest when capacity value was 20%. Furthermore, the proportion of

Capacity value	Coal reduction	Gas reduction	Mixed reduction		
c_v	$\mathrm{co}^{1.0}$	$\mathrm{ga}^{1.0}$	$\mathrm{co}^{0.25}\,\mathrm{ga}^{0.75}$	$\mathrm{co}^{0.5}\,\mathrm{ga}^{0.5}$	$\mathrm{co}^{0.75}\,\mathrm{ga}^{0.25}$
0%	111.48	70.65	80.86	91.06	101.27
5%	102.37	68.34	76.85	85.35	93.86
10%	93.25	66.03	72.84	79.64	86.45
15%	84.14	63.72	68.83	73.93	79.04
20%	75.02	61.42	64.82	68.22	71.62

Table 2.4: Value of wind LCOE ($P_{\mathrm{LC}}^{\mathrm{wi}*}$) at different scenarios of energy and capacity reduction with a 30% wind penetration.

the coal and gas components also affects the values of LCOE. The higher the energy and capacity reduction from the gas components, the lower the LCOE. In particular, the lowest LCOE for solar and wind occurred when the full energy and capacity reduction was only from the gas component (i.e., $\mathrm{ga}^{1.0}$). Therefore, from Table (2.3) and Table (2.4), the lowest values of both solar and wind LCOE is 104.32 and 61.42 respectively. These LCOE values occurred at the capacity value of 20% when the full energy and power reduction was from the gas component. Subtracting the 'bare' solar and wind LCOE values generated in Table (2.2) from the LCOE in Table (2.3) and Table (2.4) will result in the value of the extra cost of inclusion of the solar and wind power in the power grid. Considering the case of 40% solar and wind penetration in Table (2.5) and Table (2.6), the LCOE values of solar and wind increases slightly when compared to the values obtained in Table (2.3) and Table (2.4). It only remain constant when the capacity value is 0%. This implies that the higher the solar and wind penetration into the power grid, the higher their LCOE. This is generally due to the high cost of electricity generation from renewables.

Capacity value	Coal reduction	Gas reduction	Mixed reduction		
c_v	$\mathrm{co}^{1.0}$	$\mathrm{ga}^{1.0}$	$\mathrm{co}^{0.25}\,\mathrm{ga}^{0.75}$	$\mathrm{co}^{0.5}\,\mathrm{ga}^{0.5}$	$\mathrm{co}^{0.75}\,\mathrm{ga}^{0.25}$
0%	154.38	113.55	123.76	133.97	144.17
5%	147.55	111.88	120.75	129.68	138.61
10%	140.71	110.08	117.74	125.40	133.06
15%	133.87	108.36	114.73	121.12	127.50
20%	127.04	106.63	111.72	116.83	121.93

Table 2.5: Value of solar LCOE ($P_{\mathrm{LC}}^{\mathrm{so}*}$) at different scenarios of energy and capacity reduction with a 40% solar penetration.

The LCOE analysis of solar (wind) based on the integration of two renewable energy source is done based on Equation (2.2.20). The extra cost of inclusion

Capacity value	Coal reduction	Gas reduction	Mixed reduction		
c_v	$\text{co}^{1.0}$	$\text{ga}^{1.0}$	$\text{co}^{0.25}\ \text{ga}^{0.75}$	$\text{co}^{0.5}\ \text{ga}^{0.5}$	$\text{co}^{0.75}\ \text{ga}^{0.25}$
0%	111.48	70.65	80.86	91.06	101.27
5%	104.64	68.91	77.85	86.78	95.71
10%	97.81	67.19	74.84	82.49	90.16
15%	90.97	65.45	71.83	78.21	84.60
20%	84.14	63.72	68.82	73.93	79.04

Table 2.6: Value of wind LCOE ($P_{\text{LC}}^{\text{wi}*}$) at different scenarios of energy and capacity reduction with a 40% wind penetration.

of the solar (wind) power is only due to the energy reduction of the technically feasible portfolio. The result obtained for solar (wind) LCOE in the presence of wind (solar) power in a dispatchable resource-based power system is exactly the same given by the values in Table (2.3) and Table (2.4) when capacity values are 0%.

2.3 Systemic LCOE Theory with Time-Varying Pricing

In the previous section, the LCOE of a portfolio of mix technologies which includes dispatchable and non-dispatchable energy source was computed by considering the extra costs due to systemic constraints when intermittent energy sources are integrated into the power grid. This accounts for any effect due to the intermittency of solar and wind power on the power system. Nevertheless, the computation of the LCOE in the systemic LCOE framework was done based on the assumption that production and pricing of electricity did not depend explicitly on time. Solar and wind power are well known to exhibit considerable variation in their ability to generate power. These variations typically include both time of day fluctuations and seasonal cycles. If the investor faces a price schedule that varies by time of day and possibly by season, the systemic LCOE in the previous section will generally fail to capture all synergies that arise if the solar or wind power generates power above its overall average predominantly at times when electricity prices are relatively high or low. In the next section, the construction of a multiplicative correction factor called co-variation coefficient will be shown by revising the work of Reichelstein and Sahoo [41]. This will be used to append the systemic LCOE computation done earlier in this chapter. By construction, the base-load energy system, that is, the coal and gas power, have a co-variation coefficient of one. This is because they provide a continuous supply of electricity throughout the year without fluctuation with time of day

or seasonal cycle. Also, the co-variation coefficient will also be equal to one for an intermittent power source under a time-invariant pricing schedule.

2.3.1 Derivation of Co-variation Coefficient

The production capacity of solar and wind power is basically subject to significant intra-day and seasonal variations. On a given day i of a particular year, the actual capacity factor of the intermittent energy source can be defined by a function $CF_i(t)$, such that:

$$CF_i(t) = CF_i \times \epsilon_i(t) \qquad 0 \leq t \leq 24, \qquad (2.3.1)$$

where CF_i is the average capacity factor and $\epsilon_i(t) > 0$ represent the multiplicative deviation from the average capacity factor at time t. Accordingly,

$$\int_0^{24} \epsilon_i(t)dt = 24. \qquad (2.3.2)$$

Furthermore, the market value of the electricity produced in day i based on the intra-day variation can be introduced as follows. Suppose $p_i(t)$ denote the price of electricity at a particular hour of the day, such that:

$$p_i(t) = p_i \times \mu_i(t), \qquad (2.3.3)$$

where p_i is the average daily price of electricity and $\mu_i(t)$ is a multiplicative deviation from the average daily price of electricity at time t, such that:

$$\int_0^{24} \mu_i(t)dt = 24. \qquad (2.3.4)$$

The co-variation coefficient Γ_i between $CF_i(t)$ and $p_i(t)$ on a given day i is the measure of synergies or complementaries, in the intertemporal pattern of electricity generation and prices. It is given by:

$$\Gamma_i = \frac{1}{24} \int_0^{24} \epsilon_i(t)\mu_i(t)dt. \qquad (2.3.5)$$

In constructing the co-variation coefficient, it is assumed that electricity prices are non-negative. It will be equal to zero only in extreme cases when electricity is produced at times when the price is zero. The aggregate co-variation coefficient is defined as the average of the daily coefficient in a year:

$$\Gamma = \frac{1}{365} \sum_{i=1}^{365} \Gamma_i. \qquad (2.3.6)$$

The mean value of the $p(\cdot)$ is also given:

$$p = \frac{1}{365} \sum_{i=1}^{365} p_i.$$

An important proposition from [41] is stated below :

31

Proposition 1. *The intermittent power generation facility is cost competitive if and only if*

$$\Gamma \cdot p \geq P_{LC}^{\beta}, \tag{2.3.7}$$

where $\beta = $ so,wi and p is the mean value of price distribution $p(\cdot)$.

Proof. See Appendix of [41] $\qquad\qquad\qquad\qquad\qquad\qquad\qquad\qquad \square$

The term 'cost competitiveness' implies that for a renewable power generating facility with an annual price distribution, $p(\cdot)$, with mean value p, has a present value of all after-tax cash flows received or paid over the lifetime of the facility as non-negative. The proposition above shows that LCOE computation without putting into consideration the complementaries and synergies due to time-varying and pricing schedules needs to be appended by the co-variation coefficient. In addition to this, an inference from this proposition is that life-cycle cost of electricity generation improves if the intermittent energy source generates most of its output during the peak price periods. This is common with solar power which generates electricity at its peak during hot days when the price is very high due to the use of air conditioner.

Introducing the covariance of $\epsilon_i(\cdot)$ and $\mu_i(\cdot)$ is necessary in order to understand the relationship between the output of electricity and the pricing for a particular day i. The covariance is given by:

$$
\begin{aligned}
\text{cov}\left(\epsilon_i(\cdot), \mu_i(.)\right) &= \frac{1}{24} \int_0^{24} (\epsilon_i(t) - 1)(\mu_i(t) - 1) dt, \\
&= \frac{1}{24} \left(\int_0^{24} \epsilon_i(t)\mu_i(t) dt - \int_0^{24} \epsilon_i(t) dt - \int_0^{24} \mu_i(t) dt + \int_0^{24} dt \right), \\
&= \Gamma_i - 1.
\end{aligned}
$$

The third step in the equation above is obtained by using Equations (2.3.2), (2.3.4) and (2.3.5). Therefore,

$$\Gamma_i = 1 + \text{cov}\left(\epsilon_i(\cdot), \mu_i(\cdot)\right). \tag{2.3.8}$$

It must be noted from Equations (2.3.8) that an intermittent power source exhibit value synergies with the intertemporal price distribution on any given day i if and only if there is a positive covariance between $\epsilon_i(\cdot)$ and $\mu_i(\cdot)$. That is, the LCOE of electricity generation improves if the intermittent energy source generates the most of its outputs during peak price period. When $CF_i(t) = CF_i$ or $p_i(t) = p_i$ on all days, there is neither synergies or complementaries. This accounts for why the co-variation coefficient is equal to one when prices or energy generation is constant. Therefore, co-variation coefficient for the dispatchable technology is equal to one since $CF_i(t) = CF_i$ even if variation in price exists.

Statistics	Γ_{so}	Γ_{wi}
Yearly average	1.19	0.87
Yearly minimum	1.17	0.35
Yearly maximum	1.22	1.39
Summer average	1.30	0.80
Winter average	1.08	0.95

Table 2.7: Average year solar and wind co-variation coefficient.

Capacity value	Coal reduction	Gas reduction	Mixed reduction		
c_v	$\mathrm{co}^{1.0}$	$\mathrm{ga}^{1.0}$	$\mathrm{co}^{0.25}\ \mathrm{ga}^{0.75}$	$\mathrm{co}^{0.5}\ \mathrm{ga}^{0.5}$	$\mathrm{co}^{0.75}\ \mathrm{ga}^{0.25}$
0%	129.75	95.42	104.00	112.58	121.16
5%	123.99	93.97	101.47	108.98	116.48
10%	118.24	92.51	98.95	105.38	111.81
15%	112.50	91.05	96.42	101.78	107.14
20%	106.75	89.60	93.89	98.18	102.47

Table 2.8: Value of solar LCOE (P_{LC}^{so**}) adjusted with solar co-variation coefficient Γ_{so} at different scenarios of energy and capacity reduction with a 30% solar penetration.

2.3.2 Systemic LCOE with Co-variation Coefficient

The time varying generation and pricing schedule can be introduced into the systemic LCOE theory by appending the LCOEs of single technology by their respective co-variation coefficient. Following the argument outline in previous section and Prop. 2.3.1, the appended stochastic systemic LCOE portfolio (i.e $P_{LC}^{Asys}(\omega)$) can be expressed as:

$$P_{LC}^{Asys}(\omega) = w^{co}\frac{P_{LC}^{co}}{\Gamma_{co}}(\omega) + w^{ga}\frac{P_{LC}^{ga}}{\Gamma_{ga}}(\omega) + w^{wi}\frac{P_{LC}^{wi*}}{\Gamma_{wi}} + w^{so}\frac{P_{LC}^{so*}}{\Gamma_{so}}. \qquad (2.3.9)$$

By definition, the co-variation coefficient for dispatchable technologies, $\Gamma_{co} = \Gamma_{ga} = 1$, since $CF_i(t) = CF_i$, which implies that $\epsilon_i(t)$, which represent the multiplicative deviation from the average capacity factor at time t, is always equal to one since energy production is constant throughout the life cycle of the conventional power plant. Therefore, the appended stochastic systemic LCOE portfolio used for our analysis is given by:

$$P_{LC}^{Asys}(\omega) = w^{co}P_{LC}^{co}(\omega) + w^{ga}P_{LC}^{ga}(\omega) + w^{wi}\frac{P_{LC}^{wi*}}{\Gamma_{wi}} + w^{so}\frac{P_{LC}^{so*}}{\Gamma_{so}}. \qquad (2.3.10)$$

Capacity value	Coal reduction	Gas reduction	Mixed reduction		
c_v	$\text{co}^{1.0}$	$\text{ga}^{1.0}$	$\text{co}^{0.25}\,\text{ga}^{0.75}$	$\text{co}^{0.5}\,\text{ga}^{0.5}$	$\text{co}^{0.75}\,\text{ga}^{0.25}$
0%	128.14	81.20	92.94	104.67	116.40
5%	120.28	79.21	89.48	99.74	110.02
10%	112.42	77.22	86.03	94.82	103.63
15%	104.57	75.23	82.57	89.90	97.24
20%	96.71	73.25	79.11	84.98	90.85

Table 2.9: Value of wind LCOE (P_{LC}^{wi**}) adjusted with wind co-variation coefficient Γ_{wi} at different scenarios of energy and capacity reduction with a 30% wind penetration.

where Γ_{wi} is the wind co-variation coefficient which captures the synergies between wind power generation and the pricing schedule. The Γ_{so} is the solar co-variation co-efficient which captures the synergies between solar power generation and pricing schedule. Equation (2.3.10) can simply be expressed as:

$$P_{\text{LC}}^{\text{Asys}}(\omega) = w^{\text{co}} P_{\text{LC}}^{\text{co}}(\omega) + w^{\text{ga}} P_{\text{LC}}^{\text{ga}}(\omega) + w^{\text{wi}} P_{\text{LC}}^{\text{wi}**} + w^{\text{so}} P_{\text{LC}}^{\text{so}**}, \qquad (2.3.11)$$

where $P_{\text{LC}}^{\text{wi}**} = \frac{P_{\text{LC}}^{\text{wi}*}}{\Gamma_{\text{wi}}}$ is the appended wind LCOE whose computation takes into consideration all systemic constraints involved in the inclusion into the power grid and the synergies that exist between wind power generation and the time of day pricing schedule. Similarly, $P_{\text{LC}}^{\text{so}**} = \frac{P_{\text{LC}}^{\text{so}*}}{\Gamma_{\text{so}}}$ is the appended solar LCOE whose computation takes into consideration all systemic constraints involved in the inclusion into the power grid and the synergies that exist between solar power generation and the time of day pricing schedule.

For our analysis, the values for Γ_{wi} and Γ_{so} are extracted from the work of Stefan Reichelstein and Anshuman Sahoo in [41] (see Table (2.7)). The data from which the solar co-variation coefficient Γ_{so} was obtained is from northern California. The solar power generation data are based on simulations for the San Franscisco Bay Area from the PVWatts program developed by the National Renewable Energy Laboratory [35]. The wind power generation data are based on simulation recorded in the NREL Wind integration Dataset [36].

From Table (2.7), the average yearly value of the co-variation coefficient of solar power $\Gamma_{\text{so}} = 1.19$, according to Equation (2.3.8) there exist a positive correlation between energy generation and pricing in solar energy. This is true since the Sun generates energy at its peak in the hot afternoon when electricity price is also at the peak due to high demand of electricity. This occurs more often during summer which accounts for the highest values of $\Gamma_{\text{so}} = 1.30$. Due to some cloudy days in winter, radiation from the Sun is reduced thereby reducing the solar energy generation. This accounts for the value of $\Gamma_{\text{so}} = 1.08$ which is its minimum. On the other hand, the average yearly value of the co-variation

coefficient of the wind power is $\Gamma_{\mathrm{wi}} = 0.87$. This indicates a negative correlation between energy generation and pricing schedule. Wind power generation is at its maximum mostly in the night when electricity prices are off peak. This implies that most of the energy produced may be wasted, since electricity can not easily be stored in large quantity. The highest values of $\Gamma_{\mathrm{wi}} = 0.95$ occurs during winter. This is because winter period tends to be windy during both during the day and at night.

The values of the appended solar LCOE $P_{\mathrm{LC}}^{\mathrm{so}**}$ in Table (2.8) is obtained by applying the solar co-variation coefficient Γ_{so} which acts as a multiplicative correction factor which adjust the solar LCOE in Table (2.3). The adjusted solar LCOE ($P_{\mathrm{LC}}^{\mathrm{so}**}$) values obtained are 16% lower than the values of solar LCOE in Table (2.3). This implies that solar LCOE is more cost competitive than previously computed in previous literature when time-varying generation and pricing schedule are taken into consideration in the computation of intermittent energy source. On the contrary, the appended wind LCOE $P_{\mathrm{LC}}^{\mathrm{wi}**}$ values obtained in Table (2.9) are 15% higher than those obtained in Table (2.4). This implies that wind LCOE is less cost competitive than previously computed when time-varying generation and pricing schedule are taken into consideration in the computation. This is due to the fact that wind energy production is usually at its peak when electricity prices are off peak. It must be noted that this LCOE computation is markedly different from the analysis done in [41] because the analysis in this research work also involves extra costs from systemic constraints which was not considered in [41].

2.4 Conclusion

The LCOE for intermittent renewable energy sources integrated into a dispatchable resource based power grid were computed with extra cost due to the systemic constraints that account for the cost of energy and capacity reduction of the technically feasible portfolio. In addition to this, a multiplicative correction factor that account for the synergies between energy generation and time of day pricing schedule was used to append the LCOE values, thereby obtaining more realistic LCOE values for solar and wind power in a stochastic systemic LCOE portfolio. The LCOE obtained for the two intermittent renewable energy sources were higher in value than the 'bare' solar and wind LCOE due to the systemic constraints considered. Furthermore, the solar LCOE obtained are more cost competitive than the solar LCOE obtained under the stochastic systemic framework [27], while the opposite is true for wind LCOE.

Chapter 3

LCOE Risk Analysis

3.1 Introduction

Portfolio optimization was introduced in the stochastic LCOE problem in [28]. A Markowitz portfolio analysis [29] was used to show how to manage stochastic LCOE risk by computing the variance ($\sigma^{LC,w}$) for a sequence of admissible returns ($\mu^{LC,w}$) and obtaining the generation mix that minimizes the portfolio variance thereby proposing an optimal choice of the portfolio weights with minimum dispersion about the $\mu^{LC,w}$. In general, LCOE distributions are not Gaussian, having asymmetric long thick tails [14], therefore Markowitz mean-variance analysis used in the systemic LCOE risk analysis [27] are considered only as the starting point and can be extended with more suitable dispersion measures such as the CVaR deviation (CVaRD), which plays the same role as the standard deviation in a Markowitz approach. In addition to this, both theory and practice indicate that variance is not a good risk measure [1], because a risk reduction through the mean-variance approach does not only lead to low deviations from the expected return on the downside, but also on the upside [54]. Therefore an alternative is the Value at Risk (VaR), which is the maximum loss expected over a portfolio over a given time horizon at a specified confidence interval [31]. However, VaR is not subadditive and risk at the tail is non-measurable in VaR. The Conditional Value at Risk (CVaR) was introduced by Uryasev and Rockerfellar [42, 43] as an alternative to VaR. It is also known as Mean Excess Loss, Expected Shortfall (ES) or tail VaR. CVaR is defined as the conditional expectation of the loss above VaR for the time horizon and the confidence level. The CVaR is the risk measure underlying the definition of the CVaRD which will be used for LCOE risk analysis.

In this chapter, we perform a LCOE risk analysis. In particular we consider two different risk measure; the variance and the CVaR deviation and analyze the characteristics of the obtained portfolios under these two risk measures.

3.2 Minimum Variance Portfolio Analyses

3.2.1 Technical Feasible Portfolios

Using the variance as a risk measure an optimal portfolio analysis is performed for the technically feasible set of generating technology which consist of single fuel portfolio such as coal only or gas only generation portfolio and mixed portfolio including both dispatchable technologies, coal and gas. The covariance measures the degree of dependency between the two, coal-only and gas-only stochastic LCOEs, with the mutual dependence controlled by the carbon emission volatility σ^{em}. Scenario analysis was performed by considering four level of the volatility of CO_2 emission prices, namely $\sigma^{\text{em}} = 0.0, 0.10, 0.15, 0.20$. These respectively represent scenarios when the volatility of CO_2 emission prices is zero, low, medium and high.

It is well known in finance that the *global minimum variance* portfolio leads to a a well diversified portfolio (mix of the coal and gas technology) when the components in the portfolio are non correlated to each other. We recall that the stochastic LCOE for a given technically feasible portfolio can be expressed as follows:

$$P_{\text{LC}}^f(\omega) = w^{f,\text{co}} P_{\text{LC}}^{\text{co}}(\omega) + w^{f,\text{ga}} P_{\text{LC}}^{\text{ga}}(\omega). \tag{3.2.1}$$

The mean and the variance P_{LC}^f can be respectively expressed by

$$\mu_{\text{LC}}^f = w^{f,\text{co}} \mu_{\text{LC}}^{\text{co}} + w^{f,\text{ga}} \mu_{\text{LC}}^{\text{ga}} \tag{3.2.2}$$

and

$$(\sigma_{\text{LC}}^f)^2 = (w^{f,\text{co}})^2 (\sigma_{\text{LC}}^{\text{co}})^2 + (w^{f,\text{ga}})^2 (\sigma_{\text{LC}}^{\text{ga}})^2 + 2\rho w^{f,\text{co}} w^{f,\text{ga}} \sigma_{\text{LC}}^{\text{co}} \sigma_{\text{LC}}^{\text{ga}}, \tag{3.2.3}$$

where ρ is the correlation coefficient which measure the degree of interdependence between the coal and gas LCOEs. In order to find the optimal composition of coal and gas using the variance as a risk measure we solve the following optimization problem:

$$\begin{cases} \min_{\mathbf{w}} (\sigma_{\text{LC}}^f)^2 = (w^{f,\text{co}})^2 (\sigma_{\text{LC}}^{\text{co}})^2 + (w^{f,\text{ga}})^2 (\sigma_{\text{LC}}^{\text{ga}})^2 + 2\rho w^{f,\text{co}} w^{f,\text{ga}} \sigma_{\text{LC}}^{\text{co}} \sigma_{\text{LC}}^{\text{ga}} \\ s.t. \\ w^{f,\text{co}} + w^{f,\text{ga}} = 1 \\ w^{f,\text{co}}, \ w^{f,\text{ga}} \in [0, \ 1] \end{cases} \tag{3.2.4}$$

where the first constraint $(w^{f,\text{co}} + w^{f,\text{ga}})$ is the budged constraint and the second one $0 \leq w^{f,\text{co}}, \ w^{f,\text{co}} \leq 1$ is the non short selling constraint.

If we do not consider the non short selling constraint in problem (3.2.4) a closed form solution exist, given by:

$$w_{\text{mvp}}^{f,\text{co}} = \frac{(\sigma_{\text{LC}}^{\text{ga}})^2 - \rho\sigma^{\text{co}}\sigma^{\text{ga}}}{(\sigma_{\text{LC}}^{\text{ga}})^2 + (\sigma_{\text{LC}}^{\text{co}})^2 - 2\rho\sigma^{\text{co}}\sigma^{\text{ga}}}$$
$$w_{\text{mvp}}^{f,\text{ga}} = \frac{(\sigma_{\text{LC}}^{\text{co}})^2 - \rho\sigma^{\text{co}}\sigma^{\text{ga}}}{(\sigma_{\text{LC}}^{\text{ga}})^2 + (\sigma_{\text{LC}}^{\text{co}})^2 - 2\rho\sigma^{\text{co}}\sigma^{\text{ga}}}.$$

(3.2.5)

In order to solve problem (3.2.4) we first calculate the the solution given by (3.2.5). If the optimal weights obtained using the closed form solution do not satisfy the non short selling constraint we use the *quadprog* optimization function of MATLAB to solve problem (3.2.4).

It can be recalled that the mean and volatility of coal LCOE are, respectively, 102.53 and 3.73, while the mean and volatility of gas LCOE are, respectively, 63.84 and 6.72. In the following table the results obtained solving (3.2.4) considering 4 different scenarios for σ^{em} are reported.

	$\sigma^{\text{em}} = 0.00$	$\sigma^{\text{em}} = 0.10$	$\sigma^{\text{em}} = 0.15$	$\sigma^{\text{em}} = 0.20$
$w_{\text{mvp}}^{f,\text{co}}$	76%	53%	31%	6%
$w_{\text{mvp}}^{f,\text{ga}}$	24%	47%	69%	94%
$\mu_{\text{LC,mvp}}$	93.44	84.14	75.85	65.79
$\sigma_{\text{LC,mvp}}$	3.3	5.6	7.1	8.4

Table 3.1: Minimum variance portfolios.

These results are obtained using the solution given in (3.2.5). Considering that the obtained optimal weights are always positive, which satisfy the non short-selling constraint we do not run the *quadprog* MATLAB routine. It can be observed that as the volatility of $C0_2$ emission price increase from 0% to 20%, the optimal portfolio weight of coal generation reduces from 76% to as low as 6% and the average LCOE of the optimal portfolios reduce from 93.44 to 65.79. This implies that as the weight of the gas technology increases, the generating cost reduces but the riskier it is for the environment because of the uncertainty in policies that controls environmental pollution. The result presented in Table (3.1) is markedly different from those in [27], even though the same mean-variance optimization has been used. The difference is due to the fact that the fossil fuel dynamics were modeled using mean-reverting stochastic differential equations in place of the geometric Brownian motion used in [27]. A lower LCOE volatility recorded in our analysis has significant effect on the optimal weights of the coal and gas portfolio when compared to the result in [27].

3.2.2 Inclusion of Solar and Wind Assets

We recall that the inclusion of solar and wind component into the technically feasible portfolio is based on the assumption that the electricity reduction from fossil fuel generation is proportional to the share of single fuel electricity generated by the technically feasible portfolio, and that the capacity reduction of a technology α is proportional to the share of power capacity of technology α in the technically feasible portfolio. If the target solar and wind penetration are denoted by $\bar{w}^{\mathrm{so}}$ and $\bar{w}^{\mathrm{wi}}$ respectively, the power system LCOE can be expressed as

$$P_{\mathrm{LC}}^{\mathrm{sys}} = \bar{w}^{\mathrm{wi}} P_{\mathrm{LC}}^{\mathrm{wi}*} + \bar{w}^{\mathrm{so}} P_{\mathrm{LC}}^{\mathrm{so}*} + (1 - \bar{w}^{\mathrm{wi}} - \bar{w}^{\mathrm{so}}) \sum_{\alpha} w^{f,\alpha} P_{\mathrm{LC}}^{\alpha}(\omega), \qquad (3.2.6)$$

where $P_{\mathrm{LC}}^{\mathrm{sys}}$ is the systemic LCOE portfolio. It can be recalled from Equation (2.2.14) that the wind LCOE with one intermittent renewable energy source included into the power system is

$$P_{\mathrm{LC}}^{\mathrm{wi}*} = P_{\mathrm{LC}}^{\mathrm{wi}} + \sum_{\alpha} w^{f,\alpha} A^{\alpha}, \qquad (3.2.7)$$

where

$$A^{\alpha} = \left(1 - \frac{c_v}{w^{\mathrm{wi}}}\right) \left(\hat{C}^{\alpha,\mathrm{fix}} + \frac{\hat{I}_0^{\alpha} - T_c \hat{D}^{\alpha}}{1 - T_c}\right).$$

Also, it can be recalled from Equation (2.2.20) that the solar LCOE when two power sources are included in the power system is

$$P_{\mathrm{LC}}^{\mathrm{so}*} = P_{\mathrm{LC}}^{\mathrm{so}} + \sum_{\alpha} w^{f,\alpha} B^{\alpha}, \qquad (3.2.8)$$

where

$$B^{\alpha} = \hat{C}^{\alpha,\mathrm{fix}} + \frac{\hat{I}_0^{\alpha} - T_c \hat{D}^{\alpha}}{1 - T_c}.$$

Therefore substituting Equations (3.2.7) and (3.2.8) into Equation (3.2.6), we obtain:

$$P_{\mathrm{LC}}^{\mathrm{sys}} = \bar{w}^{\mathrm{wi}} P_{\mathrm{LC}}^{\mathrm{wi}} + \bar{w}^{\mathrm{so}} P_{\mathrm{LC}}^{\mathrm{so}} + \sum_{\alpha} w^{f,\alpha} \left[(1 - \bar{w}^{\mathrm{wi}} - \bar{w}^{\mathrm{so}}) P_{\mathrm{LC}}^{\alpha}(\omega) + \bar{w}^{\mathrm{wi}} A^{\alpha} + \bar{w}^{\mathrm{so}} B^{\alpha}\right].$$

The mean and the variance of the systemic LCOE portfolio $P_{\mathrm{LC}}^{\mathrm{sys}}$ can be explicitly written as

$$\mu_{\mathrm{LC}}^{\mathrm{sys}} = \bar{w}^{\mathrm{wi}} \mu_{\mathrm{LC}}^{\mathrm{wi}} + \bar{w}^{\mathrm{so}} \mu_{\mathrm{LC}}^{\mathrm{so}} \;\; + \;\; w^{f,\mathrm{co}} \left[(1 - \bar{w}^{\mathrm{wi}} - \bar{w}^{\mathrm{so}}) \mu_{\mathrm{LC}}^{\mathrm{co}} + \bar{w}^{\mathrm{wi}} A^{\mathrm{co}} + \bar{w}^{\mathrm{so}} B^{\mathrm{co}}\right]$$

$$+ \;\; w^{f,\mathrm{ga}} \left[(1 - \bar{w}^{\mathrm{wi}} - \bar{w}^{\mathrm{so}}) \mu_{\mathrm{LC}}^{\mathrm{ga}} + \bar{w}^{\mathrm{wi}} A^{\mathrm{ga}} + \bar{w}^{\mathrm{so}} B^{\mathrm{ga}}\right],$$

and

$$(\sigma_{\mathrm{LC}}^{\mathrm{sys}})^2 = \left(1 - \bar{w}^{\mathrm{wi}} - \bar{w}^{\mathrm{so}}\right)^2 \left[(w^{f,\mathrm{co}})^2(\sigma_{\mathrm{LC}}^{\mathrm{co}})^2 + (w^{f,\mathrm{ga}})^2(\sigma_{\mathrm{LC}}^{\mathrm{ga}})^2 + 2\rho w^{f,\mathrm{co}} w^{f,\mathrm{ga}} \sigma_{\mathrm{LC}}^{\mathrm{co}} \sigma_{\mathrm{LC}}^{\mathrm{ga}}\right]$$
$$= \left(1 - \bar{w}^{\mathrm{wi}} - \bar{w}^{\mathrm{so}}\right)^2 (\sigma_{\mathrm{LC}}^f)^2,$$

respectively. The composition of the minimum variance systemic portfolio is given by

$$
\begin{aligned}
w_{\mathrm{mvp}}^{\mathrm{wi}} &= \bar{w}^{\mathrm{wi}}, & (3.2.9) \\
w_{\mathrm{mvp}}^{\mathrm{so}} &= \bar{w}^{\mathrm{so}}, \\
w_{\mathrm{mvp}}^{\mathrm{co}} &= \left(1 - \bar{w}^{\mathrm{wi}} - \bar{w}^{\mathrm{so}}\right) w_{\mathrm{mvp}}^{f,\mathrm{co}}, \\
w_{\mathrm{mvp}}^{\mathrm{ga}} &= \left(1 - \bar{w}^{\mathrm{wi}} - \bar{w}^{\mathrm{so}}\right) w_{\mathrm{mvp}}^{f,\mathrm{ga}},
\end{aligned}
$$

where $w_{\mathrm{mvp}}^{f,\mathrm{co}}$ and $w_{\mathrm{mvp}}^{f,\mathrm{co}}$ are the minimum variance portfolios considering only the budget constraint, given in (3.2.5). We recall that we have a closed form solution because minimizing the variance with only budget constraint has closed form solution, given in (3.2.5), which satisfy the non short-selling constraint.

The results of the optimal minimum variance systemic portfolios under the four CO_2 price volatility scenarios at different capacity values ($c_v = 0\%, 10\%, 20\%$) are reported in Table 3.2. We assume a solar and wind penetration of 25% each, that is, $\bar{w}^{\mathrm{so}} = 25\%$, $\bar{w}^{\mathrm{wi}} = 25\%$. This is done in order to have a total of 50% penetration of renewable energy in the power system, which is chosen in accordance to the 2030 renewable commitment by some part of US and Germany [9].

The optimal weights in Table 3.2 are obtained using the closed form solution given in (3.2.10) which satisfies the non short-selling constraints. It is observed that the standard deviation ($\sigma_{\mathrm{LC,mvp}}$) recorded in Table (3.2) are lower than those of the technically feasible portfolio in Table (3.1), when compared respectively under the four CO_2 price volatility scenarios. This shows the reduction of risk through the inclusion of solar and wind components into the power system. The LCOE values of the systemic portfolio at different capacity values are higher than those of the technically feasible portfolio due to additional costs from systemic constraints when solar and wind power are integrated into the grid. As CO_2 price volatility increases, the LCOE values at different capacity decreases. The minimum cost of the systemic portfolio is 77.23, when the CO_2 price volatility $\sigma^{\mathrm{em}} = 0.20$, and the capacity value is 20%. The portfolio consist of 25% solar, 25% wind, 47% gas and 3% coal. Even though our analysis was done with 50% integration of renewable energy into power system, yet the LCOE values obtained in our analysis are lower than those values obtained in [27]. This is because of the higher percentage of gas component obtained in the optimal systemic portfolio due to a more appropriate modeling of the fossil fuel prices.

40

	$\sigma^{\mathrm{em}} = 0.00$	$\sigma^{\mathrm{em}} = 0.10$	$\sigma^{\mathrm{em}} = 0.15$	$\sigma^{\mathrm{em}} = 0.20$
$\bar{w}^{\mathrm{wi}}$	25%	25%	25%	25%
$\bar{w}^{\mathrm{so}}$	25%	25%	25%	25%
$w^{\mathrm{co}}_{\mathrm{mvp}}$	38%	26%	15%	3%
$w^{\mathrm{ga}}_{\mathrm{mvp}}$	12%	24%	35%	47%
$\mu^{c_v=0}_{\mathrm{LC,mvp}}$	108.41	98.80	89.50	80.54
$\mu^{c_v=0}_{\mathrm{LC,mvp}}$	103.90	95.27	86.93	78.88
$\mu^{c_v=0}_{\mathrm{LC,mvp}}$	99.39	91.73	84.36	77.23
$\sigma_{\mathrm{LC,mvp}}$	1.6	2.8	3.6	4.3

Table 3.2: Minimum variance systemic portfolios at different capacity values ($c_v = 0\%, 10\%, 20\%$).

Figure 3.1: Technically feasible (disp) frontier and systemic portfolio frontiers ($c_v = 0\%, 10\%, 20\%$), when carbon price volatility is $\sigma^{\mathrm{em}} = 0.0$ (Upper panel) and $\sigma^{\mathrm{em}} = 0.10$ (lower panel). The vertical axis reports the negative Portfolio mean ($-\mu_{\mathrm{LC,sys}}$ and $-\mu_{\mathrm{LC,f}}$) while the horizontal axis reports the portfolio standard deviation ($\sigma_{\mathrm{LC,sys}}$ and $\sigma_{\mathrm{LC,f}}$).

The technically feasible portfolio frontier and the systemic portfolio frontiers for different volatility scenarios are presented in Fig. (3.1) and (3.2).
The negative of $-\mu_{\mathrm{LC,sys}}$ and $-\mu_{\mathrm{LC,f}}$ were used for the risk analysis, because the higher the LCOE (which is non-negative) the higher the risk of not covering the costs of generating electricity, since the objective is to minimize the cost and risk of electricity generation in a diversified portfolio. The displacement of
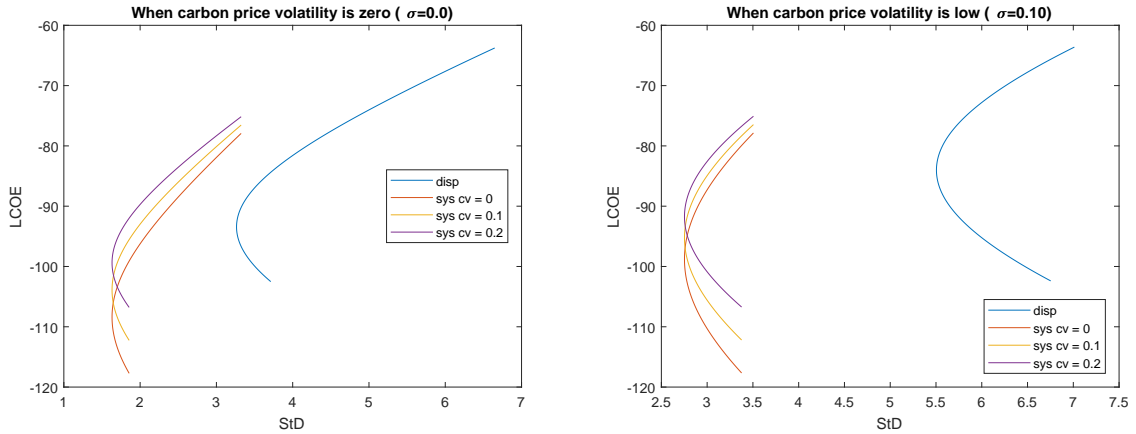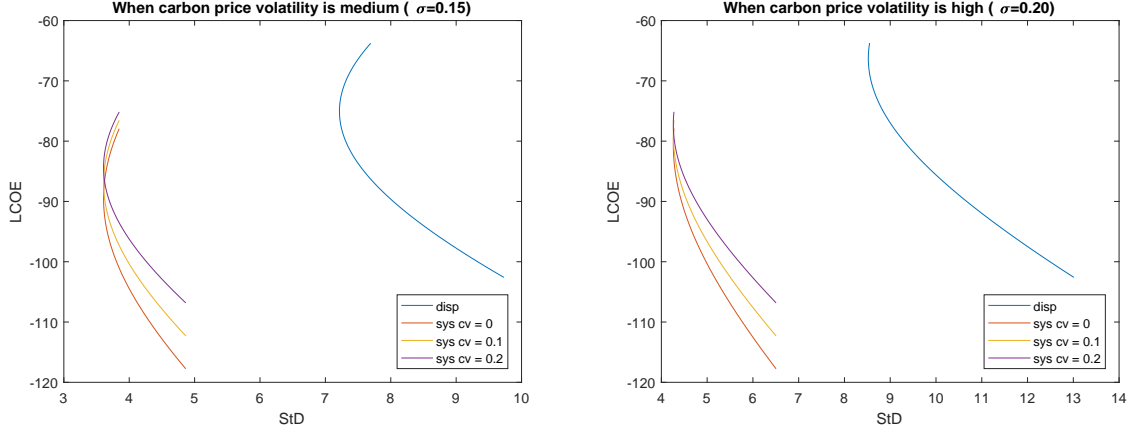
Figure 3.2: Technically feasible (disp) frontier and systemic portfolio frontiers $(c_v = 0\%, 10\%, 20\%)$, when carbon price volatility is $\sigma^{\text{em}} = 0.15$ (Upper panel) and $\sigma^{\text{em}} = 0.20$ (lower panel). The vertical axis reports the negative Portfolio mean $(-\mu_{\text{LC,sys}}$ and $-\mu_{\text{LC,f}})$ while the horizontal axis reports the portfolio standard deviation ($\sigma_{\text{LC,sys}}$ and $\sigma_{\text{LC,f}})$.

the systemic frontiers towards the southwest of the technically feasible frontier shows the combined effect of an increase in cost and risk reduction, when solar and wind components are integrated into the technically feasible portfolio. The displacement towards the south indicates an increase in cost while displacement towards the west indicates risk reduction.

When the time-varying generation and pricing schedule is considered in our systemic portfolio the appended systemic portfolio is

$$P_{\text{LC}}^{\text{Asys}} = \bar{w}^{\text{wi}} P_{\text{LC}}^{\text{wi**}} + \bar{w}^{\text{so}} P_{\text{LC}}^{\text{so**}} + (1 - \bar{w}^{\text{wi}} - \bar{w}^{\text{so}}) \sum_{\alpha} w^{f,\alpha} P_{\text{LC}}^{\alpha}(\omega), \qquad (3.2.10)$$

where $P_{\text{LC}}^{\text{wi**}} = \frac{P_{\text{LC}}^{\text{wi*}}}{\Gamma_{\text{wi}}}$ is the appended wind LCOE, whose computation takes into consideration all the systemic constraints involved in the inclusion into the power grid and the synergies that exist between wind power generation and the time of day pricing schedule. Similarly, $P_{\text{LC}}^{\text{so**}} = \frac{P_{\text{LC}}^{\text{so*}}}{\Gamma_{\text{so}}}$ is the appended solar LCOE whose computation takes into consideration all the systemic constraints involved in the inclusion into the power grid and the synergies that exist between solar power generation and the time of day pricing schedule.

The mean and the variance of $P_{\text{LC}}^{\text{Asys}}$ can be explicitly written as

$$\mu_{\text{LC}}^{\text{Asys}} = \bar{w}^{\text{wi}} \frac{\mu_{\text{LC}}^{\text{wi}}}{\Gamma_{\text{wi}}} + \bar{w}^{\text{so}} \frac{\mu_{\text{LC}}^{\text{so}}}{\Gamma_{\text{so}}} \quad + \quad w^{f,\text{co}} \left[(1 - \bar{w}^{\text{wi}} - \bar{w}^{\text{so}}) \mu_{\text{LC}}^{co} + \bar{w}^{\text{wi}} \frac{A^{\text{co}}}{\Gamma_{\text{wi}}} + \bar{w}^{\text{so}} \frac{B^{\text{co}}}{\Gamma_{\text{so}}} \right]$$

$$+ \quad w^{f,\text{ga}} \left[(1 - \bar{w}^{\text{wi}} - \bar{w}^{\text{so}}) \mu_{\text{LC}}^{ga} + \bar{w}^{\text{wi}} \frac{A^{\text{ga}}}{\Gamma_{\text{wi}}} + \bar{w}^{\text{so}} \frac{B^{\text{ga}}}{\Gamma_{\text{so}}} \right],$$
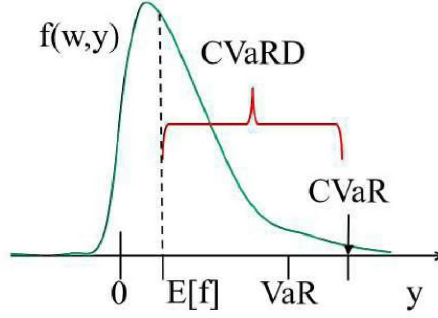
Figure 3.3: Conditional Value at Risk Deviation measure (CVaRD) described graphically [26].

and

$$(\sigma_{\text{LC}}^{\text{Asys}})^2 \;\;=\;\; \left(1 - \bar{w}^{\text{wi}} - \bar{w}^{\text{so}}\right)^2 (\sigma_{\text{LC}}^f)^2.$$

Since the solar and wind penetration in the systemic portfolio is predetermined in our analysis, the co-variation coefficient of solar and wind has no effect on neither the optimal portfolio weights nor the standard deviation. Nevertheless, the LCOE tends to be significantly lower as the solar penetration increases more than wind penetration in the appended systemic portfolio when compared to similar scenario under the systemic portfolio. This is due to the cost competitiveness of solar energy when time-varying generation and pricing of electricity is considered in the LCOE analysis. The value of LCOE for the appended systemic portfolio and the systemic portfolio will remain similar as long as the solar and wind penetration are of the same weight in the portfolio.

3.3   Conditional Value at Risk Deviation

Suppose there exist a vector of random variables y with joint probability density $p(y)$, a vector of choice variables w which denotes the portfolio weights, a loss function $f(w) = f(w, y)$, which denotes the portfolio losses, a threshold h for the losses f, and a probability α. The Value at Risk (VaR) for a given portfolio of components w at confidence level x is given by

$$\text{VaR}_{\text{x}}^{\text{w}}(f(w)) = \min_{h} \left\{ \int_{f(w,y) \leq h} p(y) dy \geq x \right\} \tag{3.3.1}$$

Equation (3.3.1) shows that $\text{VaR}_{\text{x}}^{\text{w}}$ is actually an x-quantile, and can be interpreted as the minimum threshold h above which losses are not larger than $\text{VaR}_{\text{x}}^{\text{w}}$ in x percent cases of all possible cases. Nevertheless, VaR is not suitable for the optimization of the stochastic LCOE portfolio since the underlying distribution

43

Volatility scenario		Disp.	Sys. ($c_v = 0$)	Sys. ($c_v = 10\%$)	Sys. ($c_v = 20\%$)
	VaR$_{95\%}$	90.62	101.57	98.14	94.72
$\sigma^{\mathrm{em}} = 0.00$	CVaR$_{95\%}$	93.15	102.84	99.41	96.00
	CVaRD$_{95\%}$	10.1	5.1	5.1	5.1
	VaR$_{95\%}$	93.84	103.18	99.75	96.32
$\sigma^{\mathrm{em}} = 0.10$	CVaR$_{95\%}$	97.57	105.04	101.62	98.19
	CVaRD$_{95\%}$	14.4	7.2	7.2	7.2
	VaR$_{95\%}$	97.62	105.06	101.64	98.21
$\sigma^{\mathrm{em}} = 0.15$	CVaR$_{95\%}$	103.90	108.20	104.78	101.36
	CVaRD$_{95\%}$	20.8	10.4	10.4	10.4
	VaR$_{95\%}$	100.72	106.62	103.20	99.77
$\sigma^{\mathrm{em}} = 0.20$	CVaR$_{95\%}$	111.21	111.86	108.44	105.01
	CVaRD$_{95\%}$	28.2	14.1	14.1	14.1

Table 3.3: LCOE risk analysis of technically feasible and systemic portfolios at the 95% confidence level under different volatility scenarios.

of LCOE are not Gaussian [39]. Also, since VaR is not subadditive, portfolio diversification does not lead to risk reduction in VaR. An alternative to VaR is the Conditional Value at Risk (CVaR). It is a risk measure which is sensitive to tail and asymmetry. CVaR for a portfolio of risks parameterized by w is defined as:

$$\mathrm{CVaR}_{\mathrm{x}}^{\mathrm{w}}(f(w)) = \frac{1}{1-x} \int_{f(w,y) \geq \mathrm{VaR}_{\mathrm{x}}^{\mathrm{w}}} f(w,y)p(y)dy. \qquad (3.3.2)$$

Equation (3.3.2) shows that $\mathrm{CVaR}_{\mathrm{x}}^{\mathrm{w}}$ is the expectation over the residue $1-x$ cases, i.e. the most adverse ones, this implies that $\mathrm{CVaR}_{\mathrm{x}}^{\mathrm{w}} \geq \mathrm{VaR}_{\mathrm{x}}^{\mathrm{w}}$. The CVaR is a risk measure underlying the definition of CVaR Deviation (CVaRD) which is a more appropriate measure to be used for comparison with the standard deviation. Generally speaking, risk measures evaluate outcomes in an absolute way, whereas deviation measures evaluate distribution widths. The technical difference between risk measures and deviation measures is similar to the difference between mean and the variance. Therefore the relationship between risk measure R and its partner deviation measure D is given by

$$D(f(w)) = R\Big(f(w) - E(f(w))\Big). \qquad (3.3.3)$$

According to Equation (3.3.3), the portfolio CVaRD at the confidence level x is defined [44] as

$$\mathrm{CVaRD}_{\mathrm{x}}^{\mathrm{w}}(f(w)) = \mathrm{CVaR}_{\mathrm{x}}^{\mathrm{w}}(f(w)) - E(f(w)). \qquad (3.3.4)$$

The result of LCOE risk analysis of technically feasible and systemic portfolios at 95% confidence level under different volatility scenarios are presented in Table (3.3). The $\text{VaR}_{95\%}^{\text{w}}$ implies that with 95% probability, the levelized cost of electricity in a portfolio of generation technologies can not exceed the values presented on the table at different carbon volatility scenarios. While the values of $\text{CVaR}_{95\%}^{\text{w}}$ is the average of the 5% extreme values of LCOEs at the tail end of the LCOE distribution. This accounts for unexpected cost of electricity generation that could arise throughout the lifetime of the energy generation technologies. The deviation measure $\text{CVaRD}_{95\%}^{\text{w}}$, which is comparable to the standard deviation is used to produce technically feasible and systemic portfolio frontiers in Figure (3.4) and Figure (3.5). It is observed that the graphs produced with $\text{CVaRD}_{95\%}^{\text{w}}$ are very similar to those produced with the standard deviation $\sigma_{\text{LC,sys}}$ but the former takes into consideration tail risk while the later does not. This explains the reason values of $\text{CVaRD}_{95\%}^{\text{w}}$ are higher than the values of $\sigma_{\text{LC,sys}}$ for the technically feasible and systemic portfolio under their corresponding carbon price volatility scenarios.

Figure 3.4: Technically feasible (disp) frontier and systemic portfolio frontiers ($c_v = 0\%, 10\%, 20\%$), when carbon price volatility is $\sigma^{\text{em}} = 0.0$ (Upper panel) and $\sigma^{\text{em}} = 0.10$ (lower panel). The vertical axis reports the negative Portfolio mean ($-\mu_{\text{LC,sys}}$ and $-\mu_{\text{LC,f}}$) while the horizontal axis reports the portfolio CVaRD; The CVaRD is computed at 95% confidence level.

3.4 Portfolio analysis using CVaRD

As mentioned above the variance is not a good risk measure of risk, therefore we perform the same analysis as before when the conditional value at risk deviation ($\text{CVaRD}_{95\%}^{\text{w}}$) is used as risk measure. The optimal weights for coal and gas are calculated solving the following:
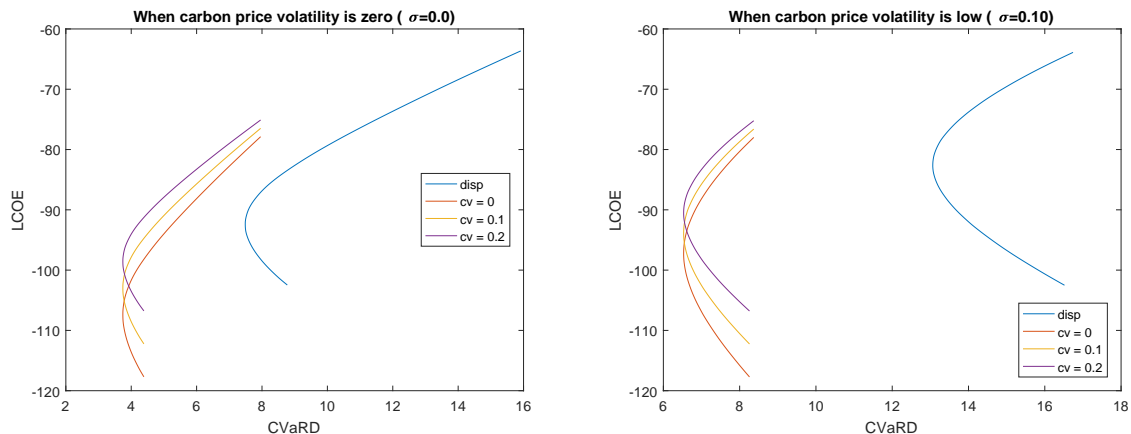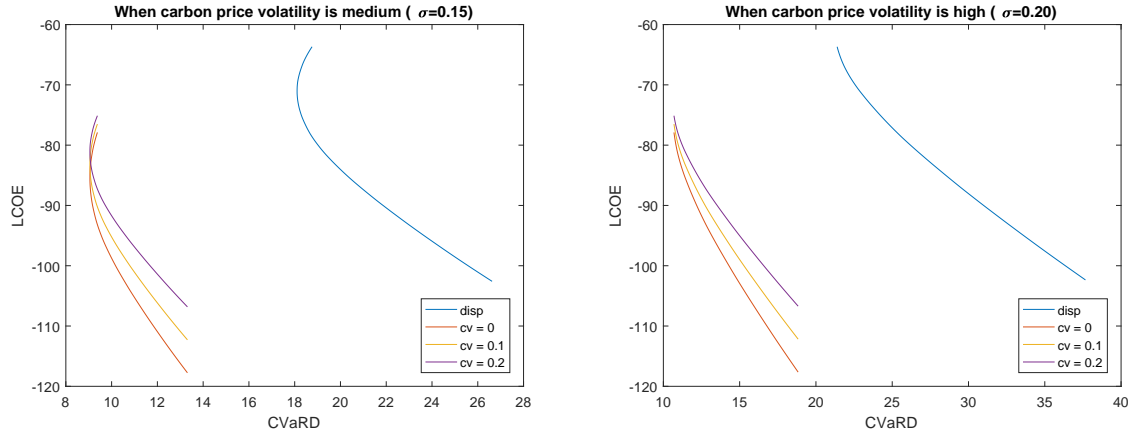
Figure 3.5: Technically feasible (disp) frontier and systemic portfolio frontiers ($c_v = 0\%, 10\%, 20\%$), when carbon price volatility is $\sigma^{\mathrm{em}} = 0.15$ (Upper panel) and $\sigma^{\mathrm{em}} = 0.20$ (lower panel). The vertical axis reports the negative Portfolio mean ($-\mu_{\mathrm{LC,sys}}$ and $-\mu_{\mathrm{LC,f}}$) while the horizontal axis reports the portfolio CVaRD; The CVaRD is computed at 95% confidence level.

$$
\begin{cases}
\min_{\mathbf{w}} CVaRD^{\mathbf{w}}_{95\%} \\
s.t. \\
w^{f,\mathrm{co}} + w^{f,\mathrm{ga}} = 1 \\
w^{f,\mathrm{co}}, \ w^{f,\mathrm{ga}} \in [0, \ 1]
\end{cases}
\tag{3.4.1}
$$

We have solved this problem for different levels of σ^{em}, as in the previous analysis, Section 3.2. The results obtained for the global $CVaRD$ are reported in Table 3.4.

	$\sigma^{\mathrm{em}} = 0.00$	$\sigma^{\mathrm{em}} = 0.10$	$\sigma^{\mathrm{em}} = 0.15$	$\sigma^{\mathrm{em}} = 0.20$
$w^{f,\mathrm{co}}_{\mathrm{cvard}}$	76%	51%	18%	0%
$w^{f,\mathrm{ga}}_{\mathrm{cvard}}$	24%	49%	82%	100%
$\mu^{\mathrm{LC,cvard}}$	93.44	83.36	70.68	63.70
$\mathrm{CVaRD}_{\mathrm{LC},95\%}$	10.1	14.4	20.8	28.2

Table 3.4: Optimal portfolio analysis for technically feasible set using CVaRD, computed at 95% confidence interval.

Comparing these results with the ones obtained using the variance as risk

46

	$\sigma^{\mathrm{em}} = 0.0$	$\sigma^{\mathrm{em}} = 0.10$	$\sigma^{\mathrm{em}} = 0.15$	$\sigma^{\mathrm{em}} = 0.20$
$\bar{w}^{\mathrm{wi}}$	25%	25%	25%	25%
$\bar{w}^{\mathrm{so}}$	25%	25%	25%	25%
$w^{\mathrm{co}}_{\mathrm{cvard}}$	38%	26%	9%	0%
$w^{\mathrm{ga}}_{\mathrm{cvard}}$	12%	24%	41%	50%
$\mu^{\mathrm{cv}=0}_{\mathrm{LC,cvard}}$	108.14	98.62	85.41	58.54
$\mu^{\mathrm{cv}=0.1}_{\mathrm{LC,cvard}}$	103.65	95.11	83.26	57.84
$\mu^{\mathrm{cv}=0.2}_{\mathrm{LC,cvard}}$	99.17	91.60	81.11	57.15
$\mathrm{CVaRD}_{\mathrm{LC},95\%}$	5.1	7.2	10.4	14.1

Table 3.5: Optimal systemic portfolio analysis using CVaRD computed at 95% confidence interval.

measure (see Section 3.2), we observe that, though the coal and gas weights seems to be similar at scenarios with zero or low carbon price volatility, as the volatility increases the optimal weights of coal and gas technology becomes clearly different. In particular, when carbon price volatility becomes high, (i.e., at 20% volatility), a gas only technology is observed under the mean-CVaRD approach.

Furthermore, the result of the portfolio optimization for the systemic portfolio using the mean-CVaRD approach is presented in Table (3.5). The analysis also follows the same argument presented earlier, with CVaRD as a deviation measure instead of the standard deviation. Comparing the results in Table (3.4) and Table (3.5), a lower value of CVaRD is observed in Table (3.5) due to the presence of solar and wind energy generating technologies in the systemic portfolio. This is similar to the effect of risk-reduction by solar and wind energy in the systemic portfolio under the mean-variance optimization. LCOE values in the mean-CVaRD approach tends to be lower than those obtained under the mean-variance approach when carbon price volatility is high (i.e. at 20% volatility). This may be due to the fact that the risk measure used to compute CVaRD is tail risk measurable. This properly captures the risk analysis involved in the gas component whose distribution is asymmetric and has long tail due to dynamics of gas prices, which includes spikes. On the other hand, the standard deviation is non-measurable at the tail. Finally, the little difference in LCOE values with the same weight proportion when carbon price volatility is 0.0% and 0.10% in Table (3.2) and Table (3.5) is due to approximation errors.

3.5 Conclusion

LCOE risk analysis was performed in this chapter. Starting from the minimum variance porfolio analyses for the technically feasible set of generating technologies. It was observed that the calculated LCOE were lower than those in the literature due to the higher percentage of gas component in the optimal portfolios of the technically feasible technology as a result of modelling fossil fuel prices of coal and gas with more appropriate dynamic model. The LCOE of the systemic portfolio were higher due to the extra cost incurred from systemic constraints involved in the integration of solar and wind energy into the power system. In addition to this, a lower volatility, which signifies risk reduction was observed under the systemic portfolios due to the presence of renewables in the portfolio of generation technology. The combined effect of risk reduction and increase in LCOE value at different capacity values can be observed in the systemic frontiers when compared to the technically feasible portfolio frontiers. When the time-varying generation and pricing of electricity is included in LCOE analysis, the cost competitiveness of solar energy has a significant effect on only the LCOE of the systemic portfolio as solar penetration increases. The CVaR deviation was used for LCOE risk analysis in order to capture the tail risk in the LCOE distribution. Portfolio optimization analysis was done using mean-CVaRD approach and the result obtained were compared with those obtained using the mean-variance approach. This mean-CVaRD approach is useful in the worst case assessment of the portfolio of generating technologies.

Chapter 4

Modeling Agent Interaction

4.1 Introduction

The second part of this research work is from the complex system perspective. A complex system is a system composed of many interacting parts called agents, which display collective behavior that do not follow trivially from the behavior of the individual parts [33]. Over the years, it has been discovered that non-linear mathematical models replicate the dynamics of real systems better than the linear ones [15, 49]. An example of such former models is the Lotka-Volterra model [22, 53].

A more specific analysis based on our previous research [48] on the effect of competition and cooperation among interacting agents along a generalized Verhulst-Lotka Volterra model is presented in this part of the thesis. In this case, interacting agents are the energy firms/investors whose aim is to minimize cost of production and the risk involved in the production of electricity in order to maximize their profit while keeping the environment clean. The agent interaction is analyzed based on agent's size with common resources to share, that is, the consumers of electricity. Agents tend to increase in size when they acquire more of the market share and reduce when any market portion is lost. A network effect was introduced through an undirected but weighted graph in order to enable a mixed-type of interactions, i.e., having a system in which competitive and cooperative scenarios are considered to occur simultaneously among various interacting agents in the presence of a realistic constraint called the market capacity. Such competition, cooperation, and mixed type of interactions are analyzed below for triad interacting agents, through the evaluation of the eigenvalues of the relevant Jacobian matrix computed at corresponding fixed points, in order to investigate the system stability. This triad system has been chosen as the most simple, yet complex enough as representative of basic networks. The effect of the agent interaction as it affects satisfying market demand, and systemic stability will be illustrated through numerical results.

49

4.2 The Generalized Verhulst-Lotka-Volterra Model

A generalized Verhulst-Lotka-Volterra Model introduced in [6] is given by:

$$\dot{s}_i = \alpha_i s_i (\beta_i - s_i) - \sum_{i \neq j} \gamma(s_i, s_j) s_i s_j, \qquad i = 1, \ldots, n, \qquad (4.2.1)$$

where s_i is the size of agent i such that $0 \leq s_i \leq 1$; $\dot{s}_i$ is its time derivative; α_i is agent's growth rate if no interaction is present, β_i is the agent's maximum capacity and $\gamma(s_i, s_j)$ is the interaction function. The first term is a Verhulst-like term [51, 52] and the others stem from the Lotka-Volterra model [22, 53].

The interaction function $\gamma(s_i, s_j)$ is defined by

$$\gamma(s_i, s_j) = K \exp\left[-\left(\frac{s_i - s_j}{\sigma}\right)^2\right]; \qquad (4.2.2)$$

it is a continuously differentiable function that allows a proper theoretical analysis of the system dynamics, leading to conclusions which will appear to be likely model independent. The positive parameter σ controls or scales the intensity of agent size similarity and the parameter K determines the scenarios of agent's interaction.

The model is used in [6] to analyze a system of n agents in competition for some common resources with competition becoming more aggressive between agents with similar size. This is because as $|s_i - s_j| \to 0$, the interaction function $\gamma(s_i, s_j) \to K$ for a constant parameter σ, its maximum value. The competition weakens when agents have distinctly different sizes, thereby suggesting a peer-to-peer competition modelling.

For the peer-to-peer interaction system, presented in [6, 7], a strength parameter K was introduced: $K > 0$ was considered to show the presence of competition in the market, while $K < 0$ implied cooperation. Under the cooperative scenario, the interaction function is defined in the interval $-K < \gamma(s_i, s_j) < 0$. In order to avoid complexity and instability of the system, the value of K was chosen carefully through fixed point analysis of agents with equal sizes [7], whose eigenvalues are

$$\lambda_{1,\ldots,n} = \frac{K - 1}{1 + (n - 1)K}, \qquad (4.2.3)$$

so that, the K range interval $-\frac{1}{n-1} < K < 0$ ensures the stability of the system.

4.3 Model Formulation

The market capacity β is defined as the amount of product/service sales that could be reached within a certain period of time by any agent in the "market" [21]. In this research work, the market capacity is said to be the overall demand for energy by consumers, which is to be satisfied by agents in the energy

market for the system to be stable. The mathematical relationship between the individual agent's maximum capacity β_i, and β is given by:

$$\beta_i = \beta - \sum_{i \neq j} s_j, \tag{4.3.1}$$

so that the initial Verhulst-Lokta-Volterra model becomes:

$$\alpha_i s_i (\beta_i - s_i) = \alpha_i s_i \left(\beta - \sum_{i=1} s_i \right). \tag{4.3.2}$$

In addition, interaction among agents is introduced and modeled by a matrix $\mathbf{K}$ with elements $k_{ij} = k_{ji}$, which are zero on the diagonal, and can be +1 or -1 off the diagonal. Thus, the interaction function becomes:

$$\gamma(s_i, s_j) = k_{ij} \exp\left[- \left(\frac{s_i - s_j}{\sigma} \right)^2 \right] \tag{4.3.3}$$

with $0 < \gamma(s_i, s_j) < |k_{ij}|$.

This matrix $\mathbf{K}$ is the adjacency matrix of a network represented by a weighted and undirected graph. The weights $0, -1$ and $+1$ indicate no interaction, cooperation and competition respectively. Furthermore, we assume that there is no loop, that is, an agent cannot compete or cooperate with herself. For some special matrices $\mathbf{K}$, we obtain the model in [6, 7]. For instance, when

$$\mathbf{K} \equiv \begin{bmatrix} 0 & 1 & . & . & 1 \\ 1 & 0 & & . & 1 \\ . & & . & & . \\ . & & & . & . \\ 1 & 1 & . & . & 0 \end{bmatrix}$$

we obtain the full competitive scenario as in [6]. For

$$\mathbf{K} \equiv \begin{bmatrix} 0 & -1 & . & . & -1 \\ -1 & 0 & & . & -1 \\ . & & . & & . \\ . & & & . & . \\ -1 & -1 & . & . & 0 \end{bmatrix},$$

this is the full cooperative scenario [7]. In addition the network matrix

$$
\mathbf{K} \equiv
\begin{bmatrix}
0 & k_{12} & . & . & k_{1n} \\
k_{21} & 0 & & . & k_{2n} \\
. & & . & & . \\
. & & & . & . \\
k_{n1} & k_{n2} & . & . & 0
\end{bmatrix}
$$

ensures a mixed-type of interaction amongst the agents in the model, when $k_{ij}(= k_{ji})$ takes the value +1 or -1. That is, when competition and cooperation occur simultaneously amongst interacting agents in the system. For example, for $n = 3$, in our model, we can have two agents collaborating in order to compete effectively with the third agent. This can be compared with the case of two small companies collaborating to compete against a big company which had previously monopolized the market.

Thus suppose that there exist n agents sharing some common resources. Let us assume that agents increase in size if they acquire some portion of the resources or have their size reduced if any market portion is lost. Our mathematical model is defined by an n-dimensional differential equation:

$$
\dot{s}_i = \alpha_i s_i \left(\beta - \sum_{i=1}^n s_i \right) - \sum_{i \neq j} k_{ij} \exp \left[-\left(\frac{s_i - s_j}{\sigma} \right)^2 \right] s_i s_j, \qquad i = 1, \ldots, n
$$

(4.3.4)

where s_i is the agent size such that $0 < s_i \leq 1$; $\dot{s}$ is its time derivative; α_i is the growth rate of agent i if no interaction is present; β is the market capacity and k_{ij} is the element of the network matrix $\mathbf{K}$ which determines the interaction between agent i and j. The interaction function $\gamma(s_i, s_j)$ is composed of dynamic parameters that result from the difference between agents in relation; the parameter σ is a positive parameter that regulates the difference in the agent's size. Note that while $\mathbf{K}$ indicates what interaction is present, σ determines the "range" of interaction of the agents. Indeed, in contrast to the "large" interaction between equal size agents, the intensity of interactions between "agents with bigger market share" and "those with small market share" occurs to be weak, since as $\mid s_i - s_j \mid \to \infty$, the interaction function $\gamma(s_i, s_j) \to 0$; on the contrary, indeed, as $\mid s_i - s_j \mid \to 0$, $\gamma(s_i, s_j) \to \pm 1$ depending on k_{ij}, which signifies a strong interaction between agents with similar sizes.

For the sake of simplicity, without much losing generality, it can be assumed that the agents have the same dynamic properties $\alpha_i = 1$, while the market

capacity can be $\beta = 1$. Therefore, equation (4.3.4) becomes:

$$\dot{s}_i = s_i \left(1 - \sum_{i=1}^{n} s_i \right) - \sum_{i \neq j} k_{ij} \exp\left[-\left(\frac{s_i - s_j}{\sigma} \right)^2 \right] s_i s_j, \qquad i = 1, \ldots, n$$

$$(4.3.5)$$

where, as stated earlier, k_{ij}, $i, j = 1, \ldots, n$ are elements of the interaction matrix $\mathbf{K}$.

4.4   Fixed Point and Stability Analysis

In this section, the fixed point analysis of the model is done in order to investigate the stability of the system for all scenarios. A triad system of agent (i.e. $n = 3$) was chosen as a simple yet complex representative of a basic network, in order to illustrate some of the properties of the model analytically.

Suppose A_1, A_2 and A_3 are triad interacting agents with market sizes s_1, s_2 and s_3 respectively, from equations (3.3) the system of triads becomes:

$$\dot{s}_1 = s_1(1 - \sum_{i=1}^{3} s_i) - k_{12} \exp^{-\left(\frac{s_1-s_2}{\sigma}\right)^2} s_1 s_2 - k_{13} \exp^{-\left(\frac{s_1-s_3}{\sigma}\right)^2} s_1 s_3, \quad (4.4.1)$$

$$\dot{s}_2 = s_2(1 - \sum_{i=1}^{3} s_i) - k_{12} \exp^{-\left(\frac{s_2-s_1}{\sigma}\right)^2} s_2 s_1 - k_{23} \exp^{-\left(\frac{s_2-s_3}{\sigma}\right)^2} s_2 s_3, \quad (4.4.2)$$

$$\dot{s}_3 = s_3(1 - \sum_{i=1}^{3} s_i) - k_{13} \exp^{-\left(\frac{s_3-s_1}{\sigma}\right)^2} s_3 s_1 - k_{23} \exp^{-\left(\frac{s_3-s_2}{\sigma}\right)^2} s_3 s_2. \quad (4.4.3)$$

The possible $\mathbf{K}$-matrices for describing the different scenarios of interaction amongst the agents A_1, A_2 and A_3 are:

$$\mathbf{K}_1 = \begin{bmatrix} 0 & 1 & 1 \\ 1 & 0 & 1 \\ 1 & 1 & 0 \end{bmatrix}, \qquad \mathbf{K}_2 = \begin{bmatrix} 0 & 1 & 1 \\ 1 & 0 & -1 \\ 1 & -1 & 0 \end{bmatrix},$$

$$\mathbf{K}_3 = \begin{bmatrix} 0 & -1 & -1 \\ -1 & 0 & 1 \\ -1 & 1 & 0 \end{bmatrix}, \qquad \mathbf{K}_4 = \begin{bmatrix} 0 & -1 & -1 \\ -1 & 0 & -1 \\ -1 & -1 & 0 \end{bmatrix}$$

where $\mathbf{K}_1$ represents the matrix for a full competitive system with three interacting agents; $\mathbf{K}_2$ is a matrix for mixed-type of interaction system, where one agent compete with two other agents in cooperation. In this case, agent A_1 competes with agent A_2 and agent A_3 which are in cooperation. $\mathbf{K}_3$ is a

matrix for mixed-type of interaction system, where one agent cooperates with two other agents in competition, in this case, agent A_1 cooperates with agent A_2 and agent A_3 which are in competition with each other. $\mathbf{K}_4$ represents the matrix for a full cooperative system amongst the three interacting agents. It can be observed that other cases of the mixed-type of interaction are isomorphic to the ones here presented.

The fixed point analysis of the system entails the evaluation of the eigenvalues of the relevant Jacobian matrix computed at each corresponding fixed point, thus used to determine the stability of the system. When the real part of all the eigenvalues is negative, the system is said to be stable. If at least one eigenvalue has a positive real part, the system is unstable.

4.4.1 Fixed Point

A fixed point is a point in the phase space where all the time derivatives are zero, i.e., $\dot{s}_i = 0$ for $i = 1 \ldots, n$. The following fixed points were detected analytically[1] from equations (4.4.1)- (4.4.3):

(I) All agents with zero size, i.e., $s_i = 0$ for $i = 1, 2, 3$.

(II) Two agents with size equal to zero: necessarily, the third agent monopolizes the market. i.e., $s_i = 1$ and $s_j = 0$ for every $i \neq j$.

(III) Two agents are of equal size in the market while the third is of size zero.

(IV) All agents own an equal share of the market, i.e, $s_i = b$ for $i = 1, 2, 3$, $0 < b \leq 1$.

Moreover it can be easily shown that the elements of the Jacobian matrix [2] of the triads are:

$$[J]_{(i,k)} = \frac{\partial \dot{s}_i}{\partial s_k} = \begin{cases} 1 - 2s_i - \sum_{i \neq j} s_j \left(1 + \gamma(s_i, s_j) \left[1 - \frac{2}{\sigma^2} s_i(s_i - s_j)\right]\right), & \text{for } k = i; \\ \\ -s_i - s_i \gamma(s_i, s_k) \left[1 - \frac{2}{\sigma^2} s_k(s_i - s_k)\right], & \text{for } k \neq i, \end{cases}$$

from which the stability conditions are to be found at each fixed point.

4.4.2 Stability Analysis

Type (I) Fixed Point

The type (I) fixed point analysis is the case in which all agents have size zero, i.e., $s_i = 0$ for $i = 1, 2, 3$. The evaluated Jacobian matrix at the type (I) fixed

---

[1]Details of fixed point analysis shown in Appendix B.
[2]Derivation of the Jacobian matrix is shown in Appendix B.

	Full Competition	Full Cooperation	Mixed Interactions	
Type	K_1	K_4	K_2	K_3
I	(0,0,0)	(0,0,0)	(0,0,0)	(0,0,0)
	(1,0,0)	(1,0,0)	(1,0,0)	(1,0,0)
II	(0,1,0)	(0,1,0)	(0,1,0)	(0,1,0)
	(0,0,1)	(0,0,1)	(0,0,1)	(0,0,1)
	(0,1/3,1/3)	(0,1,1)	(0,1,1)	(0,1/3,1/3)
III	(1/3,0,1/3)	(1,0,1)	(1/3,0,1/3)	(0,1,0)
	(1/3,1/3,0)	(1,1,0)	(1/3,1/3,0)	(1,1,0)
IV	(1/5,1/5,1/5)	(1,1,1)	-	-

Table 4.1: Coordinates of fixed points.

point, is given by:

$$\mathbf{J} = \begin{bmatrix} 1 & 0 & 0 \\ 0 & 1 & 0 \\ 0 & 0 & 1 \end{bmatrix}$$

whose eigenvalues are all equal to 1 (i.e., $\lambda_1 = \lambda_2 = \lambda_3 = 1$). Trivially, it is an unstable fixed point. At this fixed point, competition or cooperation is not applicable since all agents are at level zero. In other words, these results do not depend on the network matrix K.

Type (II) Fixed Point

The type (II) fixed point analysis corresponds to having two agents with size equal to zero; necessarily, the third agent monopolizes the market. The Jacobian matrices for the fixed points $(\beta,0,0),(0,\beta,0)$ and $(0,0,\beta)$ are:

$$J_{(\beta,0,0)} = \begin{bmatrix} 1-2\beta & -\beta-\beta\phi_{12} & -\beta-\beta\phi_{13} \\ 0 & 1-\beta-\beta\phi_{21} & 0 \\ 0 & 0 & 1-\beta-\beta\phi_{31} \end{bmatrix},$$

$$
J_{(0,\beta,0)} = \begin{bmatrix} 1 - \beta - \beta\phi_{12} & 0 & 0 \\ -\beta - \beta\phi_{21} & 1 - 2\beta & -\beta - \beta\phi_{23} \\ 0 & 0 & 1 - \beta - \beta\phi_{32} \end{bmatrix},
$$

$$
J_{(0,0,\beta)} = \begin{bmatrix} 1 - \beta - \beta\phi_{13} & 0 & 0 \\ 0 & 1 - \beta - \beta\phi_{23} & 0 \\ -\beta - \beta\phi_{31} & -\beta - \beta\phi_{32} & 1 - 2\beta \end{bmatrix},
$$

where $\phi_{ij} = k_{ij}\exp(-(\beta/\sigma)^2)$ for $i, j = 1, 2, 3$ and $i \neq j$.

1. For $J_{(\beta,0,0)}$, the corresponding eigenvalues are $\lambda_1 = 1 - 2\beta$, $\lambda_2 = 1 - \beta - \beta\phi_{21}$, $\lambda_3 = 1 - \beta - \beta\phi_{31}$. When $k_{21} = -1$ and $k_{31} = -1$, the fixed point is unstable since $\exp(-\sigma^{-2})$ is always positive for $\sigma > 0$. When $k_{21} = 1$ and $k_{31} = -1$ or $k_{21} = -1$ and $k_{31} = 1$, the fixed point still remains unstable. Stability of the fixed point $(\beta,0,0)$ occurs only when $\Gamma_{21} = 1$ and $\Gamma_{31} = 1$.

2. For $J_{(0,\beta,0)}$, the corresponding eigenvalues are $\lambda_1 = 1 - \beta - \beta\phi_{12}$, $\lambda_2 = 1 - 2\beta$, $\lambda_3 = 1 - \beta - \beta\phi_{32}$. Since $\beta = 1$ in our model, $\lambda_1 = -\phi_{12}$, $\lambda_2 = -1$, $\lambda_3 = -\phi_{32}$. When $k_{12} = 1$ and $k_{32} = 1$, the system is stable, otherwise the fixed point is unstable.

3. For $J_{(0,0,\beta)}$, the corresponding eigenvalues are $\lambda_1 = 1 - \beta - \beta\phi_{13}$, $\lambda_2 = 1 - \beta - \beta\phi_{23}$, $\lambda_3 = 1 - 2\beta$. Since $\beta = 1$ in our model, $\lambda_1 = -\phi_{13}$, $\lambda_2 = -\phi_{23}$, and $\lambda_3 = -1$. When $k_{13} = 1$ and $k_{23} = 1$, the system is stable, otherwise the fixed point is unstable.

In the fully competitive scenario, all $k_{ij} = 1$ for $i \neq j$, thereby resulting to an all negative eigenvalues of all the Jacobian matrices. Indeed, this implies stability of the system at this fixed point. This is applicable in real systems: if an agent monopolizes the competitive market, the agent will ensure that such a domination is not lost, whence keeping the market stable.

On the contrary, in the fully cooperative scenario, λ_2 and λ_3 are positive, since all $k_{ij} = -1, i \neq j$, thereby making the system unstable. This is also realistic, since in cooperation, the ultimate goal is the maximization of all agents gain in the market. Therefore, it can be emphasized that monopoly and cooperation are not compatible terms. This accounts for systemic instability.

Under the mixed interaction scenario, systemic stability is only obtained at the fixed point $(1,0,0)$ for the interaction matrix $\mathbf{K}_2$.

In conclusion, the type (II) fixed point is stable in a full competitive scenario because of the possibility of monopoly, but is unstable under full cooperation.

Type (III) Fixed Point

The type (III) fixed points analysis is the case in which two agents are of equal size in the market while the third agent is of size zero. Therefore we have the fixed points as $(0, a, a), (a, 0, a)$ and $(a, a, 0)$ where $a = \frac{1}{3}$ and $a = 1$ are the two possible cases obtained analytically.

The Jacobian Matrix $J_{(a,0,a)}$ is given by:

$$
J_{(a,0,a)} = \begin{bmatrix} 1 - 3a - ak_{13} & -a - a\theta_{12} & -a - ak_{13} \\ 0 & 1 - 2a - a(\theta_{21} + \theta_{23}) & 0 \\ -a - ak_{31} & -a - a\theta_{32} & 1 - 3a - k_{31} \end{bmatrix},
$$

where $\theta_{ij} = k_{ij} \exp^{-} \left(\frac{a}{\sigma} \right)^{2}$. It can be noted that when $a = 1$, $\theta_{ij} = \phi_{ij}$.

1. When $a = \frac{1}{3}$, the Jacobian matrix becomes

$$
J_{(\frac{1}{3},0,\frac{1}{3})} = \begin{bmatrix} -\frac{1}{3}k_{13} & -\frac{1}{3} - \frac{1}{3}\theta_{12} & -\frac{1}{3} - \frac{1}{3}k_{13} \\ 0 & -\frac{1}{3} - \frac{1}{3}(\theta_{21} + \theta_{23}) & 0 \\ -\frac{1}{3} - \frac{1}{3}k_{31} & -\frac{1}{3} - \frac{1}{3}\theta_{32} & -\frac{1}{3}k_{31} \end{bmatrix},
$$

where $\theta_{ij} = k_{ij} \exp^{-} \left(\frac{1}{3\sigma} \right)^{2}$. The corresponding eigenvalues[3] for $J_{(\frac{1}{3},0,\frac{1}{3})}$ is $\lambda_1 = \frac{1}{3}$, $\lambda_2 = \frac{1}{3} - \frac{1}{3}(k_{21} \exp^{-} \left(\frac{1}{3\sigma} \right)^{2} + k_{23} \exp^{-} \left(\frac{1}{3\sigma} \right)^{2})$ and $\lambda_3 = \frac{1}{3}$, which indicates that the system is unstable. This fixed point is possible under full competition and mixed interaction but not in the full cooperative scenario. The stability analysis of the Jacobian Matrix $J_{(0,\frac{1}{3},\frac{1}{3})}$ $J_{(\frac{1}{3},\frac{1}{3},0)}$ is similar to $J_{(\frac{1}{3},0,\frac{1}{3})}$. The full result is shown on Table 4.2.

2. When $a = 1$, the Jacobian matrix becomes

$$
J_{(1,0,1)} = \begin{bmatrix} -2 - k_{13} & -1 - \phi_{12} & -1 - k_{13} \\ 0 & -1 - (\phi_{21} + \phi_{23}) & 0 \\ -1 - k_{31} & -1 - \theta_{32} & -2 - k_{31} \end{bmatrix},
$$

where $\phi_{ij} = k_{ij} \exp^{-} \left(\frac{1}{\sigma} \right)^{2}$. The corresponding eigenvalues[4] for $J_{(1,0,1)}$ is $\lambda_1 = -1 - \phi_{12} - \phi_{23}$, $\lambda_2 = -1$ and $\lambda_3 = -3 - 2k_{13}$. The stability for the system depends mainly on the value of λ_1, since λ_2 and λ_3 is always negative. When $k_{12} = k_{23} = 1$, the system is stable. Suppose $k_{12} = -1$ and $k_{23} = 1$ or vice versa, the system still remains stable. Since the values of $\lambda_1 = -1$. The fixed point is only possible under the full cooperative

---

[3]Details of analysis is shown in Appendix B.
[4]Details of analysis is shown in Appendix B.

	Full Competition	Full Cooperation	Mixed Interactions	
Type	K_1	K_4	K_2	K_3
I	Unstable	Unstable	Unstable	Unstable
II	**Stable**	Unstable	**Stable**	Unstable
	Stable	Unstable	Unstable	Unstable
	Stable	Unstable	Unstable	Unstable
III	Unstable	**Stable**	**Stable**	Unstable
	Unstable	**Stable**	Unstable	**Stable**
	Unstable	**Stable**	Unstable	**Stable**
IV	Unstable	**Stable**	-	-

Table 4.2: Summary of Stability Analysis for Interaction Matrices.

and the mixed interaction scenarios, therefore, even though one of the agent is of size zero, the systemic stability is always observed at this fixed point. The stability analysis of $J_{(1,1,0)}$ and $J_{(0,1,1)}$ is similar to the analysis shown above.

Type (IV) Fixed Point

The type (IV) fixed point analysis is the case in which all agents are eventually owning the same share of the market, i.e., $s_i = b$ for $i = 1, 2, 3$, $0 < b \leq 1$. This is only applicable under the full competition and full cooperation interactions. When evaluating the Jacobian matrix at this fixed point, the constant b has to be calculated first by substituting $s_i = b$ and $\dot{s}_i = 0$ into Equations (4.4.1)-(4.4.3). From (4.4.1), it can be deduced that:

$$0 = b(1 - 3b) - (k_{12} + k_{13})b^2 \tag{4.4.4}$$

$$= 1 - b(3 + (k_{12} + k_{13})). \tag{4.4.5}$$

Therefore,

$$b = \frac{1}{(3 + (k_{12} + k_{13}))}. \tag{4.4.6}$$

Similarly from (4.4.2) and (4.4.3) respectively, the following is obtained:

$$b = \frac{1}{(3 + (k_{12} + k_{23}))}. \tag{4.4.7}$$

$$b = \frac{1}{(3 + (k_{13} + k_{23}))}. \tag{4.4.8}$$

Therefore, from equations (4.4.6)-(4.4.8), it can be deduced that in a fully competitive system (i.e. $k_{12} = k_{13} = k_{23} = 1$), the agent size is $b = \frac{1}{5}$. This implies that the aggregate size of the three agents does not reach the market maximum possible capacity, which may be the negative result of the competition amongst peers.

Thus, for a full competition of agents with the same size, the Jacobian matrix with $b = \frac{1}{5}$ is:

$$\mathbf{J} = \frac{1}{5} \begin{bmatrix} -1 & -2 & -2 \\ -2 & -1 & -2 \\ -2 & -2 & -1 \end{bmatrix},$$

the eigenvalues are obtained from the characteristic polynomial

$$(-1 - \lambda)^3 - 12(-1 - \lambda) - 16 = 0$$

The solution to the above cubic equation is $\lambda_1 = \lambda_2 = 1$ and $\lambda_3 = -5$. This shows that the system is unstable at this fixed point. When all the agents have an equal size in a competitive market, the system will be unstable; because the major goal of each agent is to *individually* dominate the market. According to the model, agents with "similar" sizes are strongly interacting; this leads to a "survival of the fittest" scenario in such a competitive system, - thereby making the system unstable.

In contrast, for a cooperative system (i.e. $k_{12} = k_{13} = k_{23} = -1$), we have $b = 1$, that is, collaboration makes all agents reach the market full capacity with agent sizes as a function of time possibly intersecting one another.

The corresponding Jacobian matrix for the cooperative system with $b = 1$ is:

$$\mathbf{J} = \begin{bmatrix} -1 & 0 & 0 \\ 0 & -1 & 0 \\ 0 & 0 & -1 \end{bmatrix};$$

the eigenvalues are obtained from the equation:

$$(-1 - \lambda)^3 = 0$$

which implies that the system is stable, since $\lambda_{1,2,3} = -1$. When all the agents with *quasi* equal market share cooperate, with the collective goal of maximizing their profit (size) in the market, the system will definitely be stable; their goal will be achieved since the strongest possible interaction exists amongst agents with similar sizes.

It can be noted that when $b = \frac{1}{3}$, (i.e. $k_{12} = k_{13} = k_{23} = 0$), there exists no interaction amongst the triads agents of equal sizes and this leads to the case whereby the agents "share the market" equally.

4.5 Conclusion

A summary of the fixed point analysis of our model with the network matrix $\mathbf{K}_1$, $\mathbf{K}_2$, $\mathbf{K}_3$ and $\mathbf{K}_4$ was presented in Table 4.2. On this table, it was shown that systemic stability is observed under full competitive scenario only when one agent monopolizes the market, but under the fully cooperative scenario, stability occurs when at least two of the agents own an equal share of the market. By observation, the system tends to be unstable when the agent sizes does not add up to the market capacity or when the interaction matrix is not compatible with the fixed points. For instance, the system is unstable under full cooperation when there is monopoly. In practical terms, the agents, which in this case are the energy firms, interacts together in a competitive, cooperative or mixed-type of interaction. The system becomes unstable when demands are not met in the market (i.e. when the agent sizes are not up to the market capacity). Intersection of agent sizes is assumed during collaboration. Simulation of interactions among the agents will be shown and analyzed in the next chapter.

Chapter 5

Simulation on Agent Interaction

5.1 Introduction

In this chapter, we present results from numerical simulations emphasizing the initial conditions and the convergence of triad agent sets for all interesting and possible scenarios, for each network matrix type $\mathbf{K} = \{\mathbf{K}_1, \mathbf{K}_2, \mathbf{K}_3, \mathbf{K}_4\}$.

For the sake of clarity, in Fig 5.1, the four possible scenarios are illustrated through undirected graphs with three vertices representing agents A_1, A_2 and A_3 and three edges which signify the type of interaction amongst the agents. An edge with solid line signifies a competitive interaction while an edge with dashed lines signifies a cooperative interaction. Therefore, it can be deduced that in Fig 5.1, graph $\mathbf{G}_1$ represents the full competitive scenario, $\mathbf{G}_2$ represents the first case of the mixed-interactive scenario in which agent A_1 competes with A_2 and A_3, themselves in cooperation. Graph $\mathbf{G}_3$ represents the second case of the mixed-interactive scenario in which agent A_1 cooperates with A_2 and A_3, themselves in competition and $\mathbf{G}_4$ represents the full cooperative scenario.

We have tested different sets of initial conditions; see a few exemplary cases in Table (5.1). We have verified the coherence of results. These results led to presenting only cases in which the initial conditions of agent sizes are rather different or quite similar, assuming a constant parameter that controls the size similarity, $\sigma = 1$. The dynamic change in agent's size and relative behavior have been observed for each scenario. Finally, note that agent's sizes initial conditions were chosen within a small interval in order to allow some "meaningful" interaction amongst the agents; since within our model, indeed, as $\mid s_i - s_j \mid \to \infty$, the interaction function $\gamma(s_i, s_j) \to 0$.

5.2 Fully Competitive Scenario

The fully competitive scenario with different initial conditions for the agent's size is observed in Fig 5.2 with a consideration on dynamical change in the agent size; the market eventually ends in a monopoly. For all the permutations

Figure 5.1: Graphical illustration of the four scenarios.
An edge with solid line signifies a competitive interaction while an edge with dashed line signifies a cooperative interaction. Pictures respectively refers to:
(a) G_1, (b) G_2, (c) G_3 and (d) G_4

of the initial conditions, the agent that starts with the highest initial size, i.e $s_0 = 0.4$, commenced interaction with significantly higher market share (firm's resources and capabilities) than the other agents, this creates a competitive advantage over the other agents in the market. According to Porter M. E. in [40], competitive advantage is when the firm is able to deliver the same benefits as competitors but at a lower cost (cost advantage) or deliver benefits that exceed those of competing products (differentiation advantage). The interaction results in the "Leader takes all" phenomenon which is caused by the existence of the Matthew effect also known as the "rich get richer" effect [30, 56]. This implies that the energy producing firms with competitive advantage over other firms eventually monopolize the market while satisfying demands of consumers at minimum cost, while the other two agents fade out of the market. This is possible because the two agents with smaller sizes compete too weakly with the agent that eventually dominates the market.

Competitive advantage is not permanent and therefore can be lost in the market. This may be due to lack of innovation, advancement in technology, etc. This leads to reduction in firm share in a competitive market or total exit from the market. When agents sizes are now similar as shown in Fig. 5.2, the competition becomes very "fierce" and all agents are struggling for their survival in the market. After some time span, it is observed that the agents eventually have an equal share of the market; their total market share is however lower than the market capacity. Thus, strong competition among peers is shown to lead to a reduction in the aggregate output due to the selfish interest of the individual agents. Indeed, observe that the final state is $\sum s_i = 0.6$. Convergence is generally slower in the competitive scenario when compared with the other scenarios due to the nature and effect of competition amongst the interacting agents.
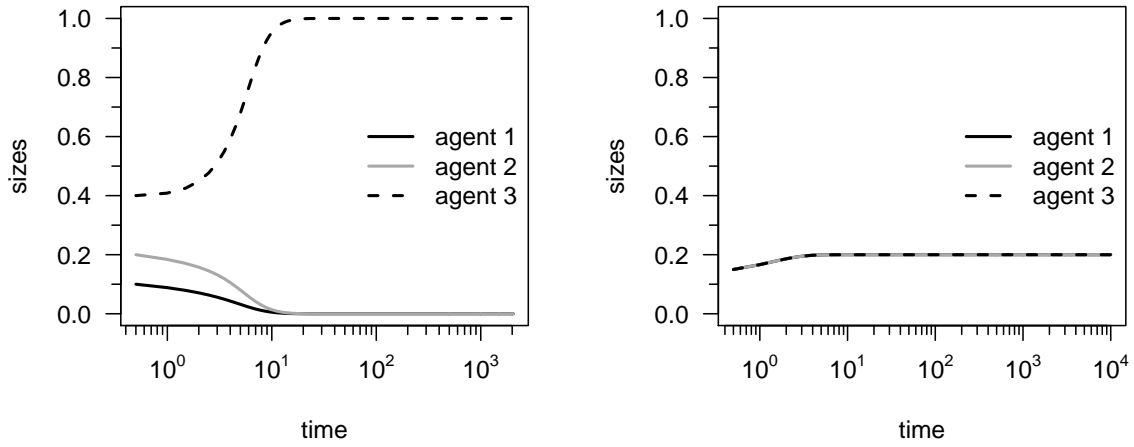
Figure 5.2: Fully Competitive Scenario (G_1) with different (lhs) and similar (rhs) agent's initial sizes.

5.3 Fully Cooperative Scenario

The fully cooperative scenario (G_4) is analyzed for different initial sizes of the triads and illustrated in Fig 5.3. It has been discovered [12] that "Collaboration is a key driver of overall performance of companies around the world. Its impact is twice as significant as a company's aggressiveness in pursuing new market opportunities (strategic orientation) and five times as significant as the external market environment (market turbulence)". It has significant impact on the firm's overall performance which determines the final market share of the firm. The collaboration amongst the agents enables all agents to grow in size up to this market capacity, thereby increasing the total market size, - which is the essence of cooperation ($\sum s_i > 1.0$). This implies that energy producing firms can collaborate together to meet demand in the market, despite their different initial sizes. Collaboration in this case involves intersection of the agent sizes.

The simulation leads to the same effect, even if the initial conditions are permuted amongst the triads and when the agents have similar initial sizes as shown in Fig 5.3. Also, agents tend to "quickly agree", thereby converging within a short time lapse.

5.4 The Single Pair Cooperation

The mixed interaction scenario (G_2), when agent A_1 competes with agents A_2 and A_3 themselves in cooperation is shown in Fig 5.4 - Fig 5.5 for different permuted initial conditions of agent's sizes. It can be observed that in all sim-
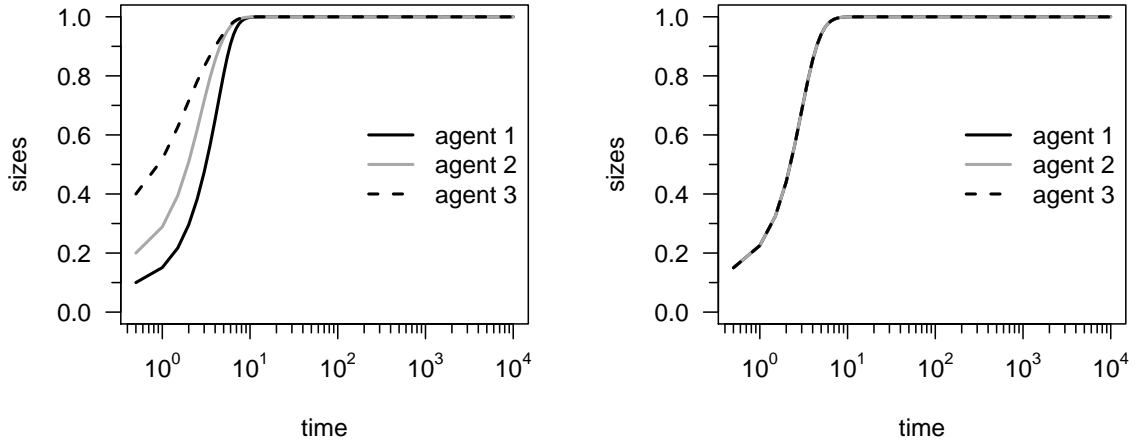
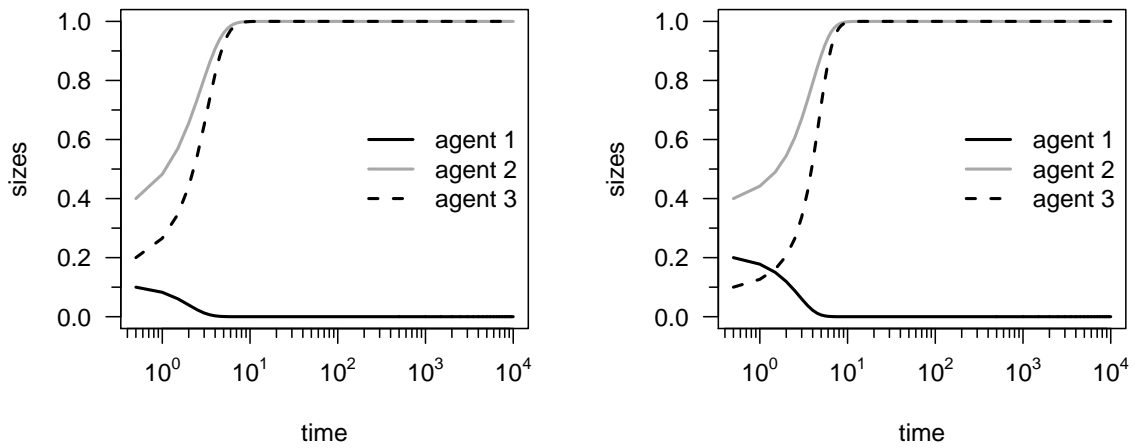Figure 5.3: Fully Cooperative Scenario (G_4) with different (lhs) and similar (rhs) agent's sizes.

Figure 5.4: Mixed Interaction Scenario (G_2), A_1 competes with A_2 and A_3 in pair cooperation, for different initial sizes.
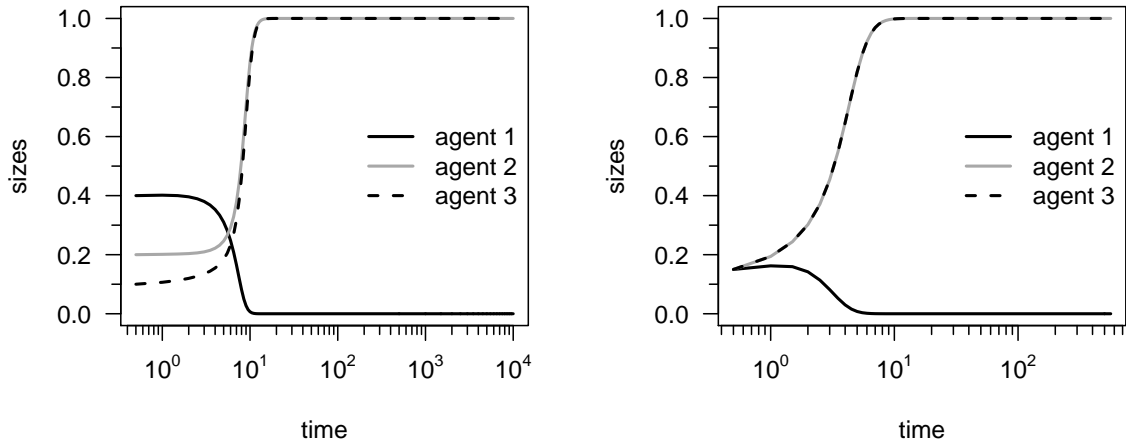
Figure 5.5: Mixed Interaction Scenario (G_2): A_1 competes with A_2 and A_3 in a pair cooperation, for different (lhs) or similar (rhs) initial sizes.

ulations, the sizes of agents A_2 and A_3 in cooperation grow dynamically with time up to the market capacity but agent A_1 decreases in size until it fades out of the market. The most interesting simulation is seen in Fig 5.5, with different initial conditions $s_0 = \{0.4, 0.2, 0.1\}$ where agent A_1 initially possesses the biggest share of the market with $s_1 = 0.4$, competes with the two other agents A_2 and A_3 that alternate a smaller size 0.1 and 0.2. Note that the sum of the two initial shares of the cooperating agents is lower than the share of the competing agents. Interestingly, after some time, the collaboration between agents A_2 and A_3 knocks out agent A_1 from the market. This affirms the words of Jaclyn Kostner, Ph.D., best-selling author, and expert on high-performance virtual collaboration which says, *"As a general rule, global companies that collaborate better, perform better. Those that collaborate less, do not perform as well. It's just that simple"*[12]. However, this is not possible if the intensity of interactions is very low amongst the agents; that is, when A_1 is "extremely bigger" in size when compared to agents A_2 and A_3.

When all the agents have similar initial conditions, the pattern is similar with agents A_2 and A_3 totally taking over the market by growing up to the market capacity as seen in Fig 5.5.

5.5 The Double Pair Cooperation

Finally, the second possible case of mixed interaction scenario (G_3) is shown in Fig 5.6 - Fig 5.7; agent A_1 cooperates with agents A_2 and A_3 themselves in
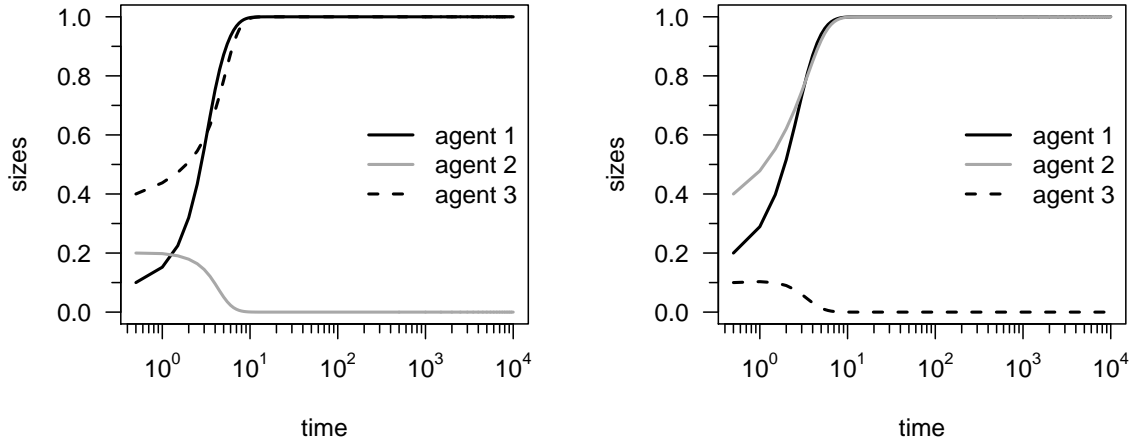
Figure 5.6: Mixed Interaction Scenario (G_3), A_1 cooperates with A_2 and A_3 in competition for different initial sizes.
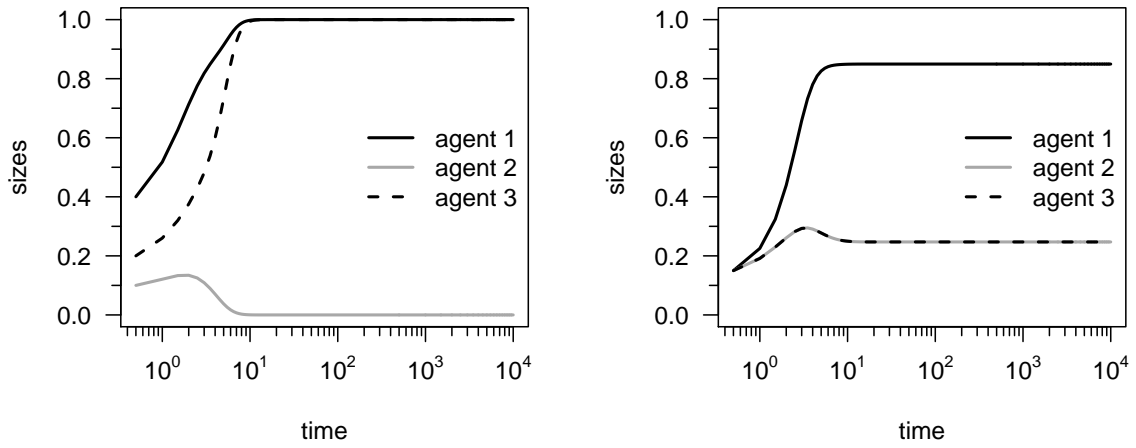

Figure 5.7: Mixed Interaction Scenario(G_3), A_1 cooperates with A_2 and A_3 in competition for different (lhs) or similar (rhs) initial sizes.

competition, for different permuted initial conditions of agent's sizes.

When agent A_1 cooperates strongly with the agent with a higher initial condition and cooperates weakly with the other one. Such strategic decision by small firms to collaborate with larger firms accelerate growth and create stability which in turn gives them a competitive advantage over other competing firms in market. Also, as written in [17], start-up firms are likely to be more informed, innovative and more creative than long standing larger firm. Therefore, partnership with such start-up firms is also beneficial to the growth of the larger firm as observed in Fig 5.6 - Fig 5.7. The effect of cooperation makes agent A_1 (irrespective of its initial condition) and any one of the two agents that cooperates strongly with agent A_1 grows up to the market capacity, while the effect of weak cooperation and competition between agents A_2 and A_3 makes the agent with the lower initial condition vanishing from the market.

Surprisingly, when the three agents have the same initial size, the simulation turns out interesting also, as seen in Fig 5.7, - unlike the first case of mixed interaction. When agent A_1 cooperates strongly with agents A_2 and A_3 which are in strong competition with each other, the effect of this strong and opposite interaction in the system results in a final state in which no agent is attaining the market capacity, but each agent nevertheless grows above its initial size; all three agents remained active in the market. Nevertheless, agent A_1 possesses the "lion share" of the market by taking advantage of the competition between the other agents to collaborate differently with them.

5.6   Conclusion

A summary of the simulations of the triad interaction agents is presented in Table (5.1). The characteristic values pertain to agent's size initial conditions, final size and the time of convergence. It can be observed that convergence is slower during competition, due to the conflicting interests of interacting agents; in contrast, during cooperation, agents tend to "agree", thereby converging within a shorter time lapse. For the mixed interaction cases, when agent A_1 competes with agents A_2 and A_3 in cooperation, a scenario with two collaborating agents in conflict with one, the time of convergence is seen to be faster than when agent A_1 cooperates with agents A_2 and A_3 in competition: this can be understood due to the collaborative effect of mixed interactions being higher in the first case than in the second case.
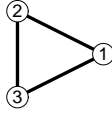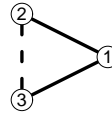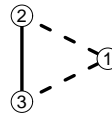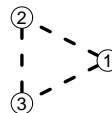
Scenario	Initial Sizes $s_i(0)$			Growth (+) / Decay (-)		
Full Competition G_1	0.1	0.2	0.4	-	-	+
	0.1	0.4	0.2	-	+	-
	0.4	0.1	0.2	+	-	-
	0.4	0.2	0.1	+	-	-
	0.2	0.4	0.1	-	+	-
	0.2	0.1	0.4	-	-	+
	0.15	0.15	0.15	+	+	+
	0.3	0.3	0.3	-	-	-
Mixed Interaction G_2	0.1	0.2	0.4	-	+	+
	0.1	0.4	0.2	-	+	+
	0.4	0.1	0.2	-	+	+
	0.4	0.2	0.1	-	+	+
	0.2	0.4	0.1	-	+	+
	0.2	0.1	0.4	-	+	+
	0.15	0.15	0.15	-	+	+
	0.3	0.3	0.3	-	+	+
Mixed Interaction G_3	0.1	0.2	0.4	+	-	+
	0.1	0.4	0.2	+	+	-
	0.4	0.1	0.2	+	-	+
	0.4	0.2	0.1	+	+	-
	0.2	0.4	0.1	+	+	-
	0.2	0.1	0.4	+	-	+
	0.15	0.15	0.15	+	+	+
	0.3	0.3	0.3	+	-	-
Full Cooperation G_4	0.1	0.2	0.4	+	+	+
	0.1	0.4	0.2	+	+	+
	0.4	0.1	0.2	+	+	+
	0.4	0.2	0.1	+	+	+
	0.2	0.4	0.1	+	+	+
	0.2	0.4	0.1	+	+	+
	0.15	0.15	0.15	+	+	+
	0.3	0.3	0.3	+	+	+

Table 5.1: Summary of the effect of initial size conditions for the various scenarios as obtained from simulations, i.e. changing the relative initial sizes of the agents.

Appendix A

Technical Terms in LCOE Computation

1. **Capacity Factor**: The net capacity factor is the unitless ratio of an actual electrical energy output over a given period of time to the maximum possible electrical energy output over the same amount of time. It is generally measured as a percentage.

2. **Capacity Value**: This refers to the contribution of a power plant to reliably meet demand. The capacity value (or capacity credit) is measured either in kilowatt (kW), megawatt(MW), or gigawatt (GW) or the fraction of its nameplate capacity (%). For instance, the plant with a nameplate capacity of 150 MW could have a capacity value of 75 MW or 50%.

3. **Heat Rate**: Heat rate is generally defined as the amount of fuel required to generate one unit of electricity in a power plant.

4. **Nameplate Capacity**: This is generally referred to as the maximum output (i.e., generation) of a power plant. Nameplate capacity is typically measured in a kilowatt (kW), megawatt(MW), or gigawatt (GW) rating. It may also be referred to as nominal capacity or installed capacity. This may be further distinguished as the net capacity of the plant after plant parasitic loads have been considered, which are subtracted from gross capacity.

Asset depreciation D_n^α used in the LCOE model through out the thesis is technology dependent and it is computed using the MACRS system (Modified Accelerated Cost Recovery System) displayed in Table (A).

	MACRS,15	MACRS,20
Year 1	5.00%	3.750%
Year 2	9.50%	7.219%
Year 3	8.55%	6.677%
Year 4	7.70%	6.177%
Year 5	6.93%	5.713%
Year 6	6.23%	5.285%
Year 7	5.90%	4.888%
Year 8	5.90%	4.522%
Year 9	5.91%	4.462%
Year 10	5.90%	4.461%
Year 11	5.91%	4.462%
Year 12	5.90%	4.461%
Year 13	5.91%	4.462%
Year 14	5.90%	4.461%
Year 15	5.91%	4.462%
Year 16	2.95%	4.461%
Year 17		4.462%
Year 18		4.461%
Year 19		4.462%
Year 20		4.461%
Year 21		2.231%

Table A.1: Depreciation Schedule.

Appendix B

Details on Fixed Point and Stability Analyses

B.1 Mathematical Model

Our mathematical model is defined by an n-dimensional differential equation:

$$\dot{s}_i = s_i \left(1 - \sum_{i=1}^{n} s_i \right) - \sum_{i \neq j} k_{ij} \exp \left[- \left(\frac{s_i - s_j}{\sigma} \right)^2 \right] s_i s_j, \qquad i = 1, \ldots, n.$$

For simplicity, when $n = 3$, the above differential equations becomes:

$$\begin{aligned}
\dot{s}_1 &= s_1(1 - s_1 - s_2 - s_3) - \gamma(s_1, s_2)s_1s_2 - \gamma(s_1, s_3)s_1s_3, & \text{(B.1.1)} \\
\dot{s}_2 &= s_2(1 - s_1 - s_2 - s_3) - \gamma(s_2, s_1)s_2s_1 - \gamma(s_2, s_3)s_2s_3, & \text{(B.1.2)} \\
\dot{s}_3 &= s_3(1 - s_1 - s_2 - s_3) - \gamma(s_3, s_1)s_3s_1 - \gamma(s_3, s_2)s_3s_2, & \text{(B.1.3)}
\end{aligned}$$

where

$$\gamma(s_i, s_j) = k_{ij} \exp \left[- \left(\frac{s_i - s_j}{\sigma} \right)^2 \right]. \qquad \text{(B.1.4)}$$

B.2 Fixed Point Analysis

A fixed point is a point in the phase space where all the time derivatives are zero, i.e., $\dot{s}_i = 0$ for $i = 1, \ldots, n$.

(I) Trivially, the point (0,0,0) is a fixed point. That is, when $s_1 = 0$, $s_2 = 0$ and $s_3 = 0$, then $\dot{s}_i = 0$ for $i = 1, \ldots, 3$ is satisfied.

(II) Trivially, the points (1,0,0), (0,1,0) and (0,0,1) are fixed points.

(III) Computation for the type (III) fixed point from Equations (B.1.1)-B.1.3) at $\dot{s}_i = 0$ is shown below:

(a.) When $s_1 = 0$, $s_2 \neq 0$ and $s_3 \neq 0$, Equations (B.1.1)- (B.1.3) becomes:

$$0 = s_2(1 - s_2 - s_3) - \gamma(s_2, s_3)s_2s_3, \qquad \text{(B.2.1)}$$
$$0 = s_3(1 - s_2 - s_3) - \gamma(s_3, s_2)s_3s_2. \qquad \text{(B.2.2)}$$

They can be further simplified as

$$s_2(1 - s_2 - s_3) = \gamma(s_2, s_3)s_2s_3,$$
$$s_3(1 - s_2 - s_3) = \gamma(s_3, s_2)s_3s_2,$$

this implies that

$$s_2(1 - s_2 - s_3) = s_3(1 - s_2 - s_3),$$

since $\gamma(s_2, s_3) = \gamma(s_3, s_2)$. Hence $s_2 = s_3$. Substituting our result into Equation (B.2.1), we obtain

$$0 = s_2(1 - 2s_2) - \gamma(s_2, s_3)s_2^2,$$
$$0 = (1 - 2s_2 - \gamma(s_2, s_3)s_2),$$
$$s_2 = \frac{1}{2 + \gamma(s_2, s_3)}.$$

Since $s_2 = s_3$, from Equation (B.1.4) we can deduce that the interaction function $\gamma(s_2, s_3) = k_{23} = k_{32}$. Hence,

$$s_2 = \frac{1}{2 + k_{23}}. \qquad \text{(B.2.3)}$$

Therefore, the fixed point is $\left(0, \frac{1}{2+k_{23}}, \frac{1}{2+k_{32}}\right)$.

When $k_{23} = k_{32} = +1$, the fixed point is $\left(0, \frac{1}{3}, \frac{1}{3}\right)$; when $k_{23} = k_{32} = -1$ the fixed point is $(0, 1, 1)$.

(b.) When $s_1 \neq 0$, $s_2 = 0$ and $s_3 \neq 0$, Equations (B.1.1)- (B.1.3) becomes:

$$0 = s_1(1 - s_1 - s_3) - \gamma(s_1, s_3)s_1s_3,$$
$$0 = s_3(1 - s_1 - s_3) - \gamma(s_3, s_1)s_3s_1.$$

The computation follows a similar approach to that shown in (a.) above. Therefore, the fixed point is $\left(\frac{1}{2+k_{13}}, 0, \frac{1}{2+k_{31}}\right)$.

When $k_{13} = k_{31} = +1$, the fixed point is $\left(\frac{1}{3}, 0, \frac{1}{3}\right)$; when $k_{23} = k_{32} = -1$ the fixed point is $(1, 0, 1)$.

(c.) When $s_1 \neq 0$, $s_2 \neq 0$ and $s_3 = 0$, Equations (B.1.1)- (B.1.3) becomes:

$$0 = s_1(1 - s_1 - s_2) - \gamma(s_1, s_2)s_1 s_2,$$
$$0 = s_3(1 - s_1 - s_2) - \gamma(s_2, s_1)s_2 s_1.$$

The computation follows similar a approach as shown in (a.) above. Therefore, the fixed point is $\left(\frac{1}{2+k_{12}}, \frac{1}{2+k_{21}}, 0\right)$.

When $k_{13} = k_{31} = +1$, the fixed point is $\left(\frac{1}{3}, \frac{1}{3}, 0\right)$; when $k_{23} = k_{32} = -1$ the fixed point is $(1, 1, 0)$.

(IV) Computation of the type (IV) fixed point from Equations (B.1.1)- (B.1.3) at $\dot{s}_i = 0$ is shown below:
When $s_1 \neq 0$, $s_2 \neq 0$ and $s_3 \neq 0$, for simplicity, we assume $s_1 = s_2 = s_3 = b$, where $0 < b \leq 1$. Equations (B.1.1)- (B.1.3) becomes:

$$0 = b(1 - 3b) - \gamma(s_1, s_2)b^2 - \gamma(s_1, s_3)b^2,$$
$$0 = b(1 - 3b) - \gamma(s_2, s_1)b^2 - \gamma(s_2, s_3)b^2,$$
$$0 = b(1 - 3b) - \gamma(s_3, s_1)b^2 - \gamma(s_3, s_2)b^2.$$

Since, $s_1 = s_2$, from Equation (B.1.4) we can deduce that the interaction function $\gamma(s_1, s_2) = k_{12} = k_{21}$, also, since $s_1 = s_3$, the interaction function $\gamma(s_1, s_3) = k_{13} = k_{31}$ and since $s_2 = s_3$, the interaction function $\gamma(s_2, s_3) = k_{23} = k_{32}$. Therefore, from the argument above, we have

$$0 = b(1 - 3b) - k_{12}b^2 - k_{13}b^2,$$
$$0 = b(1 - 3b) - k_{12}b^2 - k_{23}b^2,$$
$$0 = b(1 - 3b) - k_{13}b^2 - k_{23}b^2.$$

This implies that

$$(1 - 3b) = k_{12}b + k_{13}b,$$
$$(1 - 3b) = k_{12}b + k_{23}b,$$
$$(1 - 3b) = k_{13}b + k_{23}b.$$

Hence, $k_{12}b + k_{13}b = k_{12}b + k_{23}b = k_{13}b + k_{23}b$, which implies that, for this fixed point, $k_{12} = k_{13} = k_{23}$.

The value of b is given by

$$b = \frac{1}{3 + k_{12} + k_{13}} = \frac{1}{3 + k_{12} + k_{23}} = \frac{1}{3 + k_{13} + k_{23}}.$$

Therefore, when $k_{12} = k_{13} = k_{23} = +1$, the fixed point is $\left(\frac{1}{5}, \frac{1}{5}, \frac{1}{5}\right)$; when $k_{12} = k_{13} = k_{23} = -1$, the fixed point is $(1, 1, 1)$.

The summary of the fixed point analysis presented in Table (B.1) below:

	Full Competition	Full Cooperation	Mixed Interactions	
Type	K_1	K_4	K_2	K_3
I	(0,0,0)	(0,0,0)	(0,0,0)	(0,0,0)
II	(1,0,0)	(1,0,0)	(1,0,0)	(1,0,0)
	(0,1,0)	(0,1,0)	(0,1,0)	(0,1,0)
	(0,0,1)	(0,0,1)	(0,0,1)	(0,0,1)
III	(0,1/3,1/3)	(0,1,1)	(0,1,1)	(0,1/3,1/3)
	(1/3,0,1/3)	(1,0,1)	(1/3,0,1/3)	(0,1,0)
	(1/3,1/3,0)	(1,1,0)	(1/3,1/3,0)	(1,1,0)
IV	(1/5,1/5,1/5)	(1,1,1)	-	-

Table B.1: Coordinates of fixed points.

B.3 Jacobian Matrix

The Jacobian matrix $[\mathbf{J}]_{(i,k)} = \frac{\partial \dot{s}_i}{\partial s_k}$, for $i, k = 1, \ldots, 3$. That is,

$$\mathbf{J} = \begin{bmatrix} \frac{\partial \dot{s}_1}{\partial s_1} & \frac{\partial \dot{s}_1}{\partial s_2} & \frac{\partial \dot{s}_1}{\partial s_3} \\ \frac{\partial \dot{s}_2}{\partial s_1} & \frac{\partial \dot{s}_2}{\partial s_2} & \frac{\partial \dot{s}_2}{\partial s_3} \\ \frac{\partial \dot{s}_3}{\partial s_1} & \frac{\partial \dot{s}_3}{\partial s_2} & \frac{\partial \dot{s}_3}{\partial s_3} \end{bmatrix}$$

The solutions of the elements of the Jacobian matrix are presented below:

$$
\begin{aligned}
\frac{\partial \dot{s}_1}{\partial s_1} &= 1 - 2s_1 - s_2 - s_3 - \gamma(s_1, s_2)s_2 - \frac{2(s_1 - s_2)}{\sigma^2}\gamma(s_1, s_2)s_1 s_2 - \gamma(s_1, s_3)s_3 - \frac{2(s_1 - s_3)}{\sigma^2}\gamma(s_1, s_3)s_1 s_3, \\
&= 1 - 2s_1 - s_2\left(1 + \gamma(s_1, s_2) + \frac{2}{\sigma^2}\gamma(s_1, s_2)s_1(s_1 - s_2)\right) - s_3\left(1 + \gamma(s_1, s_3) + \frac{2}{\sigma^2}\gamma(s_1, s_3)s_1(s_1 - s_3)\right);
\end{aligned}
$$

$$
\frac{\partial \dot{s}_1}{\partial s_2} = -s_1 - s_1\gamma(s_1, s_2) + \frac{2(s_1 - s_2)}{\sigma^2}\gamma(s_1, s_2)s_1 s_2;
$$

$$
\frac{\partial \dot{s}_1}{\partial s_3} = -s_1 - s_1\gamma(s_1, s_3) + \frac{2(s_1 - s_3)}{\sigma^2}\gamma(s_1, s_3)s_1 s_3;
$$

$$
\frac{\partial \dot{s}_2}{\partial s_1} = -s_2 - s_2\gamma(s_1, s_2) + \frac{2(s_2 - s_1)}{\sigma^2}\gamma(s_1, s_2)s_1 s_2;
$$

$$
\frac{\partial \dot{s}_2}{\partial s_2} = 1 - 2s_2 - s_1\left(1 + \gamma(s_1, s_2) + \frac{2(s_2 - s_1)}{\sigma^2}\gamma(s_1, s_2)s_2\right) - s_3\left(1 + \gamma(s_2, s_3) + \frac{2(s_2 - s_3)}{\sigma^2}\gamma(s_2, s_3)s_2\right);
$$

$$
\frac{\partial \dot{s}_2}{\partial s_3} = -s_2 - s_2\gamma(s_2, s_3) + \frac{2(s_2 - s_3)}{\sigma^2}\gamma(s_2, s_3)s_2 s_3;
$$

$$
\frac{\partial \dot{s}_3}{\partial s_1} = -s_3 - s_3\gamma(s_1, s_3) + \frac{2(s_3 - s_1)}{\sigma^2}\gamma(s_1, s_3)s_1 s_3;
$$

$$
\frac{\partial \dot{s}_3}{\partial s_2} = -s_3 - s_3\gamma(s_2, s_3) + \frac{2(s_3 - s_2)}{\sigma^2}\gamma(s_2, s_3)s_2 s_3;
$$

$$
\frac{\partial \dot{s}_3}{\partial s_3} = 1 - 2s_3 - s_1\left(1 + \gamma(s_1, s_3) + \frac{2(s_3 - s_1)}{\sigma^2}\gamma(s_1, s_3)s_3\right) - s_2\left(1 + \gamma(s_2, s_3) + \frac{2(s_3 - s_2)}{\sigma^2}\gamma(s_2, s_3)s_3\right).
$$

Where the interaction function $\gamma(s_i, s_j)$ is given as:

$$
\gamma(s_i, s_j) = k_{ij} \exp\left[-\left(\frac{s_i - s_j}{\sigma}\right)^2\right].
$$

Therefore the Jacobian matrix $[J]_{(i,k)} = \frac{\partial \dot{s}_i}{\partial s_k}$, with $i, k = 1, \ldots 3$, can be generalized as:

$$
[J]_{(i,k)} = \frac{\partial \dot{s}_i}{\partial s_k} =
\begin{cases}
1 - 2s_i - \sum_{i \neq j} s_j \left(1 + \gamma(s_i, s_j)\left[1 - \frac{2}{\sigma^2}s_i(s_i - s_j)\right]\right), & \text{for } k = i; \\
\\
-s_i - s_i\gamma(s_i, s_k)\left[1 - \frac{2}{\sigma^2}s_k(s_i - s_k)\right], & \text{for } k \neq i.
\end{cases}
$$

B.4 Type III Fixed Point Analysis

The details of the stability analysis for the type III fixed point is shown below:

1. When $a = \frac{1}{3}$, the Jacobian matrix $J_{(a,0,a)}$ is given by

$$
J_{(\frac{1}{3},0,\frac{1}{3})} =
\begin{bmatrix}
-\frac{1}{3}k_{13} & -\frac{1}{3} - \frac{1}{3}\theta_{12} & -\frac{1}{3} - \frac{1}{3}k_{13} \\
0 & -\frac{1}{3} - \frac{1}{3}(\theta_{21} + \theta_{23}) & 0 \\
-\frac{1}{3} - \frac{1}{3}k_{31} & -\frac{1}{3} - \frac{1}{3}\theta_{32} & -\frac{1}{3}k_{31}
\end{bmatrix},
$$

where $\theta_{ij} = k_{ij} \exp^{-\left(\frac{1}{3\sigma}\right)^2}$.

The characteristic equation is obtained by

$$|J_{\left(\frac{1}{3},0,\frac{1}{3}\right)} - \lambda I| = 0$$

This implies that

$$
\begin{aligned}
0 &= \left(-\frac{1}{3}k_{13} - \lambda\right)\left[\left(-\frac{1}{3} - \frac{1}{3}(\theta_{21} + \theta_{23}) - \lambda\right)\left(-\frac{1}{3}k_{31} - \lambda\right)\right] \\
&- \left(-\frac{1}{3} - \frac{1}{3}k_{13}\right)\left[\left(-\frac{1}{3} - \frac{1}{3}(\theta_{21} + \theta_{23}) - \lambda\right)\left(-\frac{1}{3} - \frac{1}{3}k_{31}\right)\right].
\end{aligned}
$$

Furthermore,

$$
0 = \left(-\frac{1}{3} - \frac{1}{3}(\theta_{21} + \theta_{23}) - \lambda\right)\left[\left(-\frac{1}{3}k_{13} - \lambda\right)\left(-\frac{1}{3}k_{31} - \lambda\right) - \left(-\frac{1}{3} - \frac{1}{3}k_{13}\right)\left(-\frac{1}{3} - \frac{1}{3}k_{31}\right)\right].
$$

Therefore,

$$
\begin{aligned}
0 &= \left(-\frac{1}{3} - \frac{1}{3}(\theta_{21} + \theta_{23}) - \lambda\right) \\
\implies \lambda &= -\frac{1}{3} - \frac{1}{3}(\theta_{21} + \theta_{23}) \\
\lambda &= -\frac{1}{3} - \frac{1}{3}\left(k_{21}\exp^{-\left(\frac{1}{3\sigma}\right)^2} + k_{23}\exp^{-\left(\frac{1}{3\sigma}\right)^2}\right);
\end{aligned}
$$

or

$$
0 = \left[\left(-\frac{1}{3}k_{13} - \lambda\right)\left(-\frac{1}{3}k_{31} - \lambda\right) - \left(-\frac{1}{3} - \frac{1}{3}k_{13}\right)\left(-\frac{1}{3} - \frac{1}{3}k_{31}\right)\right].
$$

This implies:

$$
\left(-\frac{1}{3}k_{13} - \lambda\right)\left(-\frac{1}{3}k_{31} - \lambda\right) = \left(-\frac{1}{3} - \frac{1}{3}k_{13}\right)\left(-\frac{1}{3} - \frac{1}{3}k_{31}\right),
$$

$$
\lambda^2 + \frac{2}{3}\lambda k_{13} + \frac{1}{9}k_{13}^2 = \frac{1}{9} + \frac{2}{9}\lambda k_{13} + \frac{1}{9}k_{13}^2,
$$

where $k_{13} = k_{31}$ is applied to obtain the second equation. Therefore by comparing coefficients, the value of $\lambda = \frac{1}{3}$ twice.

The eigenvalues of the Jacobian matrix $J_{\left(\frac{1}{3},0,\frac{1}{3}\right)}$ is therefore equals to $\frac{1}{3}$, $\frac{1}{3}$ and $-\frac{1}{3} - \frac{1}{3}\left(k_{21}\exp^{-\left(\frac{1}{3\sigma}\right)^2} + k_{23}\exp^{-\left(\frac{1}{3\sigma}\right)^2}\right)$. This shows the fixed point is Unstable since at least one of the eigenvalues is positive.

2. When $a = 1$, the Jacobian matrix becomes

$$J_{(1,0,1)} = \begin{bmatrix} -2 - k_{13} & -1 - \phi_{12} & -1 - k_{13} \\ 0 & -1 - (\phi_{21} + \phi_{23}) & 0 \\ -1 - k_{31} & -1 - \theta_{32} & -2 - k_{31} \end{bmatrix},$$

where $\phi_{ij} = k_{ij} \exp^- \left(\frac{1}{\sigma}\right)^2$.

The characteristic equation is obtained by

$$|J_{(1,0,1)} - \lambda I| = 0$$

This implies that

$$\begin{aligned} 0 &= (-2 - k_{13} - \lambda)\left[(-1 - (\phi_{21} + \phi_{23}) - \lambda)(-2 - k_{31} - \lambda)\right] \\ &\quad - (-1 - k_{13})\left[(-1 - (\phi_{21} + \phi_{23}) - \lambda)(-1 - k_{31})\right]. \end{aligned}$$

It can be deduce from above that

$$\begin{aligned} 0 &= (-1 - (\phi_{21} + \phi_{23}) - \lambda), \\ \implies \lambda &= -1 - (\phi_{21} + \phi_{23}). \end{aligned}$$

or

$$0 = (-2 - k_{13} - \lambda)(-2 - k_{31} - \lambda) - (-1 - k_{13})(-1 - k_{31}).$$

Putting $k_{13} = k_{31}$ into the above equation, we have

$$\begin{aligned} (-2 - k_{13} - \lambda)^2 &= (-1 - k_{13})^2, \\ \lambda^2 + 2(2 + k_{13})\lambda &= (-1 - k_{13})^2 - (-2 - k_{13})^2, \\ \lambda^2 + 2(2 + k_{13})\lambda + (3 + 2k_{13}) &= 0. \end{aligned}$$

Solving for λ, we have

$$\begin{aligned} \lambda &= \frac{-2(2 + k_{13}) \pm \sqrt{(4 + 2k_{13})^2 - 4(3 + 2k_{13})}}{2} \\ &= \frac{-2(2 + k_{13}) \pm \sqrt{(2 + 2k_{13})^2}}{2} \end{aligned}$$

Therefore the value of λ can be computed firstly as

$$\begin{aligned} \lambda &= \frac{-2(2 + k_{13}) + (2 + 2k_{13})}{2} \\ &= \frac{-4 - 2k_{13} + 2 + 2k_{13}}{2} \\ &= -1 \end{aligned} \tag{B.4.1}$$

77

and secondly as

$$
\begin{aligned}
\lambda &= \frac{-2(2 + k_{13}) - (2 + 2k_{13})}{2} \\
&= \frac{-4 - 2k_{13} - 2 - 2k_{13}}{2} \\
&= -3 - 2k_{13}
\end{aligned}
$$

The eigenvalues of the Jacobian matrix $J_{(1,0,1)}$ is therefore equals to -1, $-3 - 2k_{13}$ and $-1 - (\phi_{21} + \phi_{23})$.

Bibliography

[1] Artzner, P., Delbaen, F., Eber, J.M. and Heath, D., 1999. Coherent measures of risk. *Mathematical finance, 9*(3), pp.203-228.

[2] Barabàsi A.L., 2003. Linked: How everything is connected to everything else and what it means, *Perseus, Cambridge.*

[3] Barbose, G.L., 2010. Tracking the Sun II: The Installed Cost of Photovoltaics in the US from 1998-2008. *Lawrence Berkeley National Laboratory.*

[4] Blair, N.J., Dobos, A.P. and Gilman, P., 2013, April. Comparison of photovoltaic models in the system advisor model. *In Proceedings of the Solar.*

[5] Boccaletti, S., Latora, V., Moreno, Y., Chavez, M. and Hwang, D.U., 2006. Complex networks: Structure and dynamics. *Physics reports, 424*(4), pp.175-308

[6] Caram, L.F., Caiafa, C.F., Proto, A.N. and Ausloos, M., 2010. Dynamic peer-to-peer competition. Physica A: *Statistical Mechanics and its Applications, 389*(13), pp.2628-2636.

[7] Caram, L.F., Caiafa, C.F., Ausloos, M. and Proto, A.N., 2015. Cooperative peer-to-peer multiagent-based systems. *Physical Review E, 92*(2), p.022805.

[8] Comes, C.A., 2012. Banking system: Three level Lotka-Volterra model. *Procedia Economics and Finance, 3*, pp.251-255.

[9] Dallinger, D., Gerda, S. and Wietschel, M., 2013. Integration of intermittent renewable power supply using grid-connected vehicles–A 2030 case study for California and Germany. *Applied Energy, 104*, pp.666-682.

[10] EIA, 2016. *Annual energy outlook 2016.* U.S. Energy Information Administration, Department of Energy.

[11] EIA, 2016. *Updated capital cost estimates for utility scale electricity generating plants.* U.S. Energy Information Administration, Department of Energy.

[12] Frost and Sullivan, 2006. *New Research Reveals Collaboration Is a Key Driver of Business Performance Around the World.* Whitepaper. Microsoft Press Release. Redmond, Washington.

[13] Garcìa-Martos, C., Rodrìguez, J., Sànchez, M.J., 2013. Modelling and forecasting fossil fuels, CO_2 and electricity and their volatilities. *Applied Energy 101*, pp.363-375.

[14] Gonzàlez-Pedraz, C., Moreno, M., Pena, J.I., 2014. Tail risk in energy portfolios, *Energy Economics 46*, pp.422-434.

[15] Hilborn, R.C., 2000. *Chaos and Nonlinear Dynamics: An Introduction for Scientist and Engineers* Oxford University Press, Oxford.

[16] Huisman, R. and Mahieu, R., 2003. Regime jumps in electricity prices. *Energy economics, 25*(5), pp.425-434.

[17] https://www.theguardian.com/small-business-network/2013/aug/20/big-company-partnership-grow-small-business

[18] https://www.scientificamerican.com/article/wind-and-solar-are-better-together/

[19] Jacobson, M.Z. and Delucchi, M.A., 2009. A path to sustainable energy by 2030. *Scientific American, 301*(5), pp.58-65.

[20] Joskoaw, P.L., 2011. Comparing the costs of intermittent and dispatchable electricity generating technologies. *The American Economic Review, 101*(3), pp.238-241.

[21] Knyviene, I., Girdzijauskas, S. and Grundey, D., 2010. Market capacity from the viewpoint of logistic analysis. *Technological and Economic Development of economy, 16*(4), pp.690-702.

[22] Lotka, A.J., 1926. Elements of physical biology. *Science Progress in the Twentieth Century (1919-1933), 21*(82), pp.341-343.

[23] Lucheroni, C. and Mari, C., 2014, October. Stochastic LCOE and risk/cost trade-off in electricity generation portfolio selection. In *Sustainable Energy Policy and Strategies for Europe, 14th IAEE European Conference, October 28-31, 2014.* International Association for Energy Economics.

[24] Lucheroni, C. and Mari, C., 2014, May. Stochastic LCOE for optimal electricity generation portfolio selection. In *European Energy Market (EEM), 2014 11th International Conference on the* (pp. 1-8). IEEE.

[25] Lucheroni, C. and Mari, C., 2015. Risk Shaping of Optimal Electricity Portfolios in the Stochastic LCOE Theory. *Energy Econ.*

[26] Lucheroni, C. and Mari, C., 2017. CO$_2$ volatility impact on energy portfolio choice: A fully stochastic LCOE theory analysis. *Applied Energy, 190*, pp.278-290.

[27] Lucheroni, C. and Mari, C., 2016. Stochastic systemic LCOE: Integration of non-dispatchable renewable power sources in the LCOE theory. https://doi.org/10.13140/rg.2.1.1025.3042

[28] Mari, C., 2014. Hedging electricity price volatility using nuclear power. *Applied Energy, 113*, pp.615-621.

[29] Markowitz, H., 1952. Portfolio selection. *The journal of finance, 7*(1), pp.77-91.

[30] Maurer, S.M. and Huberman, B.A., 2003. Competitive dynamics of web sites. *Journal of Economic Dynamics and Control, 27*(11), pp.2195-2206.

[31] Philippe, J., 1997. Value at Risk: The New Benchmark for controlling Derivatives Risk. New York: McGraw-Hill;.

[32] MIT, 2003. *The future of nuclear power*, Cambridge, United State.

[33] Newman, M.E., 2011. Complex systems: A survey, a*rXiv preprint arXiv:1112.1440.*

[34] NREL, 2012. *Renewable Electricity Futures Study*, National Renewable Energy Laboratory.

[35] NREL, 2012. *PVWatts Version 1*: http://rredc.nrel.gov/solar/calculators/ PVWATTS/version1.

[36] NREL, 2012. *Wind Integration Datasets*: http//www.nrel.gov/elecrticity/ transmission/ wind_integration_dataset.html.

[37] OECD NEA/IEA, 2010. *Projected Costs of Generating Electricity*, Organisation for Economic Co-operation and Development, Nuclear Energy Agency/International Energy Agency, Paris, France.

[38] Ouyang, X. and Lin, B., 2014. Levelized cost of electricity (LCOE) of renewable energies and required subsidies in China. *Energy policy, 70*, pp.64-73.

[39] Pachamanova, D. A., and F. J. Fabozzi, 2010. *Simulation and Optimization in Finance: Modeling with MATLAB,@ RISK, or VBA*, Vol. 173. John Wiley & Sons.

[40] Porter, M. E., 1985. The Competitive Advantage: Creating and Sustaining Superior Performance. NY: Free Press.

[41] Reichelstein, S. and Sahoo, A., 2015. Time of day pricing and the levelized cost of intermittent power generation. *Energy Economics, 48,* pp.97-108.

[42] Rockafellar, R.T. and Uryasev, S., 2000. Optimization of conditional value-at-risk. *Journal of risk, 2,* pp.21-42.

[43] Rockafellar, R.T. and Uryasev, S., 2002. Conditional value-at-risk for general loss distributions. *Journal of banking & finance, 26*(7), pp.1443-1471.

[44] Rockafellar, R.T., Uryasev, S. and Zabarankin, M., 2006. Generalized deviations in risk analysis. *Finance and Stochastics, 10*(1), pp.51-74.

[45] Roth, I.F. and Ambs, L.L., 2004. Incorporating externalities into a full cost approach to electric power generation life-cycle costing. *Energy, 29*(12), pp.2125-2144.

[46] Short, W., Packey, D.J. and Holt, T., 1995. A *manual for the economic evaluation of energy efficiency and renewable energy technologies (No. NREL/TP–462-5173).* National Renewable Energy Lab., Golden, CO (United States).

[47] Singh, P.P. and Singh, S., 2010. Realistic generation cost of solar photovoltaic electricity. *Renewable Energy, 35*(3), pp.563-569.

[48] Sonubi, A., Arcagni, A., Stefani, S. and Ausloos, M., 2016. Effects of competition and cooperation interaction between agents on networks in the presence of a market capacity. *Physical Review E, 94*(2), p.022303.

[49] Strogatz, S., Friedman, M., Mallinckrodt, A.J. and McKay, S., 1994. Nonlinear dynamics and chaos: With applications to physics, biology, chemistry, and engineering. *Computers in Physics, 8*(5), pp.532-532.

[50] Taylor, G. and Tanton, T., 2012. The Hidden Costs of Wind Electricity: Why the full cost of wind generation is unlikely to match the cost of natural gas, coal or nuclear generation. *Washington, DC: American Tradition Institute: Center for Energy Studies.*

[51] Verhulst, P. F., 1845. Recherches mathématiques sur la loi d'accroissement de la population, *Nouv. mém. de l'Academie Royale des Sci. et Belles-Lettres de Bruxelles 18*, pp.1-41.

[52] Verhulst, P. F., 1847. Deuxième mémoire sur la loi d'accroissement de la population. *Mém. de l'Academie Royale des Sci., des Lettres et des Beaux-Arts de Belgique 20*, pp.1-32.

[53] Volterra, V., 1926. Variazioni e fluttuazioni del numero d'individui in specie animali conviventi. *Mem. R. Accad. Naz. dei Lincei VI, 2*, 31.

[54] Wang, J., 2000. Mean-variance-VaR based portfolio optimization. *Valdosta State University.*

[55] Weron, R., 2009. Heavy-tails and regime-switching in electricity prices. *Mathematical Methods of Operations Research, 69*(3), pp.457-473.

[56] Yanhui, L. and Siming, Z., 2007. Competitive dynamics of e-commerce web sites. *Applied mathematical modelling, 31*(5), pp.912-919.

[57] Zhang, L., Barakat, G. and Yassine, A., 2012. Deterministic optimization and cost analysis of hybrid PV/wind/battery/diesel power system. *International Journal of Renewable Energy Research (IJRER), 2*(4), pp.686-696.